

ISSN 1881-7831 Online ISSN 1881-784X

DD & T

Drug Discoveries & Therapeutics

Volume 6, Number 2
April, 2012



www.ddtjournal.com

DD & T

Drug Discoveries & Therapeutics



ISSN: 1881-7831
Online ISSN: 1881-784X
CODEN: DDTRBX
Issues/Year: 6
Language: English
Publisher: IACMHR Co., Ltd.

Drug Discoveries & Therapeutics is one of a series of peer-reviewed journals of the International Research and Cooperation Association for Bio & Socio-Sciences Advancement (IRCA-BSSA) Group and is published bimonthly by the International Advancement Center for Medicine & Health Research Co., Ltd. (IACMHR Co., Ltd.) and supported by the IRCA-BSSA and Shandong University China-Japan Cooperation Center for Drug Discovery & Screening (SDU-DDSC).

Drug Discoveries & Therapeutics publishes contributions in all fields of pharmaceutical and therapeutic research such as medicinal chemistry, pharmacology, pharmaceutical analysis, pharmaceuticals, pharmaceutical administration, and experimental and clinical studies of effects, mechanisms, or uses of various treatments. Studies in drug-related fields such as biology, biochemistry, physiology, microbiology, and immunology are also within the scope of this journal.

Drug Discoveries & Therapeutics publishes Original Articles, Brief Reports, Reviews, Policy Forum articles, Case Reports, News, and Letters on all aspects of the field of pharmaceutical research. All contributions should seek to promote international collaboration in pharmaceutical science.

Editorial Board

Editor-in-Chief:

Kazuhisa SEKIMIZU
The University of Tokyo, Tokyo, Japan

Co-Editors-in-Chief:

Xishan HAO
Tianjin Medical University, Tianjin, China

Norihiro KOKUDO
The University of Tokyo, Tokyo, Japan

Hongxiang LOU
Shandong University, Ji'nan, China

Yun YEN
City of Hope National Medical Center, Duarte, CA, USA

Chief Director & Executive Editor:

Wei TANG
The University of Tokyo, Tokyo, Japan

Managing Editor:

Hiroshi HAMAMOTO
The University of Tokyo, Tokyo, Japan
Munehiro NAKATA
Tokai University, Hiratsuka, Japan

Senior Editors:

Guanhua DU
Chinese Academy of Medical Science and Peking Union Medical College, Beijing, China

Xiao-Kang LI
National Research Institute for Child Health and Development, Tokyo, Japan

Masahiro MURAKAMI
Osaka Ohtani University, Osaka, Japan

Yutaka ORIHARA
The University of Tokyo, Tokyo, Japan

Tomofumi SANTA
The University of Tokyo, Tokyo, Japan

Wenfang XU
Shandong University, Ji'nan, China

Web Editor:

Yu CHEN
The University of Tokyo, Tokyo, Japan

Proofreaders:

Curtis BENTLEY
Roswell, GA, USA
Thomas R. LEBON
Los Angeles, CA, USA

Editorial and Head Office:

Pearl City Koishikawa 603,
2-4-5 Kasuga, Bunkyo-ku,
Tokyo 112-0003, Japan
Tel.: +81-3-5840-9697
Fax: +81-3-5840-9698
E-mail: office@ddtjournal.com

Drug Discoveries & Therapeutics

Editorial and Head Office

Pearl City Koishikawa 603, 2-4-5 Kasuga, Bunkyo-ku,
Tokyo 112-0003, Japan

Tel: +81-3-5840-9697, Fax: +81-3-5840-9698
E-mail: office@ddtjournal.com
URL: www.ddtjournal.com

Editorial Board Members

Alex ALMASAN (Cleveland, OH)	Yu HUANG (Hong Kong)	Xiao-Ming OU (Jackson, MS)	Takako YOKOZAWA (Toyama, Toyama)
John K. BUOLAMWINI (Memphis, TN)	Hans E. JUNGINGER (Marburg, Hesse)	Weisan PAN (Shenyang, Liaoning)	Rongmin YU (Guangzhou, Guangdong)
Shousong CAO (Buffalo, NY)	Amrit B. KARMARKAR (Karad, Maharashtra)	Rakesh P. PATEL (Mehsana, Gujarat)	Guangxi ZHAI (Ji'nan, Shandong)
Jang-Yang CHANG (Tainan)	Toshiaki KATADA (Tokyo)	Shivanand P. PUTHLI (Mumbai, Maharashtra)	Liangren ZHANG (Beijing)
Fen-Er CHEN (Shanghai)	Gagan KAUSHAL (Charleston, WV)	Shafiqur RAHMAN (Brookings, SD)	Lining ZHANG (Ji'nan, Shandong)
Zhe-Sheng CHEN (Queens, NY)	Ibrahim S. KHATTAB (Kuwait)	Adel SAKR (Cairo)	Na ZHANG (Ji'nan, Shandong)
Zilin CHEN (Wuhan, Hubei)	Shiroh KISHIOKA (Wakayama, Wakayama)	Gary K. SCHWARTZ (New York, NY)	Ruiwen ZHANG (Amarillo, TX)
Chandradhar DWIVEDI (Brookings, SD)	Robert Kam-Ming KO (Hong Kong)	Yuemao SHEN (Ji'nan, Shandong)	Xiu-Mei ZHANG (Ji'nan, Shandong)
Mohamed F. EL-MILIGI (6th of October City)	Nobuyuki KOBAYASHI (Nagasaki, Nagasaki)	Brahma N. SINGH (New York, NY)	Yongxiang ZHANG (Beijing)
Hao FANG (Ji'nan, Shandong)	Toshiro KONISHI (Tokyo)	Tianqiang SONG (Tianjin)	(As of April 2012)
Marcus L. FORREST (Lawrence, KS)	Chun-Guang LI (Melbourne)	Sanjay K. SRIVASTAVA (Amarillo, TX)	
Takeshi FUKUSHIMA (Funabashi, Chiba)	Minyong LI (Ji'nan, Shandong)	Hongbin SUN (Nanjing, Jiangsu)	
Harald HAMACHER (Tübingen, Baden-Württemberg)	Jikai LIU (Kunming, Yunnan)	Chandan M. THOMAS (Bradenton, FL)	
Kenji HAMASE (Fukuoka, Fukuoka)	Xinyong LIU (Ji'nan, Shandong)	Murat TURKOGLU (Istanbul)	
Xiaojiang HAO (Kunming, Yunnan)	Yuxiu LIU (Nanjing, Jiangsu)	Fengshan WANG (Ji'nan, Shandong)	
Kiyoshi HASEGAWA (Tokyo)	Xingyuan MA (Shanghai)	Hui WANG (Shanghai)	
Waseem HASSAN (Rio de Janeiro)	Ken-ichi MAFUNE (Tokyo)	Quanxing WANG (Shanghai)	
Langchong HE (Xi'an, Shaanxi)	Sridhar MANI (Bronx, NY)	Stephen G. WARD (Bath)	
Rodney J. Y. HO (Seattle, WA)	Tohru MIZUSHIMA (Tokyo)	Yuhong XU (Shanghai)	
Hsing-Pang HSIEH (Zhunan, Miaoli)	Abdulla M. MOLOKHIA (Alexandria)	Bing YAN (Ji'nan, Shandong)	
Yongzhou HU (Hangzhou, Zhejiang)	Yoshinobu NAKANISHI (Kanazawa, Ishikawa)	Yasuko YOKOTA (Tokyo)	

Review

- 55 - 61 **Up-frameshift protein 1 (UPF1): Multitalented entertainer in RNA decay.**
Naoto Imamachi, Hidenori Tani, Nobuyoshi Akimitsu

Original Articles

- 62 - 68 **A facile method for the synthesis of *N*-(α -aminoacyl) sulfonamides.**
Shaolei Wu, Minglu Chen, Yutao Wang, Xuben Hou, Xinying Yang, Li Su, Hao Fang
- 69 - 77 **In silico ligand based design of indolylpiperidinyl derivatives as novel histamine H₁ receptor antagonists.**
Sarvesh Paliwal, Supriya Singh, Mahima Pal
- 78 - 87 **Synthesis, analgesic, anti-inflammatory and ulcerogenic properties of some novel *N'*-((1-(substituted amino)methyl)-2-oxoindolin-3-ylidene)-4-(2-(methyl/phenyl)-4-oxoquinazolin-3(4*H*)-yl)benzohydrazide derivatives.**
Govindaraj Saravanan, Veerachamy Alagarsamy, Chinnasamy Rajaram Prakash
- 88 - 93 **Evaluation of innate immune stimulating activity of polysaccharides using a silkworm (*Bombyx mori*) muscle contraction assay.**
Tomoko Fujiyuki, Hiroshi Hamamoto, Kenichi Ishii, Makoto Urai, Keiko Kataoka, Tadahiro Takeda, Shoji Shibata, Kazuhisa Sekimizu
- 94 - 101 **Regulation of Janus-activated kinase-2 (JAK2) by diindolylmethane in ovarian cancer *in vitro* and *in vivo*.**
Prabodh K. Kandala, Sanjay K. Srivastava
- 102 - 107 **Analyzing global trends of biomarker use in drug interventional clinical studies.**
Kunihiko Hayashi, Sachiko Masuda, Hiromichi Kimura

CONTENTS

(Continued)

Commentary

- 108 - 111 **Standardization of perioperative management on hepato-biliarypancreatic surgery.**
*Jianjun Gao, Peipei Song, Sumihito Tamura, Kiyoshi Hasegawa, Yasuhiko Sugawara,
Norihiko Kokudo, Kanji Uchida, Ryo Orii, Fanghua Qi, Jiahong Dong, Wei Tang*

Guide for Authors

Copyright

Up-frameshift protein 1 (UPF1): Multitalented entertainer in RNA decay

Naoto Imamachi¹, Hidenori Tani², Nobuyoshi Akimitsu^{1,*}

¹ Radioisotope Center, The University of Tokyo, Tokyo, Japan;

² Research Institute for Environmental Management Technology, National Institute of Advanced Industrial Science and Technology (AIST), Tsukuba, Japan.

ABSTRACT: Up-frameshift protein 1 (UPF1) is an evolutionarily conserved protein with RNA/DNA-dependent ATPase and RNA helicase activity. The protein is well known for its central role in nonsense-mediated mRNA decay (NMD), which eliminates aberrant mRNAs harboring premature termination codon (PTC), preventing the accumulation of nonfunctional or potentially harmful truncated proteins. NMD is also involved in the regulation of the state-levels of many normal physiological mRNAs. Moreover UPF1 is not only a key player in NMD but is also involved in non-NMD RNA degradation, such as stau1 (STAU1)-mediated mRNA decay (SMD) and replication-dependent histone mRNA decay. Thus, UPF1 is an important factor for the RNA quality control system and the regulation of physiological gene expression. Further, recent studies have clarified that UPF1 contributes to DNA replication, DNA repair, telomere metabolism, and stabilization of HIV-1 genomic RNA. In the review, we summarize numerous functions of UPF1.

Keywords: UPF1, RNA surveillance, post-transcriptional gene regulation, RNA replication, S phase progression, telomere, HIV-1

1. Introduction

Up-frameshift protein 1 (UPF1) is evolutionarily conserved and ubiquitously expressed phosphoprotein with RNA/DNA-dependent ATPase and RNA helicase activity (1). UPF1 has been characterized as an essential factor for nonsense-mediated mRNA decay (NMD), which eliminates aberrant mRNAs harboring premature termination codon (PTC) generated by a nonsense mutation or frameshift (2). NMD is one of the important

RNA surveillance mechanisms, which prevent the accumulation of nonfunctional or potentially harmful truncated proteins (3,4). The pathway is also involved in regulating the expression of 1-10% normal physiological mRNAs (5). UPF1 interacts with several NMD factors, such as UPF2, NCBP1 (also known as CBP80), SMG1, SMG5-SMG7, SMG6, and eRF1-eRF3 (6-16). In addition to its role in quality control mechanism by NMD, UPF1 also functions two non-NMD decay pathways: stau1 (STAU1)-mediated mRNA decay (SMD) and replication-dependent histone mRNA decay. SMD, unlike NMD, involves in the regulation of functional mRNAs harboring double-stranded RNA region called STAU1-binding site (SBS) in their 3'-untranslated region (3' UTR) (17,18). Replication-dependent histone mRNA decay degrades cell cycle-regulated histone mRNAs harboring stem-loop structure in the 3' UTR (19). Thus, UPF1 is an important factor in RNA surveillance mechanism for the degradation of abnormal mRNAs and the post-transcriptional regulation of gene expression for the degradation of normal mRNAs.

Interestingly, recent studies have revealed that UPF1 is not only a key player in several RNA degradation pathways but is also involved in several unique roles such as DNA replication, DNA repair, telomere metabolism, and stabilization of HIV-1 genomic RNA. UPF1 physically interacts with the DNA polymerase δ during S-phase of the cell cycle, controls telomere length and telomeric silencing, and regulates the HIV-1 RNA metabolism and translation (20-23). In the review, we describe that the roles of UPF1 in RNA surveillance mechanism, the post-transcriptional regulation of physiological mRNAs, and several unique functions in the cells.

2. Evolutional conservation of UPF1

UPF1 (Figure 1) was originally isolated in yeast (24). UPF1 is known as regulator of nonsense transcript 1 (Rent1) in mice, and suppressor with morphogenetic defects in genitalia 2 (Smg2) in fruitfly (1,25). For UPF1, the sequence identities among human, plant, fruitfly, nematode, and yeast are between 40-62% compared to 59-67% for ribosomal proteins. Especially,

*Address correspondence to:

Dr. Nobuyoshi Akimitsu, Radioisotope Center, The University of Tokyo, 2-11-16 Yayoi, Bunkyo-ku, Tokyo 113-0032, Japan.

E-mail: akimitsu@ric.u-tokyo.ac.jp

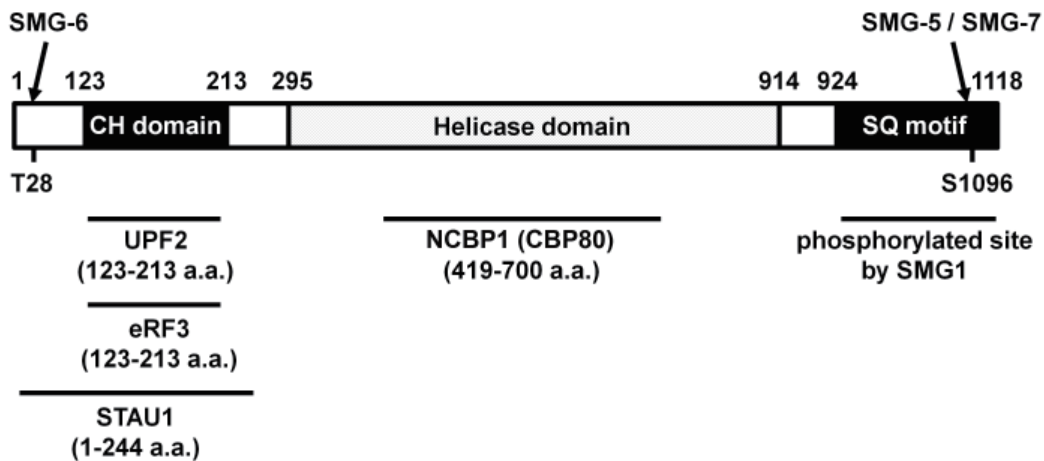


Figure 1. The structure of UPF1 protein. Schematic diagram explaining domains of human UPF1 protein. Cysteine/histidine-rich domain (CH domain) is present at N-terminus. Helicase domain is important for NMD. Serine/glutamine motif (SQ motif) is present at C-terminus. The numbers above the schematic diagram represent the amino acid positions of the domain or the motif boundary. The alphameric characters below the schematic diagram represent the phosphorylated positions. Phosphorylation of UPF1 at T28 is important for SMG6 binding to UPF1. Phosphorylation of UPF1 at S1096 is important for SMG5/SMG7 binding to UPF1. UPF1 is phosphorylated by SMG1 at SQ motif. The binding site of each NMD factor is represented below the schematic diagram. a.a., amino acids.

the sequence identities among zebrafish, mouse, and human are over 90% (26). Thus, UPF1 is highly conserved throughout eukaryotes. High evolutionary conservation suggests its importance in biological systems. Actually, UPF1 is essential for embryonic viability in plant, fruitfly, zebrafish, and mice (27-31). For instance, loss of UPF1 function inhibits cell growth and induces apoptosis in *Drosophila melanogaster* (27). Thus, UPF1 plays important roles in various organisms.

3. Nonsense-mediated mRNA decay (NMD)

RNA degradation, as well as RNA transcription, plays a crucial role in the regulation of gene expression. RNA degradation can be divided into two classes; the mechanisms for regulating of gene expression and the mechanisms for rapidly degrading aberrant mRNAs (32). Generally, mRNA decay rates of house-keeping genes are slow, while those of regulatory genes such as transcription factor and replication-dependent histones are comparatively fast (33). The expression level of regulatory genes is frequently modulated by RNA decay pathway (34). Rapid degradation is also occurred by the generation of aberrant mRNAs, such as mRNAs harboring PTC (35). NMD is best known as mRNA surveillance mechanism for the elimination of such aberrant PTC-containing mRNAs generated as a result of a nonsense mutation or frameshift (3,4). Previous bioinformatic analyses predicted that one-third alternatively spliced transcripts have the potential to contain PTCs, which trigger NMD (36). Thus, the NMD pathway is essential to ensure the fidelity of transcripts, preventing the production of harmful truncated proteins with dominant-negative or deleterious gain-of-function activities and, as a consequence, human diseases

(37,38). Interestingly, NMD contributes to not only the degradation of aberrant mRNAs harboring PTC, but also the regulation of normal physiological mRNAs. The previous studies suggested that NMD is involved in the degradation of 1-10% physiological transcripts from a wide variety of species, including yeast, nematode, fruitfly, plants, and mammals (5,39-47).

The NMD pathway in human cells comprises the factors UPF1, UPF2, UPF3A, UPF3B, SMG1, SMG5, SMG6, SMG7, SMG8, SMG9, NAG, and DHX34 (4,48). Among these factors, the UPF proteins constitute the core NMD machinery. Of all the UPF genes, UPF1 is functionally the most important factor for NMD (26,49). Newly synthesized mRNAs harbor cap-binding protein heterodimer NCBP1-NCBP2 (also known as CBP80-CBP20) at the 5' cap structure and exon-exon junction complex (EJC) as result of precursor mRNA (pre-mRNA) splicing (32,50). An important step in NMD is the translation-dependent recognition of transcripts with aberrant termination events and then targeting those mRNAs for degradation. EJC, deposited 20-24 nucleotides upstream of exon-exon junctions, plays a central role to distinguish aberrant PTC-containing mRNA from normal mRNA in mammalian cells (51). Although EJCs locating within an open reading frame (ORF) are removed by elongating ribosomes, EJCs locating downstream of the termination codon remain associated with the ribonucleoprotein (RNP) (52). This remaining EJC during a pioneer round of translation recruits NMD factors, including UPF1, to PTC-containing mRNAs and stimulates mRNA degradation (51). NCBP1-NCBP2 complex is also retained in PTC-containing mRNAs during the pioneer-round of translation (3,4). UPF1 interacts with NCBP1, and this interaction

contributes to the process of NMD at the initial step (16). The NCBP1-UPF1 interaction promotes the binding of SMG1-UPF1 to eRF1-eRF3 so as to form the SURF (SMG1-UPF1-eRF1-eRF3) complex and then promotes the interaction of SMG1-UPF1 with EJC (6-9,15,16,51). Thus, UPF1 plays a central role in NMD pathway, especially initial step.

UPF1 regulates the degradation of NMD-sensitive mRNAs and the remodeling of the mRNA surveillance complex through phosphorylation/dephosphorylation cycle (10-14). Namely, UPF1 is phosphorylated by SMG1, a phosphatidylinositol 3-kinase-related protein kinase (PIKK), at specific serine residues in its C-terminus serine/glutamine motifs (SQ motifs: 924-1,118 amino acids) (10,11). UPF1 phosphorylation facilitates the assembly of degradation factor, consequently, triggers the degradation of NMD-sensitive mRNAs (53). RNA degradation requires for the assembly of degradation factors and translational repression during NMD. UPF1 phosphorylation triggers eIF3-dependent translational repression during the process of NMD. Phosphorylated UPF1 but not hypophosphorylated UPF1 directly interacts with eIF3, a component of the 43S pre-initiation complex and then prevents the joining of 60S ribosomal subunit (54). Thus, UPF1 phosphorylation induces translational repression. Moreover, phosphorylated UPF1 also interacts with SMG5, SMG6, SMG7, and human proline-rich nuclear receptor coregulatory protein 2 (PNRC2) and then triggers the degradation of NMD-sensitive mRNAs (53,55-59). The association of SMG6 with phosphorylated UPF1 triggers RNA degradation by SMG6 endonuclease (SMG6-mediated endonucleolytic decay) (55,56,58,59). In contrast, the association of heterodimer SMG5/SMG7 with phosphorylated UPF1 triggers RNA degradation by deadenylase and decapping enzyme (SMG5/SMG7-mediated exonucleolytic decay) (57,59). PNRC2 interacts with UPF1 and DCP1a, a component of decapping complex. The mediation of PNRC2 triggers 5'-to-3' exonucleolytic decay (53). However, the biological importance of multiple decay pathways is still unclear.

Disassembly of mRNP complex is critical in the final step of RNA degradation. The recent study revealed that ATP hydrolysis by UPF1 leads to disassemble mRNP complex targeted to NMD (60). Thus, disassembly of mRNP complex by UPF1 is involved in recycling of NMD factors and other RNA-binding proteins derived from NMD substrates and UPF1 ATPase activity plays an important role in ATPase-dependent mRNP disassembly in NMD.

4. Staufen1-mediated mRNA decay (SMD)

Staufen, a double-stranded RNA-binding protein, was originally identified as maternal factor required for the localization of *bicoid* mRNAs at the anterior pole and

oskar mRNAs at the posterior pole during oogenesis (61). Mammalian genomes encode two homologous Staufen genes, STAU1 and STAU2, although the functional discrimination between STAU1 and STAU2 is largely unknown (62). STAU1 is involved in the degradation of certain mRNAs containing SBS in their 3' UTR. SBS is divided into two groups: intramolecular base-pairing within a 3' UTR or intermolecular base-pairing between an mRNA 3' UTR and a long noncoding RNA named half-STAU1-binding site RNAs (1/2-sbsRNAs) (17,63). STAU1-dependent RNA degradation is named as SMD (64). SMD targets not only NCBP1-NCBP2-bound mRNAs but also eIF4E-bound mRNAs. SMD does not require EJC for the target selection (15). To date, the best-characterized SMD target is ADP-ribosylation factor 1 (ARF1) mRNA, containing a 19-bp stem loop structure recognized by STAU1 (17). Plasminogen activator inhibitor 1 (SERPINE1) and paired box 2 (PAX2) mRNAs are also targeted by SMD (14). In contrast to NMD, SMD regulates the stability of mRNAs encoding functional protein, namely, regulates physiological transcripts (18). NMD and SMD share several features; both systems require translation process (7). UPF1 is also involved in SMD through the direct binding with STAU1 (17). Hence, UPF1 regulates physiological transcripts as well as NMD-targeted mRNAs.

Intriguingly, recent studies revealed that SMD and NMD pathways fight over UPF1. STAU1-binding domain within UPF1 is overlapped with UPF2, a core factor of NMD. siRNA-mediated knockdown of STAU1, which inhibits SMD, increases the NMD activity while siRNA-mediated knockdown of UPF2, which consequently inhibits NMD, increases SMD (64). Moreover, the differentiation of myoblasts to myotubes in the mouse skeletal C2C12 cells is associated with the decreased contribution of SMD and the increased contribution of NMD. For example, the mRNA expression level of SMD targets such as JUN or SERPINE1 are decreased upon differentiation while those of NMD targets such as BAG1 or TGM2 are increased (64). The competition of SMD and NMD also contributes to the differentiation process. PAX3 mRNA, which inhibits myogenic differentiation, is an SMD target while myogenin mRNA, which encodes a protein required for myogenesis, is a UPF2-dependent NMD target (64). Thus, the interaction between SMD and NMD pathways forms an important gene expression network, where UPF1 plays a central role.

5. Replication-dependent histone mRNA decay

Histone proteins are essential components of chromosomes. In mammalian cells, the regulation of histone proteins is coupled to the rate of DNA replication. Replication-dependent histone genes encode the core histones (H2A, H2B, H3, and H4) and the

linker histones (H1). The expression of histone mRNAs increases when cells progress G1 to S phase of the cell cycle, and these mRNAs rapidly decrease at the end of S phase. Regulation of histone mRNA levels contributes for the coordination between DNA replication and chromatin assembly during S phase to ensure the proper replication of chromatin structure (65,66). The rapid destabilization of mRNA mainly contributes to rapidly reduce the mRNA level. Therefore, rapid degradation of histone mRNAs plays a crucial role in a main regulatory step to ensure proper histone mRNA levels at the end of S phase. Transcripts encoding histone proteins lack polyadenylated tails, although they are transcribed by RNA polymerase II (19). This conjures up an image of presence of special mechanism for the regulation of histone mRNA stabilities. Actually, 3' UTRs of replication-dependent histone mRNAs harbor the special stem-loop structure that is required for rapid regulatory degradation of histone mRNAs (19,66). The structure at the 3' end of histone mRNA interacts with the stem-loop binding proteins (SLBP) (65,66). UPF1 plays a crucial role in histone mRNA degradation through an interaction with SLBP at the end of S phase or after the inhibition of DNA synthesis (19). Moreover, the function of UPF1 in histone mRNA degradation is regulated by phosphorylation (19,67). The serine/glutamine motifs (SQ motifs) and threonine/glutamine motifs (TQ motifs) of UPF1 are phosphorylated by phosphatidylinositol 3-kinase-related protein kinase (PIKK) family (11). The phosphorylation of UPF1 triggers histone mRNA degradation (19,67).

Ataxia telangiectasia mutated (ATM) and DNA-dependent protein kinase (DNA-PK) are mainly activated by double-strand breaks (DSBs) generated by ionizing radiation. Ataxia telangiectasia and Rad3 related (ATR) is by single stranded DNA and stalled replication forks generated by UV light, replication block, and hypoxia. ATR, DNA-PK, and ATM are other members of the PIKK family (68). Recent studies revealed that the phosphorylation activity of ATR and DNA-PK but not ATM is required for histone mRNA degradation after the inhibition of DNA synthesis (67).

6. S phase progression & DNA replication

Recent studies revealed that UPF1 physically interacts with DNA polymerase δ and is crucial to S phase progression and DNA replication in NMD-independent manner (20,69). It was found that 4% of UPF1 proteins were bound chromatin-associated protein fraction while UPF1 mostly exists in the soluble fraction. The amount of chromatin-associated UPF1 is low in M phase and early G1 phase, starts to increase in mid-G1, and is highest level in S phase. Depletion of UPF1 but not UPF2 results in an early S phase arrest and stalls replication fork progression (20,69). This inhibition of replication fork progression triggers ATR-

dependent DNA damage response and replication block (64,70). UPF1 may be involved in DNA damage response in S phase of the cell cycle. In support of the physiological importance of UPF1 in S phase, UPF1 depletion also induces the accumulation of nuclear foci containing a sensitive marker for DNA damage such as phosphorylated histone H2AX (γ -H2AX) (20,69). Moreover, chromatin-associated and phosphorylated UPF1 are reduced in cells depleted for ATR, while UPF1 accumulates on the chromatin in cells irradiated gamma-ray for induction of DNA damage (20,69). Those results suggest that gamma-ray irradiation triggers ATR-mediated phosphorylation and then chromatin-associated UPF1 is phosphorylated by active ATR. Furthermore, UPF1 interacts with the p66 subunit and p125 catalytic subunit of DNA polymerase δ . In contrast, UPF2 does not detectably interact with DNA polymerase δ . UPF1 may assist DNA polymerase δ to trigger replication fork progression or DNA repair in NMD-independent manner (20,69). Thus, UPF1 plays an important role in DNA replication and S phase progression through non-NMD pathway.

7. Telomere homeostasis

Telomeres are the heterochromatic structures located at the end of eukaryotic chromosomes. In mammal, telomeres consist of tandem arrays of duplex 5'-TTAGGG-3' repeats. The structure plays a crucial role in genome stability at the cellular level and contributes to tumor suppressors at the organismal level (71). There are a lot of proteins associated with telomeric DNA and these proteins are involved in telomere length regulation and telomere protection. The association of NMD factor with telomere function was previously reported. Mutations of UPF1, UPF2, and UPF3 shorten telomere length and reduced telomeric silencing in *Saccharomyces cerevisiae* (72,73). UPF mutant strains lead to increased mRNA levels of telomere-related proteins such as telomerase catalytic subunit (EST2), regulators of telomerase (EST1, EST3, STN1, and TEN1), and telomeric chromatin structure-related genes (SAS2 and ORC5) (73).

Telomeres originally are believed to be transcriptionally silent. However, recent studies revealed that telomeric repeats are transcribed by DNA-dependent RNA polymerase II into telomeric repeat-containing RNA (TERRA: also known as TelRNA) (72-74). TERRA is a long-noncoding RNA in animals and fungi, co-localizes with telomeres not only in interphase cells but also in transcriptionally inactive metaphase cells and blocks the activity of telomerase, a reverse transcriptase-like enzyme required for the maintenance of telomere length. Knockdown of *UPF1*, *SMG1* or *SMG6* leads to increase the number of telomere-associated TERRA foci on RNA fluorescence in situ hybridization (RNA-FISH). However, neither

the mRNA expression level nor the half-life of TERRA are not increased in cells depleted for UPF1 or SMG6 on northern blot (73,74). Thus, NMD factors including UPF1 may be not likely to be involved in the degradation of TERRA and be only required for the disassembly of TERRA and telomeres. Otherwise, there is the possibility that those NMD factors are involved in TERRA degradation locally at the telomere because the local change of TERRA mRNA level may be undetectable on northern blot.

8. HIV-1 genomic RNA stability

The stability of viral genomic RNA is crucial to a successful viral infection and proper replication within the cells. Therefore, viral RNAs have an ability to avoid RNA degradation by the host machinery. Interestingly, viruses have evolved mechanisms not only to escape the elimination by these decay pathways, but also to manipulate them for enhanced viral replication and gene expression (75).

The HIV-1 RNP consists of HIV-1 genomic RNA, pr55^{Gag} (the major structural protein), STAU1 (the host protein) (76,77). Recent study revealed that UPF1 is one of HIV-1 RNP components and is involved in HIV-1 genomic RNA stability (23). Knockdown of *UPF1* decreases the level of HIV-1 genomic RNA and pr55^{Gag} synthesis. Conversely, overexpression of UPF1 increases the level of HIV-1 genomic RNA and pr55^{Gag} synthesis (23). The effects of UPF1 on HIV-1 genomic RNA stability are dependent on ATPase domain of UPF1 but not the association of UPF1 with UPF2 (23). Thus, the association of UPF1 with HIV-1 genomic RNA is important for the stability of the virus RNA, and the effect may be on NMD-independent manner.

9. Conclusion

UPF1 was originally known as a central factor in NMD. As we have seen in this review, UPF1 is a multitasking entertainer to be involved in RNA surveillance, the regulation of physiological transcripts, DNA replication, S phase progression, telomere homeostasis, and HIV-1 metabolism (Figure 1). However, the overview of UPF1 is still unclear. It is hoped that future studies will uncover new insights into the complicated roles of UPF1.

References

1. Applequist SE, Selg M, Raman C, Jack HM. Cloning and characterization of HUPF1, a human homolog of the *Saccharomyces cerevisiae* nonsense mRNA reducing UPF1 protein. *Nucleic Acids Res.* 1997; 25:814-821.
2. Bhattacharya A, Czaplinski K, Trifillis P, He F, Jacobson A, Peltz SW. Characterization of the biochemical properties of the human Upf1 gene product that is involved in nonsense mediated mRNA decay. *RNA.*

- 2000; 6:1226-1235.
3. Chang YF, Imam JS, Wilkinson MF. The nonsense-mediated decay RNA surveillance pathway. *Annu Rev Biochem.* 2007; 76:51-74.
4. Nicholson P, Yepiskoposyan H, Metz S, Zamudio Orozco R, Kleinschmidt N, Muhlemann O. Nonsense-mediated mRNA decay in human cells: Mechanistic insights, functions beyond quality control and the double-life of NMD factors. *Cell Mol Life Sci.* 2010; 67:677-700.
5. Mendell JT, Sharifi NA, Meyers JL, Martinez-Murillo F, Dietz HC. Nonsense surveillance regulates expression of diverse classes of mammalian transcripts and mutes genomic noise. *Nat Genet.* 2004; 36:1073-1078.
6. Kadlec J, Guilligay D, Ravelli RB, Cusack S. Crystal structure of the UPF2-interacting domain of nonsense-mediated mRNA decay factor UPF1. *RNA.* 2006; 12:1817-1824.
7. Chamieh H, Ballut L, Bonneau F, Le Hir H. NMD factors UPF2 and UPF3 bridge UPF1 to the exon junction complex and stimulate its RNA helicase activity. *Nat Struct Mol Biol.* 2008; 15:85-93.
8. Czaplinski K, Ruiz-Echevarria MJ, Paushkin SV, Han X, Weng Y, Perlick HA, Dietz HC, Ter-Avanesyan MD, Peltz SW. The surveillance complex interacts with the translation release factors to enhance termination and degrade aberrant mRNAs. *Genes Dev.* 1998; 12:1665-1677.
9. Ivanov PV, Gehring NH, Kunz JB, Hentze MW, Kulozik AE. Interactions between UPF1, eRFs, PABP and the exon junction complex suggest an integrated model for mammalian NMD pathways. *EMBO J.* 2008; 27:736-747.
10. Denning G, Jamieson L, Maquat LE, Thompson EA, Fields AP. Cloning of a novel phosphatidylinositol kinase-related kinase: Characterization of the human SMG-1 RNA surveillance protein. *J Biol Chem.* 2001; 276:22709-22714.
11. Yamashita A, Ohnishi T, Kashima I, Taya Y, Ohno S. Human SMG-1, a novel phosphatidylinositol 3-kinase-related protein kinase, associates with components of the mRNA surveillance complex and is involved in the regulation of nonsense mediated mRNA decay. *Genes Dev.* 2001; 15:2215-2228.
12. Ohnishi T, Yamashita A, Kashima I, Schell T, Anders KR, Grimson A, Hachiya T, Hentze MW, Anderson P, Ohno S. Phosphorylation of hUPF1 induces formation of mRNA surveillance complexes containing hSMG-5 and hSMG-7. *Mol Cell.* 2003; 12:1187-1200.
13. Anders KR, Grimson A, Anderson P. SMG-5, required for *C.elegans* nonsense-mediated mRNA decay, associates with SMG-2 and protein phosphatase 2A. *EMBO J.* 2003; 22:641-650.
14. Chiu SY, Serin G, Ohara O, Maquat LE. Characterization of human Smg5/7a: A protein with similarities to *Caenorhabditis elegans* SMG5 and SMG7 that functions in the dephosphorylation of Upf1. *RNA.* 2003; 9:77-87.
15. Hosoda N, Kim YK, Lejeune F, Maquat LE. CBP80 promotes interaction of Upf1 with Upf2 during nonsense-mediated mRNA decay in mammalian cells. *Nature Struct Mol Biol.* 2005; 12:893-901.
16. Hwang J, Sato H, Tang Y, Matsuda D, Maquat LE. UPF1 association with the cap-binding protein, CBP80, promotes nonsense-mediated mRNA decay at two distinct steps. *Mol Cell.* 2010; 39:396-409.

17. Kim YK, Furic L, Desgroseillers L, Maquat LE. Mammalian Stauf1 recruits Upf1 to specific mRNA 3'UTRs so as to elicit mRNA decay. *Cell*. 2005; 120:195-208.
18. Kim YK, Furic L, Parisien M, Major F, DesGroseillers L, Maquat LE. Stauf1 regulates diverse classes of mammalian transcripts. *EMBO J*. 2007; 26:2670-2681.
19. Kaygun H, Marzluff WF. Regulated degradation of replication-dependent histone mRNAs requires both ATR and Upf1. *Nat Struct Mol Biol*. 2005; 12:794-800.
20. Azzalin CM, Lingner J. The human RNA surveillance factor UPF1 is required for S phase progression and genome stability. *Curr Biol*. 2006; 16:433-439.
21. Dahlseid JN, Lew-Smith J, Lelivelt MJ, Enomoto S, Ford A, Desruisseaux M, McClellan M, Lue N, Culbertson MR, Berman J. mRNAs encoding telomerase components and regulators are controlled by *UPF* genes in *Saccharomyces cerevisiae*. *Eukaryot Cell*. 2003; 2:134-142.
22. Lew JE, Enomoto S, Berman J. Telomere length regulation and telomeric chromatin require the nonsense-mediated mRNA decay pathway. *Mol Cell Biol*. 1998; 18:6121-6130.
23. Ajamian L, Abrahamyan L, Milev M, Ivanov PV, Kulozik AE, Gehring NH, Mouland AJ. Unexpected roles for UPF1 in HIV-1 RNA metabolism and translation. *RNA*. 2008; 14:914-927.
24. Leeds P, Peltz SW, Jacobson A, Culbertson MR. The product of the yeast *UPF1* gene is required for rapid turnover of mRNAs containing a premature translational termination codon. *Genes Dev*. 1991; 5:2303-2314.
25. Page MF, Carr B, Anders KR, Grimson A, Anderson P. SMG-2 is a phosphorylated protein required for mRNA surveillance in *Caenorhabditis elegans* and related to Upf1p of yeast. *Mol Cell Biol*. 1999; 19:5943-5951.
26. Culbertson MR, Leeds PF. Looking at mRNA decay pathways through the window of molecular evolution. *Curr Opin Genet Dev*. 2003; 13:207-214.
27. Avery P, Vicente-Crespo M, Francis D, Nashchekina O, Alonso CR, Palacios IM. *Drosophila* Upf1 and Upf2 loss of function inhibits cell growth and causes animal death in a Upf3-independent manner. *RNA*. 2011; 17:624-638.
28. Wittkopp N, Huntzinger E, Weiler C, Sauliere J, Schmidt S, Sonawane M, Izaurralde E. Nonsense-mediated mRNA decay effectors are essential for zebrafish embryonic development and survival. *Mol Cell Biol*. 2009; 29:3517-3528.
29. Medghalchi SM, Frischmeyer PA, Mendell JT, Kelly AG, Lawler AM, Dietz HC. Rent1, a trans-effector of nonsense-mediated mRNA decay, is essential for mammalian embryonic viability. *Hum Mol Genet*. 2001; 10:99-105.
30. Riehs-Kearman N, Gloggnitzer J, Dekrout B, Jonak C, Riha K. Aberrant growth and lethality of *Arabidopsis* deficient in nonsense-mediated RNA decay factors is caused by autoimmune-like response. *Nucleic Acids Res*. In press.
31. Hwang J, Maquat LE. Nonsense-mediated mRNA decay (NMD) in animal embryogenesis: To die or not to die, that is the question. *Curr Opin Genet Dev*. 2011; 21:422-430.
32. Schoenberg DR, Maquat LE. Regulation of cytoplasmic mRNA decay. *Nat Rev Genet*. 2012; 13:246-259.
33. Tani H, Mizutani R, Salam KA, Tano K, Ijiri K, Wakamatsu A, Isogai T, Suzuki Y, Akimitsu N. Genome-wide determination of RNA stability reveals hundreds of short-lived noncoding transcripts in mammals. *Genome Res*. 2012; 22:947-956.
34. Keene JD. Mini review: Global regulation and dynamics of ribonucleic acid. *Endocrinology*. 2010; 151:1391-1397.
35. Akimitsu N. Messenger RNA surveillance systems monitoring proper translation termination. *J Biochem*. 2008; 143:1-8.
36. Lewis BP, Green RE, Brenner SE. Evidence for the widespread coupling of alternative splicing and nonsense-mediated mRNA decay in humans. *Proc Natl Acad Sci U S A*. 2003; 7:189-192.
37. Holbrook JA, Neu-Yilik G, Hentze MW, Kulozik AE. Nonsense-mediated decay approaches the clinic. *Nat Genet*. 2004; 36:801-808.
38. Bhuvanagiri M, Schlitter AM, Hentze MW, Kulozik AE. NMD: RNA biology meets human genetic medicine. *Biochem J*. 2010; 430:365-377.
39. Lelivelt MJ, Culbertson MR. Yeast Upf proteins required for RNA surveillance affect global expression of the yeast transcriptome. *Mol Cell Biol*. 1999; 19:6710-6719.
40. He F, Li X, Spatrick P, Casillo R, Dong S, Jacobson A. Genome-wide analysis of mRNAs regulated by the nonsense-mediated and 5' to 3' mRNA decay pathways in yeast. *Mol Cell*. 2003; 12:1439-1452.
41. Guan Q, Zheng W, Tang S, Liu X, Zinkel RA, Tsui KW, Yandell BS, Culbertson MR. Impact of nonsense-mediated mRNA decay on the global expression profile of budding yeast. *PLoS Genet*. 2006; 2:e203.
42. Ramani AK, Nelson AC, Kapranov P, Bell I, Gingeras TR, Fraser AG. High resolution transcriptome maps for wild-type and nonsense-mediated decay-defective *Caenorhabditis elegans*. *Genome Biol*. 2009; 10:R101.
43. Rehwinkel J, Letunic I, Raes J, Bork P, Izaurralde E. Nonsense-mediated mRNA decay factors act in concert to regulate common mRNA targets. *RNA*. 2005; 11:1530-1544.
44. Hori K, Watanabe Y. UPF3 suppresses aberrant spliced mRNA in *Arabidopsis*. *Plant J*. 2005; 43:530-540.
45. Yoine M, Nishii T, Nakamura K. Arabidopsis UPF1 RNA helicase for nonsense-mediated mRNA decay is involved in seed size control and is essential for growth. *Plant Cell Physiol*. 2006; 47:572-580.
46. Kurihara Y, Matsui A, Hanada K, Kawashima M, Ishida J, Morosawa T, Tanaka M, Kaminuma E, Mochizuki Y, Matsushima A, Toyoda T, Shinozaki K, Seki M. Genome-wide suppression of aberrant mRNA-like noncoding RNAs by NMD in *Arabidopsis*. *Proc Natl Acad Sci U S A*. 2009; 106:2453-2458.
47. Wittmann J, Hol EM, Jack HM. hUPF2 silencing identifies physiologic substrates of mammalian nonsense-mediated mRNA decay. *Mol Cell Biol*. 2006; 26:1272-1287.
48. Rebbapragada I, Lykke-Andersen J. Execution of nonsense-mediated mRNA decay: What defines a substrate? *Curr Opin Cell Biol*. 2009; 21:394-402.
49. Perlick HA, Medghalchi SM, Spencer FA, Kendzior RJ Jr, Dietz HC. Mammalian orthologues of a yeast regulator of nonsense transcript stability. *Proc Natl Acad Sci U S A*. 1996; 93:10928-10932.
50. Ishigaki Y, Li X, Serin G, Maquat LE. Evidence for a pioneer round of mRNA translation: mRNAs subject to nonsense-mediated decay in mammalian cells are bound by CBP80 and CBP20. *Cell*. 2001; 106:607-617.
51. Kashima I, Yamashita A, Izumi N, Kataoka N, Morishita R, Hoshino S, Ohno M, Dreyfuss G, Ohno S. Binding of

- a novel SMG-1-Upfl-eRF1-eRF3 complex (SURF) to the exon junction complex triggers Upfl phosphorylation and nonsense-mediated mRNA decay. *Genes Dev.* 2006; 20:355-367.
52. Le Hir H, Izaurralde E, Maquat LE, Moore MJ. The spliceosome deposits multiple proteins 20-24 nucleotides upstream of mRNA exon-exon junctions. *EMBO J.* 2000; 19:6860-6869.
 53. Cho H, Kim KM, Kim YK. Human proline-rich nuclear receptor coregulatory protein 2 mediates an interaction between mRNA surveillance machinery and decapping complex. *Mol Cell.* 2009; 33:75-86.
 54. Isken O, Kim YK, Hosoda N, Mayeur GL, Hershey JW, Maquat LE. Upfl phosphorylation triggers translational repression during nonsense-mediated mRNA decay. *Cell.* 2008; 133:314-327.
 55. Eberle AB, Lykke-Andersen S, Muhlemann O, Jensen TH. SMG6 promotes endonucleolytic cleavage of nonsense mRNA in human cells. *Nat Struct Mol Biol.* 2009; 16:49-55.
 56. Huntzinger E, Kashima I, Fauser M, Sauliere J, Izaurralde E. SMG6 is the catalytic endonuclease that cleaves mRNAs containing nonsense codons in metazoan. *RNA.* 2008; 14:2609-2617.
 57. Unterholzner L, Izaurralde E. SMG7 acts as a molecular link between mRNA surveillance and mRNA decay. *Mol Cell.* 2004; 16:587-596.
 58. Okada-Katsuhata Y, Yamashita A, Kutsuzawa K, Izumi N, Hirahara F, Ohno S. N- and C-terminal Upfl phosphorylations create binding platforms for SMG-6 and SMG-5:SMG-7 during NMD. *Nucleic Acids Res.* 2012; 40:1251-1266.
 59. Muhlemann O, Lykke-Andersen J. How and where are nonsense mRNAs degraded in mammalian cells? *RNA Biol.* 2010; 7:28-32.
 60. Franks TM, Singh G, Lykke-Andersen J. Upfl ATPase-dependent mRNP disassembly is required for completion of nonsense-mediated mRNA decay. *Cell.* 2010; 143:938-950.
 61. Roegiers F, Jan YN. Staufen: A common component of mRNA transport in oocytes and neurons? *Trends Cell Biol.* 2000; 10:220-224.
 62. Furic L, Maher-Laporte M, DesGroseillers L. A genome-wide approach identifies distinct but overlapping subsets of cellular mRNAs associated with Staufen1- and Staufen2-containing ribonucleoprotein complexes. *RNA.* 2008; 14:324-335.
 63. Gong C, Maquat LE. IncRNAs transactivate Staufen1-mediated mRNA decay by duplexing with 3' UTRs via Alu elements. *Nature.* 2011; 470:284-288.
 64. Gong C, Kim YK, Woeller CF, Tang Y, Maquat LE. SMD and NMD are competitive pathways that contribute to myogenesis: Effects on PAX3 and myogenin mRNAs. *Genes Dev.* 2009; 23:54-66.
 65. Marzluff WF. Metazoan replication-dependent histone mRNAs: A unique set of RNA polymerase II transcripts. *Curr Opin Cell Biol.* 2005; 17:274-280.
 66. Marzluff WF, Wagner EJ, Duronio RJ. Metabolism and regulation of canonical histone mRNAs: Life without a poly (A) tail. *Nat Rev Genet.* 2008; 9:843-854.
 67. Muller B, Blackburn J, Feijoo C, Zhao X, Smythe C. DNA-activated protein kinase functions in a newly observed S phase checkpoint that links histone mRNA abundance with DNA replication. *J Cell Biol.* 2007; 179:1385-1398.
 68. Branzei D, Foiani M. Regulation of DNA repair throughout the cell cycle. *Nat Rev Mol Cell Biol.* 2008; 9:297-308.
 69. Azzalin CM, Lingner J. The double life of UPF1 in RNA and DNA stability pathways. *Cell Cycle.* 2006; 5:1496-1498.
 70. Branzei D, Foiani M. Maintaining genome stability at the replication fork. *Nature Rev Mol Cell Biol.* 2010; 11:208-219.
 71. O' Sullivan RJ, Karlseder J. Telomeres: Protecting chromosomes against genome instability. *Nat Rev Mol Cell Biol.* 2010; 11:171-181.
 72. Schoeftner S, Blasco MA. Developmentally regulated transcription of mammalian telomeres by DNA-dependent RNA polymerase II. *Nat Cell Biol.* 2008; 10:228-236.
 73. Azzalin CM, Reichenbach P, Khoriauli L, Giulotto E, Lingner J. Telomeric repeat containing RNA and RNA surveillance factors at mammalian chromosome ends. *Science.* 2007; 318:798-801.
 74. Luke B, Lingner J. TERRA: Telomeric repeat-containing RNA. *EMBO J.* 2009; 28:2503-2510.
 75. Gaglia MM, Glaunsinger BA. Viruses and the cellular RNA decay machinery. *Wiley Interdiscip Rev RNA.* 2010; 1:47-59.
 76. Moulant AJ, Mercier J, Luo M, Bernier L, DesGroseillers L, Cohen EA. The double-stranded RNA-binding protein staufen is incorporated in human immunodeficiency virus type1: Evidence for a role in genomic RNA encapsidation. *J Virol.* 2000; 74:5441-5451.
 77. Chatel-Chaix L, Clement JF, Martel C, Beriault V, Gatignol A, DesGroseillers L, Moulant AJ. Identification of Staufen in the human immunodeficiency virus type 1 Gag ribonucleoprotein complex and a role in generating infectious viral particles. *Mol Cell Biol.* 2004; 24:2637-2648.

(Received April 3, 2012; Accepted April 21, 2012)

A facile method for the synthesis of *N*-(α -aminoacyl) sulfonamides

Shaolei Wu, Minglu Chen, Yutao Wang, Xuben Hou, Xinying Yang, Li Su, Hao Fang*

School of Pharmacy, Shandong University, Ji'nan, Shandong, China.

ABSTRACT: *N*-Acylsulfonamide derivatives have important applications in organic synthesis and drug discovery. It was found that many problems occurred preparing amino acid derived *N*-acylsulfonamides with the commonly used coupling approach in our previous studies. In this paper, we report an efficient approach to synthesize various amino acids derived *N*-acylsulfonamides in high yields without any racemization.

Keywords: Synthesis, amino acid-derived *N*-acylsulfonamides, the mixed anhydride method

1. Introduction

Currently, *N*-acylsulfonamide derivatives are used in various applications in organic chemistry and medicinal chemistry. According to the literature, *N*-acylsulfonamide derivatives can assist tandem C-H olefination for the synthesis of isoindolinones (1), and act as safety-catch linkers for the solid phase synthesis of peptide (2) and hyaluronic acid oligosaccharides (3). In addition, proline-derived *N*-sulfonylcarboxamides have been reported to be good chiral catalysts for asymmetric mannich reactions and anti-aldol reactions (4-7). For biological applications, *N*-acylsulfonamide derivatives not only can be used as therapeutic agents for Alzheimer's disease (8), but also can act as RNase A inhibitors (9), prostaglandin E receptor 3 (EP3) receptor antagonists (10), prostacyclin receptor agonists (11), HCV NS5B polymerase allosteric inhibitors (12), and HCV NS3 protease inhibitors. In a recent study, *N*-acylsulfonamide structures have been regarded as good moieties for Bcl-2 inhibitors. For example, ABT-737 has been confirmed as a potent Bcl-2 inhibitor for cancer treatment (13).

Recently, many efforts have been devoted to the synthesis of *N*-acylsulfonamides derivatives. Generally speaking, sulfonamide is the commonly

used starting material which reacts with different acylating reagents, such as acyl chlorides (3), anhydrides (14), *N*-acyl benzotriazoles (15), and coupling reagents for peptide synthesis (e.g. 1-ethyl-3-(3-dimethylaminopropyl)carbodiimide hydrochloride (EDCI), dicyclohexylcarbodiimide (DCC), and carbonyl diimidazole) (16,17). On the other hand, *N*-acylsulfonamides can also be accessed through the reaction of amides and sulfonyl chlorides (18). All the methods mentioned above have their advantages, but some problems and inconveniences still occur during the process, such as long reaction time, and low product yield (19). Recently, a palladium-catalyzed amidocarbonylation protocol was disclosed producing *N*-acylsulfonamides in excellent yields when Mo(CO)₆ was employed as a carbon monoxide source (20). The reaction was efficient; however, the high-density microwave heating conditions necessary limit functional compatibility and potential substrate scope. Moreover, Williams documented that *N*-acylsulfonamides can be obtained from carboxylic acids through thio acid/azide amidation, which is highly compatible with acid- and base-sensitive amino acid protection (21). However, sulfonylazides are not easy to handle, and the method might have problems with large-scale manipulation. Therefore, development of a mild, simple, efficient and atom-economical method for synthesis of *N*-acylsulfonamides is still a worthwhile project.

In our recent studies, the phenylalanine derived *N*-acylsulfonamide lead compound, WL-276, was investigated as a Bcl-2 inhibitor to overcome drug resistance and suppress prostate tumor growth (22,23). However, low yield, a long reaction time (more than 48 h) and racemization give us problems when EDCI and related coupling reagents were used for synthesis of *N*-acylsulfonamides. To overcome these problems, we developed a convenient and facile method for preparing amino acids derived *N*-acylsulfonamides using a modified mixed anhydride method without product racemization.

2. Materials and Methods

2.1. General methods

Solvents were reagent grade and purified and dried using standard methods when necessary. All melting

*Address correspondence to:

Dr. Hao Fang, School of Pharmacy, Shandong University, No. 44, Wenhuxi Road, Ji'nan 250012, Shandong, China.
e-mail: haofangcn@sdu.edu.cn

points were determined on a micromelting point apparatus (are uncorrected). $^1\text{H-NMR}$ and $^{13}\text{C-NMR}$ spectra were obtained on a Bruker Avance-300 in the indicated solvent. Chemical shifts are expressed in delta (δ) units with tetramethyl-silane (TMS) as the internal reference. Electrospray ionization-mass spectrometry (ESI-MS) was determined on an API 4000 spectrometer. All reactions were monitored using thin-layer chromatography (TLC) on 0.25 mm silica gel plates (60GF-254) and visualized with UV light. Flash column chromatography was performed on a column packed with silica gel 60 (200-300 mesh). Concentration of reaction solutions involved use of a rotary evaporator at reduced pressure. Specific rotation was determined on Modular Circular Polarimeter (MCP200). Enantiomeric excess analysis by HPLC used a Shimidazol LC-10Avp UV detector.

2.2. General procedure for the preparation of amino acid-derived *N*-acylsulfonamides

In our initial studies, the reaction of *N*^α-protected phenylalanine and benzenesulfonamide (1:1.1, molar ratios) was selected as the model to test the mixed anhydride method (24). However, no desired product was observed and all the starting materials were recovered. We believed that the possible reason for this phenomenon is the weak nucleophilicity of the sulfonamide. Therefore, different bases such as sodium hydroxide, sodium ethoxide and sodium hydride, were tested to deprotonate the sulfonamide so as to increase the nucleophilicity of the sulfonamide. The method is described as followed (Figure 1): First, to a solution of NaH or EtONa (2.5 eq) in anhydrous tetrahydrofuran (THF) (10 mL) benzenesulfonamide **3** was added at 0°C, and the mixture stirred at 0°C for 30 min and at room temperature for 3-4 h (with NaOH as base we needed 12 h) to give benzenesulfonamide sodium salt **3'**. Second, to a solution of *N*^α-protected phenylalanine I(1 eq) in 10 mL anhydrous THF *N*-methyl morpholine (NMM) (1.1 eq) was added at -20°C. Ten min later, isobutylchloroformate (1.1 eq) was added. After another 45 min, the mixture was added to a solution of **3'**, the reaction was allowed to warm to room temperature gradually, and stirred for

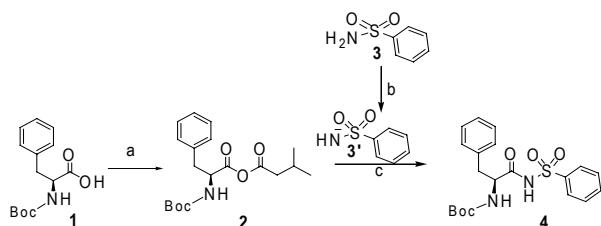


Figure 1. Synthesis of product 4. (a): i) **1**, NMM, THF, -20°C, 10 min; ii) isobutylchloroformate, 45 min. (b): i) **3** (1 eq), base (2.5 eq), THF, 0°C, 30 min; ii) rt, 3-4 h. (c): 0°C, 30 min, and then rose to room temperature, 5-8 h.

5-8 h. After removal of the solvent, ethyl acetate was added and the mixture was washed successively with 1 M citric acid, then brine, and dried over MgSO_4 . After removal of the solvent, the crude mixture was purified by recrystallization with ethanol or flash chromatography (petroleum ether/ethyl acetate, 5:1) to give the pure products **4**.

3. Results and Discussion

The results suggest that sodium hydride should be the best base to give excellent isolated yield (98%) and shortest time (Table 1). On the other hand, EtONa also afforded a good yield (87%), but the reaction time is over 16 h; sodium hydroxide did not work in this reaction. Therefore, sodium hydride was selected as the optimal base for further investigations.

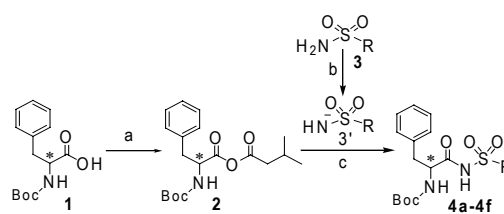
The enantiomeric excess of (*S*)-**4** and (*R*)-**4** prepared with our modified mixed anhydride method (compound **4a** and **4b** in Table 2) were determined by HPLC on a Chiralpak IA column (Figure 2). Both of them gave a > 99% enantiomeric excess analysis, which demonstrated that our method could effectively overcome the problem of racemization when using EDCI and related coupling reagents.

Table 1. The reaction of *N*^α-protected phenylalanine with benzenesulfonamide

Entry	Base	Time (h)	Isolated yield (%) of 4
1	None	16	0
2	NaOH	16	0
3	EtONa	16	87
4	NaH	6	98

Table 2. The reaction of *N*^α-protected phenylalanine with substituted benzenesulfonamides or alkylsulfonamide

Entry	Configuration of the amino acid 1	R	Base	Product	Isolated yield (%)
1	<i>S</i>	Phenyl	NaH	4a	98
2	<i>R</i>	Phenyl	NaH	4b	98
3	<i>S</i>	4-Nitrophenyl	NaH	4c	96
4	<i>S</i>	3-Chloro-4-nitro-phenyl	NaH	4d	97
5	<i>S</i>	4-Chloro-phenyl	NaH	4e	94
6	<i>S</i>	Methyl	NaH	4f	97



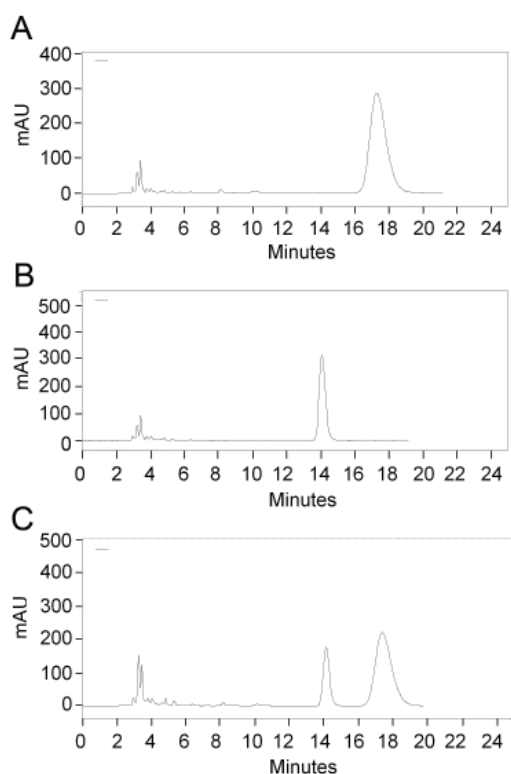
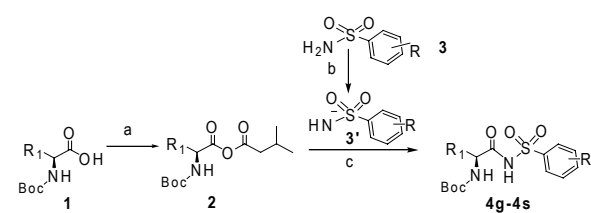


Figure 2. HPLC trace of **4a** and **4b**. Condition: Chiralpak IA 4.6 × 150 mm; mobile phase: 100/30 hexane/isopropyl alcohol (containing 0.05% trifluoroacetic acid) detection at 230 nm, flow rate: 1.0 mL/min. (A): Compound **4a** with *S* configuration; (B): Compound **4b** with *R* configuration; (C): mixture of compound **4a** and **4b**.

Various benzenesulfonamides and alkylsulfonamide were further examined to react with different *N^α*-protected phenylalanine, and the results are summarized in Table 2. Generally speaking, excellent yields (94-98%) were obtained. Our improved mixed anhydride method shows many advantages such as cheap reagents, easy and safe operation, and is suitable for amino acid substrates.

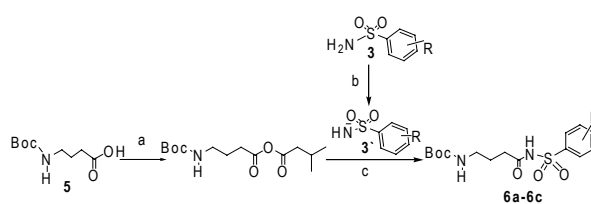
To demonstrate the generality of this approach, a broad range of *N^α*-protected amino acids were chosen to explore the scope of this reaction (Table 3). In general, good to excellent (73-98%) yields were obtained not only for the selected *N^α*-protected amino acids substrates, but also for substituted benzenesulfonamides. According to the results, the electron withdraw group (EWG) substituents on the phenyl ring of benzenesulfonamides also gave good isolated yields (e.g. entries 2, 3, 5, and 6). On the other hand, Boc-protected gamma-aminobutanoic acid was used to react with different substituted benzenesulfonamides in our studies. The results demonstrate that good isolated yield can be achieved through our procedures (Table 4).

Table 3. Synthesis of *N*-(*N^α*-protected aminoacyl) sulfonamides



Entry	R	R ₁	Products	Isolated Yield %
1	H		4g	90
2	4-Nitro		4h	96
3	3-Chloro-4-nitro		4i	85
4	H		4j	97
5	4-Nitro		4k	87
6	3-Chloro-4-nitro		4l	98
7	H		4m	91
8	4-Nitro		4n	88
9	3-Chloro-4-nitro		4o	84
10	H	H	4p	92
11	4-Nitro	H	4q	90
12	3-Chloro-4-nitro	H	4r	81
13	H	CH ₃ -	4s	73

Table 4. The reaction of *N*-protected γ -amino acid with benzenesulfonamide



Entry	R	Products	Isolated yield(%) of 4
1	H	6a	80
2	4-Nitro	6b	85
3	3-Chloro-4-nitro	6c	79

4. Conclusion

In summary, a modified mixed anhydride method was developed for preparation of amino acids derived *N*-(α -aminoacyl) sulfonamides. This method shows the advantages of efficiency, convenience and economics, which could overcome problems of low yields, long reaction time and racemization when using common coupling methodology. This would greatly help the organic chemists and medicinal chemists to prepare more bioactive compounds in the future.

Acknowledgements

This work was supported by National Natural Foundation Research Grant (Grant No. 30728031, No. 21172133, and No. 20602023), Natural Science Foundation for Young Scholars of Shandong Province (2006BS03021) and Scientific Research Foundation for the Returned Overseas Chinese Scholars, State Education Ministry.

References

- Zhu C, Falck JR. *N*-Acylsulfonamide assisted tandem C-H Olefination/Annulation: Synthesis of isoindolinones. *Org Lett*. 2011; 13:1214-1217.
- Ellman JA, Backes BJ. An alkanesulfonamide "safety-catch" linker for solid-phase synthesis. *J Org Chem*. 1999; 64:2322-2330.
- Massah AR, Azadi D, Aliyan H, Momeni AR, Naghash HJ, Kazemi F. An efficient method for the synthesis of *N*-acylsulfonamides: One-Pot sulfonylation and acylation of primary arylamines under solvent-free conditions. *Monatsh Chem*. 2008; 139:233-240.
- Nakamura S, Hara N, Nakashima H, Kubo K, Shibata N, Toru T. Enantioselective synthesis of (*R*)-convolutamydin A with new *N*-heteroarylsulfonylprolin amides. *Chemistry*. 2008; 14:8079-8081.
- Wu Y, Zhang Y, Yu M, Zhao G, Wang S. Highly efficient and reusable dendritic catalysts derived from *N*-prolylsulfonamide for the asymmetric direct aldol reaction in water. *Org Lett*. 2006; 8:4417-4420.
- Chowdari NS, Ahmad M, Albertshofer K, Tanaka F, Barbas CF 3rd. Expedient synthesis of chiral 1, 2- and 1, 4-diamines: Protecting group dependent regioselectivity in direct organocatalytic asymmetric Mannich reactions. *Org Lett*. 2006; 8:2839-2842.
- Yang H, Carter RG. Development of an enantioselective route toward the lycopodium alkaloids: Total synthesis of lycopodine. *J Org Chem*. 2010; 75:4929-4938.
- Hasegawa T, Yamamoto H. A practical synthesis of optically active (*R*)-2-propyloctanoic acid: Therapeutic agent for Alzheimer's disease. *Bull Chem Soc Jpn*. 2000; 73:423-428.
- Thiyagarajan N, Smith BD, Raines RT, Acharya KR. Functional and structural analyses of *N*-acylsulfonamide-linked dinucleoside inhibitors of RNase A. *FEBS J*. 2011; 278:541-549.
- Asada M, Obitsu T, Kinoshita A, Nakai Y, Nagase T, Sugimoto I, Tanaka M, Takizawa H, Yoshikawa K, Sato K, Narita M, Ohuchida S, Nakai H, Toda M. Discovery of novel *N*-acylsulfonamide analogs as potent and selective EP3 receptor antagonists. *Bioorg Med Chem Lett*. 2010; 20:2639-2643.
- Nakamura A, Yamada T, Asaki T. Synthesis and evaluation of *N*-acylsulfonamide and *N*-acylsulfonylurea prodrugs of a prostacyclin receptor agonist. *Bioorg Med Chem*. 2007; 15:7720-7725.
- Lampa A, Ehrenberg AE, Gustafsson SS, Vema A, Kerblom E, Lindeberg G, Karlén A, Danielson UH, Sandström A. Improved P2 phenylglycine-based hepatitis C virus NS3 protease inhibitors with alkenylic prime-side substituents. *Bioorg Med Chem*. 2010; 18:5413-5424.
- Kang MH, Reynolds CP. Bcl-2 inhibitors: Targeting mitochondrial apoptotic pathways in cancer therapy. *Clin Cancer Res*. 2009; 15:1126-1132.
- Singh DU, Singh PR, Samant SD. Fe-exchanged montmorillonite K10 – the first heterogeneous catalyst for acylation of sulfonamides with carboxylic acid anhydrides. *Tetrahedron Lett*. 2004; 45:4805-4807.
- Katritzky AR, Hoffmann S, Suzuki K. *N*-Acylation of sulfonamides using *N*-acylbenzotriazoles. *Arkivoc*. 2004(xii):14-22.
- Banwell MG, Crasto CF, Easton CJ, Forrest AK, Karoli T, March DR, Mensah L, Nairn MR, O'Hanlon PJ, Oldham MD, Yue W. Analogues of SB-203207 as inhibitors of tRNA synthetases. *Bioorg Med Chem Lett*. 2000; 10:2263-2266.
- Wang Y, Soper DL, Dirr MJ, deLong MA, De B, Wos JA. The synthesis and human FP receptor binding affinity of 13, 14-dihydro prostaglandin F1 α sulfonamides: Potential treatments for osteoporosis. *Chem Pharm Bull*. 2000; 48:1332-1337.
- Ellis D. Racemisation-free synthesis of chiral acylsulfonamides. *Tetrahedron Asymm*. 2001; 12:1589-1593.
- Johnson DC II, Widlanski TS. Facile synthesis of 5'-(*N*-acyl sulfonamide) derivatized nucleosides. *Tetrahedron Lett*. 2001; 42:3677-3679.
- Wu X, Ronn R, Gossas T, Larhed M. Easy-to-execute carbonylations: Microwave synthesis of acyl sulfonamides using Mo(CO)₆ as a solid carbon monoxide source. *J Org Chem*. 2005; 70:3094-3098.
- Barlett KN, Kolakowski RV, Katukojvala S, Williams LJ. Thio acid/azide amidation: An improved route to *N*-acyl sulfonamides. *Org Lett*. 2006; 8:823-826.
- Wang L, Sloper DT, Addo SN, Tian D, Slaton JW, Xing C. WL-276, an Antagonist against Bcl-2 proteins, overcomes drug resistance and suppresses prostate tumor growth. *Cancer Res*. 2008; 68:4377-4383.
- Xiao G, Fang H, Xing C, Xu W. Structure, function and inhibition of Bcl-2 family proteins: A new target for anti-tumor agents. *Mini Rev Med Chem*. 2009; 9:1596-1604.
- Valeur E, Bradley M. Amide bond formation: Beyond the myth of coupling reagents. *Chem Soc Rev*. 2009; 38:606-631.

(Received March 13, 2012; Revised April 16, 2012; Accepted April 16, 2012)

Appendix

Synthesis of *N*-acylsulfonamide derivatives **4a-4s**, **6a-6c**

(*S*)-*Tert*-butyl (1-oxo-3-phenyl-1-(phenylsulfonamido)propan-2-yl) carbamate (**4a**)

Yield: 98%. $[\alpha]_D^{20} = 8.6$ ($c = 0.50$, CH₃OH). ¹H-NMR (300 MHz, CDCl₃): δ (ppm) = 9.34 (s, 1H), 8.04-8.06 (d, $J = 7.5$ Hz, 2H), 7.57-7.66 (tt, 1H), 7.52-7.57 (dt, 2H), 7.04-7.23 (3H), 7.02-7.04 (2H), 4.90 (s, 1H), 4.31 (s, 1H), 3.02-3.08 (dd, $J = 14.1$ Hz, 6.3 Hz, 1H), 2.89-2.97 (dd, 1H), 1.38 (s, 9H). ¹³C-NMR (300 MHz, CDCl₃): $\delta = 169.5, 155.7, 138.4, 135.3, 134.0, 129.2, 128.9, 128.5, 127.3, 81.5, 55.9, 36.9, 28.1$. HRMS (ESI): calcd. for C₂₀H₂₃N₂O₅S⁻ 403.1333, found 403.1311 [M - H]. Melting point: 133-135°C.

(*R*)-*Tert*-butyl (1-oxo-3-phenyl-1-(phenylsulfonamido)propan-2-yl) carbamate (**4b**)

Yield: 98%. $[\alpha]_D^{20} = -8.6$ ($c = 0.50$, CH₃OH). ¹H-NMR (300 MHz, CDCl₃): δ (ppm) = 9.23 (s, 1H), 8.04-8.06 (d, $J = 7.5$ Hz, 2H), 7.64-7.69 (tt, 1H), 7.53-7.61 (dt, 2H), 7.22-7.24 (3H), 7.03-7.06 (2H), 4.83-1.85 (d, 1H), 4.29 (s, 1H), 3.02-3.09 (dd, $J = 14.1$ Hz, 6.3 Hz, 1H), 2.91-2.98 (dd, $J = 14.1$ Hz, 7.5 Hz, 1H), 1.38 (s, 9H). ¹³C-NMR (300 MHz, CDCl₃): $\delta = 169.5, 155.8, 138.5, 135.3, 133.9, 129.2, 128.9, 128.5, 127.3, 81.5, 56.1, 36.9, 28.1$. HRMS (ESI): calcd. for C₂₀H₂₃N₂O₅S⁻ 403.1333, found 403.1311 [M - H]. Melting point: 133-135°C.

(*S*)-*Tert*-butyl(1-(4-nitrophenylsulfonamido)-1-oxo-3-phenylpropan-2-yl) carbamate (**4c**)

Yield: 96%. $[\alpha]_D^{20} = 8.2$ ($c = 0.50$, CH₃OH). ¹H-NMR (300 MHz, CDCl₃): δ (ppm) = 9.57 (s, 1H), 8.35-8.38 (d, $J = 8.7$ Hz, 1H), 8.22-8.24 (d, $J = 8.7$ Hz, 1H), 7.25-7.26 (3H), 7.06-7.07 (2H), 4.84-4.86 (d, $J = 6.9$ Hz, 1H), 4.24-4.26 (q, 1H), 3.04-3.108 (dd, $J = 14.1$ Hz, 6.3 Hz, 1H), 2.93-2.99 (dd, $J = 14.1$ Hz, 7.8 Hz, 1H), 1.40 (s, 9H). ¹³C-NMR (300 MHz, CDCl₃): $\delta = 169.6, 156.1, 150.8, 143.9, 135.0, 129.9, 129.1, 128.9, 127.46, 124.0, 82.0, 56.2, 36.5, 28.1$. HRMS (ESI): calcd. for C₂₀H₂₂N₃O₇S⁻ 4483.1184, found 448.1314 [M - H]. Melting point: 244-245°C.

(*S*)-*Tert*-butyl(1-(4-chloro-3-nitrophenylsulfonamido)-1-oxo-3-phenylpropan-2-yl)carbonate (**4d**)

Yield: 97%. $[\alpha]_D^{20} = 12.8$ ($c = 0.50$, CH₃OH). ¹H-NMR (300 MHz, CDCl₃): δ (ppm) = 9.50 (s, 1H), 8.48-8.49 (d, $J = 2.1$ Hz, 1H), 8.18-8.21 (dd, $J = 8.4$ Hz, 2.1 Hz,) 7.72-7.75 (d, $J = 8.4$ Hz, 1H), 7.26 (3H), 7.07-7.10 (2H), 4.80-4.82 (d, $J = 6.6$ Hz, 1H), 4.20-4.27 (q, 1H), 3.04-3.11 (dd, $J = 14.1$ Hz, 6.3 Hz, 1H), 2.93-2.99 (dd, $J = 14.1$ Hz, 7.8 Hz, 1H), 1.40 (s, 9H). ¹³C-NMR (300

MHz, CDCl₃): $\delta = 169.5, 156, 147.7, 138.3, 135.0, 133.1, 132.7, 129.1, 129.0, 127.5, 125.8, 82.2, 56.4, 36.3, 28.1$. HRMS (ESI): calcd. for C₂₀H₂₁ClN₃O₇S⁻ 482.0794, found 482.0977 [M - H]. Melting point: 147-150°C.

(*S*)-*Tert*-butyl(1-(4-chlorophenylsulfonamido)-1-oxo-3-phenylpropan-2-yl) carbamate (**4e**)

Yield: 94%. $[\alpha]_D^{20} = 6.8$ ($c = 0.50$, CH₃OH). ¹H-NMR (300 MHz, CDCl₃): δ (ppm) = 9.55 (s, 1H), 7.95-7.98 (d, $J = 8.7$ Hz, 2H), 7.49-7.52 (d, $J = 8.7$ Hz, 2H), 7.22-7.23 (3H), 7.02-7.04 (2H), 4.96 (s, 1H), 4.32 (1H), 3.01-3.08 (dd, $J = 14.1$ Hz, 6.3 Hz, 1H), 2.88-2.95 (dd, $J = 14.1$ Hz, 7.8 Hz, 1H), 1.38 (s, 9H). ¹³C-NMR (300 MHz, CDCl₃): $\delta = 169.8, 155.9, 140.7, 136.8, 135.2, 130.0, 129.2, 129.2, 128.8, 127.3, 81.5, 55.9, 37.1, 28.2$. HRMS (ESI): calcd. for C₂₀H₂₂ClN₂O₅S⁻ 437.0943, found 437.0950 [M - H]. Melting point: 132-134°C.

(*S*)-*Tert*-butyl (1-(methylsulfonamido)-1-oxo-3-phenylpropan-2-yl)carbamate (**4f**)

Yield: 98%. $[\alpha]_D^{20} = 17.6$ ($c = 0.50$, CH₃OH). ¹H-NMR (300 MHz, CDCl₃): δ (ppm) = 9.05 (s, 1H), 7.30-7.36 (m, 3H), 7.19-7.21 (dd, 2H), 4.94-4.97 (d, 1H), 4.38 (s, 1H), 3.24 (s, 3H), 3.16-3.24 (dd, $J = 14.1$ Hz, 6 Hz, 1H), 2.99-3.07 (dd, $J = 14.1$ Hz, 8.1 Hz, 1H), 1.41 (s, 9H). ¹³C-NMR (300 MHz, CDCl₃): $\delta = 170.9, 155.9, 135.4, 129.3, 128.93, 127.4, 81.6, 56.2, 41.4, 37.1, 28.2$. HRMS (ESI): calcd. for C₁₅H₂₁N₂O₅S⁻ 341.1177, found 347.1192 [M - H]. Melting point: 145-147°C.

(*S*)-*Tert*-butyl(4-methyl-1-oxo-1-(phenylsulfonamido)pentan-2-yl) carbamate (**4g**)

Yield: 90%. $[\alpha]_D^{20} = -9.4$ ($c = 0.50$, CH₃OH). ¹H-NMR (300 MHz, CDCl₃): δ (ppm) = 9.54 (s, 1H), 8.049-8.074 (d, $J = 7.5$ Hz, 2H), 7.61-7.66 (tt, 1H), 7.51-7.56 (td, 2H), 4.76 (s, 1H), 4.04 (s, 1H), 1.56-1.66 (m, 2H), 1.43 (s, 9H), 1.26 (1H), 0.85-0.91 (dd, 6H). ¹³C-NMR (300 MHz, CDCl₃): $\delta = 170.4, 156.3, 138.6, 133.9, 128.9, 128.4, 81.4, 53.5, 39.3, 28.2, 24.5, 22.8, 21.7$. HRMS (ESI): calcd. for C₁₇H₂₅N₂O₅S⁻ 369.1490, found 369.1501 [M - H]. Melting point: 152-155°C.

(*S*)-*Tert*-butyl(4-methyl-1-(4-nitrophenylsulfonamido)-1-oxopentan-2-yl)carbamate (**4h**)

Yield: 96%. $[\alpha]_D^{20} = 4.6$ ($c = 0.50$, CH₃OH). ¹H-NMR (300 MHz, CDCl₃): δ (ppm) = 9.85 (s, 1H), 8.35-8.39 (d, 2H), 8.23-8.28 (d, 2H), 4.75 (s, 1H), 4.00 (s, 1H), 1.63-1.65 (m, 3H), 1.45 (s, 9H), 0.86-0.93 (dd, 6H). ¹³C-NMR (300 MHz, CDCl₃): $\delta = 170.6, 156.6, 150.8, 144.0, 129.9, 124.1, 81.8, 53.4, 39.0, 28.2, 24.5, 22.8, 21.6$. HRMS (ESI): calcd. for C₁₇H₂₄N₃O₇S⁻ 414.1340, found 414.1360 [M - H]. Melting point: 121-123°C.

(S)-Tert-butyl(1-(4-chloro-3-nitrophenylsulfonamido)-4-methyl-1-oxopentan-2-yl)carbamate (4i)

Yield: 85%. $[\alpha]_D^{20} = 23.2$ (c = 0.50, CH₃OH). ¹H-NMR (300 MHz, CDCl₃): δ (ppm) = 9.91 (s, 1H), 8.5-8.52 (d, *J* = 2.1 Hz, 2H), 8.20-8.23 (dd, *J* = 8.4 Hz, 2.1 Hz, 2H), 7.72-7.75 (d, *J* = 8.7 Hz, 2H), 4.78 (s, 1H), 4.02 (s, 1H), 1.61-1.65 (m, 2H), 1.43-1.51 (m, 10H), 0.87-0.96 (dd, 6H). ¹³C-NMR (300 MHz, CDCl₃): δ = 170.9, 156.6, 152.5, 147.6, 138.5, 132.9, 132.7, 125.8, 82.0, 53.4, 39.2, 28.1, 24.6, 22.8, 21.6. HRMS (ESI): calcd. for C₁₇H₂₃ClN₃O₇S⁻ 448.0951, found 448.0924 [M - H]⁻. Melting point: 142-144°C.

Tert-butyl((2S)-3-methyl-1-oxo-1-(phenylsulfonamido)pentan-2-yl)carbamate (4j)

Yield: 97%. $[\alpha]_D^{20} = -11.8$ (c = 0.50, CH₃OH). ¹H-NMR (300 MHz, CDCl₃): δ (ppm) = 9.34 (s, 1H), 8.05-8.08 (d, *J* = 7.5 Hz, 2H), 7.61-7.66 (tt, *J* = 7.5 Hz, 1H), 7.51-7.56 (dt, *J* = 7.5 Hz, 2H), 4.9 (s, 1H), 3.89 (s, 1H), 1.85 (m, 1H), 1.67 (m, 2H), 1.42 (s, 9H), 1.06-1.13 (m, 1H), 0.82-0.88 (m, 6H). ¹³C-NMR (300 MHz, CDCl₃): δ = 170.0, 156.1, 138.5, 133.9, 128.9, 128.4, 81.1, 59.6, 36.4, 28.2, 24.6, 15.4, 11.1. HRMS (ESI): calcd. for C₁₇H₂₃N₂O₅S⁻ 369.1490, found 369.1592 [M - H]⁻. Melting point: 152-154°C.

Tert-butyl((2S)-3-methyl-1-(4-nitrophenylsulfonamido)-1-oxopentan-2-yl)carbamate (4k)

Yield: 87%. $[\alpha]_D^{20} = 3.2$ (c = 0.50, CH₃OH). ¹H-NMR (300 MHz, CDCl₃): δ (ppm) = 9.99 (s, 1H), 8.353-8.39 (d, *J* = 9.0 Hz, 2H), 8.25-8.28 (d, *J* = 9.0 Hz, 2H), 5.02 (s, 1H), 3.94 (s, 1H), 1.79-1.81 (m, 1H), 1.43-1.49 (10H), 1.04-1.18 (m, 1H), 0.83-0.88 (m, 6H). ¹³C-NMR (300 MHz, CDCl₃): δ = 170.7, 156.5, 150.8, 144.0, 129.9, 124.1, 81.6, 59.5, 36.5, 28.2, 24.7, 15.4, 10.9. HRMS (ESI): calcd. for C₁₇H₂₄N₃O₇S⁻ 414.1340, found 414.1359 [M - H]⁻. Melting point: 119-120°C.

Tert-butyl((2S)-1-(4-chloro-3-nitrophenylsulfonamido)-3-methyl-1-oxopentan-2-yl)carbamate (4l)

Yield: 98%. $[\alpha]_D^{20} = 6.8$ (c = 0.50, CH₃OH). ¹H-NMR (300 MHz, CDCl₃): δ (ppm) = 10.17 (s, 1H), 8.53-8.54 (d, *J* = 8.4 Hz, 1H), 8.22-8.24 (d, *J* = 8.4 Hz, 1H), 7.74-7.76 (d, *J* = 8.7 Hz, 2H), 5.07 (s, 1H), 3.90-3.96 (s, 1H), 1.81 (1H), 1.43 (10H), 1.10-1.14 (m, 1H), 0.84-0.89 (m, 6H). ¹³C-NMR (300 MHz, CDCl₃): δ = 170.8, 156.0, 147.6, 138.5, 132.9, 132.8, 132.7, 125.9, 81.7, 59.5, 36.6, 28.2, 24.69, 15.4, 10.9. HRMS (ESI): calcd. for C₁₇H₂₃ClN₃O₇S⁻ 448.0951, found 448.0967 [M - H]⁻. Melting point: 125-127°C.

(S)-Tert-butyl(3-methyl-1-oxo-1-(phenylsulfonamido)butan-2-yl)carbamate (4m)

Yield: 91%. $[\alpha]_D^{20} = -13.4$ (c = 0.50, CH₃OH). ¹H-NMR (300 MHz, CDCl₃): δ (ppm) = 9.61 (s, 1H), 8.06-8.09 (d, *J* = 7.5 Hz, 2H), 7.61-7.66 (tt, *J* = 7.2 Hz, 1H), 7.51-7.56 (dt, 2H), 5.02 (s, 2H), 3.95 (s, 1H), 2.06-2.08 (m, 1H), 1.42 (s, 9H), 0.84-0.90 (dd, 6H). ¹³C-NMR (300 MHz, CDCl₃): δ = 170.4, 156.2, 138.6, 133.9, 128.9, 128.4, 80.8, 59.9, 30.4, 28.2, 19.0, 17.6. HRMS (ESI): calcd. for C₁₆H₂₃N₂O₅S⁻ 355.1333, found 355.1320 [M - H]⁻. Melting point: 165-167°C.

(S)-Tert-butyl(3-methyl-1-(4-nitrophenylsulfonamido)-1-oxobutan-2-yl)carbamate (4n)

Yield: 88%. $[\alpha]_D^{20} = 2.2$ (c = 0.50, CH₃OH). ¹H-NMR (300 MHz, CDCl₃): δ (ppm) = 9.85 (s, 1H), 8.35-8.42 (d, *J* = 9 Hz, 2H), 7.25-7.28 (d, *J* = 9 Hz, 2H), 4.97 (s, 1H), 3.83-3.90 (t, 1H), 2.03-2.14 (m, 1H), 1.43 (s, 9H), 0.89-0.93 (dd, 6H). ¹³C-NMR (300 MHz, CDCl₃): δ = 170.6, 156.3, 150.8, 144.0, 129.9, 124.1, 81.6, 60.3, 30.2, 28.2, 19.0, 17.9. HRMS (ESI): calcd. for C₁₆H₂₂N₃O₇S⁻ 400.1184, found 400.1193 [M - H]⁻. Melting point: 155-157°C.

(S)-Tert-butyl(1-(4-chloro-3-nitrophenylsulfonamido)-3-methyl-1-oxobutan-2-yl)carbamate (4o)

Yield: 84%. $[\alpha]_D^{20} = 26.6$ (c = 0.50, CH₃OH). ¹H-NMR (300 MHz, CDCl₃): δ (ppm) = 9.89 (s, 1H), 8.53-8.54 (d, *J* = 2.1 Hz, 1H), 8.2-8.24 (dd, *J* = 8.4 Hz, *J* = 2.1 Hz, 1H), 7.73-7.76 (d, *J* = 8.4 Hz, 1H), 4.98 (s, 2H), 3.82-3.87 (t, 1H), 2.04-2.15 (m, 1H), 1.43 (s, 9H), 0.91-0.955 (dd, 6H). ¹³C-NMR (300 MHz, CDCl₃): δ = 170.6, 156.6, 147.6, 138.5, 133.0, 132.8, 132.7, 125.9, 81.7, 60.3, 30.2, 28.3, 19.1, 17.9. HRMS (ESI): calcd. for C₁₆H₂₂ClN₃O₇S⁻ 434.0794, found 434.0806 [M - H]⁻. Melting point: 127-130°C.

Tert-butyl (2-oxo-2-(phenylsulfonamido)ethyl) carbamate (4p)

Yield: 92%. ¹H-NMR (300 MHz, CDCl₃): δ (ppm) = 9.60 (s, 1H), 8.06-8.08 (d, *J* = 7.5 Hz, 2H), 7.61-7.67 (tt, *J* = 8.7 Hz, 1H), 7.52-7.57 (td, 2H), 5.242 (s, 1H), 3.823 (s, 2H), 1.44 (s, 9H). ¹³C-NMR (300 MHz, CDCl₃): δ = 168.0, 156.3, 138.5, 134.0, 129.0, 128.3, 81.1, 44.8, 28.2. HRMS (ESI): calcd. for C₁₃H₁₇N₂O₅S⁻ 313.0864, found 313.0866 [M - H]⁻. Melting point: 116-120°C.

Tert-butyl(2-(4-nitrophenylsulfonamido)-2-oxoethyl) carbamate (4q)

Yield: 90%. ¹H-NMR (300 MHz, CDCl₃): δ (ppm) = 9.80 (s, 1H), 8.37-8.40 (d, *J* = 8.7 Hz, 2H), 8.26-8.29 (d, *J* = 8.7 Hz, 2H), 5.21 (s, 1H), 3.81-3.83 (d, *J* = 5.7 Hz, 2H), 1.46 (s, 9H). ¹³C-NMR (300 MHz, CDCl₃): δ = 167.7, 156.7, 150.9, 143.9, 129.9, 124.2, 82.0, 45.4, 28.2. HRMS (ESI): calcd. for C₁₃H₁₆N₃O₇S⁻ 358.0714, found 358.0697 [M - H]⁻. Melting point: 144-147°C.

Tert-butyl(2-(4-chloro-3-nitrophenylsulfonamido)-2-oxoethyl)carbamate (4r)

Yield: 81%. ¹H-NMR (300 MHz, CDCl₃): δ (ppm) = 9.720 (s, 1H), 8.53-8.54 (d, *J* = 2.1 Hz, 1H), 8.21-8.25 (dd, *J* = 2.1 Hz, *J* = 8.4 Hz, 1H), 7.74-7.77 (d, *J* = 8.4 Hz, 1H), 5.11-5.15 (t, 1H), 3.79-3.81 (d, 2H), 1.47 (s, 9H). ¹³C-NMR (300 MHz, CDCl₃): δ = 167.7, 156.9, 147.8, 138.4, 133.2, 132.7, 132.6, 125.8, 82.2, 45.6, 28.2. HRMS (ESI): calcd. for C₁₃H₁₅ClN₃O₇S⁻ 392.0325, found 392.0331 [M - H]⁻. Melting point: 142-145°C.

(S)-Tert-butyl(1-oxo-1-(phenylsulfonamido)propan-2-yl)carbamate (4s)

Yield: 73%. [α]_D²⁰ = -23.4 (c = 0.50, CH₃OH). ¹H-NMR (300 MHz, CDCl₃): δ (ppm) = 9.76 (s, 1H), 8.05-8.08 (d, *J* = 7.8 Hz, 2H), 7.62-7.67 (tt, 1H), 7.51-7.56 (dt, 2H), 4.89 (s, 1H), 4.11 (s, 1H), 1.44 (s, 9H), 1.29-1.46 (d, 3H). ¹³C-NMR (300 MHz, CDCl₃): δ = 170.6, 156.2, 138.6, 133.9, 128.9, 128.3, 81.4, 50.4, 28.2, 16.7. HRMS (ESI): calcd. for C₁₄H₁₉N₂O₅S⁻ 327.1020, found 327.1101 [M - H]⁻. Melting point: 142-145°C.

Tert-butyl (4-oxo-4-(phenylsulfonamido)butyl)carbamate (6a)

Yield: 80%. ¹H-NMR (300 MHz, CDCl₃): δ (ppm) = 10.19 (s, 1H), 8.07-8.09 (d, *J* = 14.1 Hz, 1H), 7.61-7.66 (tt, 1H), 7.51-7.56 (td, 2H), 4.76 (s, 1H), 3.07-3.13 (q, 2H),

2.27-2.31 (t, *J* = 12.9 Hz, 2H), 1.66-1.77 (m, 2H), 1.46 (s, 9H). ¹³C-NMR (300 MHz, CDCl₃): δ = 171.2, 157.2, 139.0, 133.7, 128.9, 128.3, 80.1, 39.1, 33.44, 28.4, 26.1. HRMS (ESI): calcd. for C₁₅H₂₁N₂O₅S⁻ 341.1177, found 341.1188 [M - H]⁻. Melting point: 139-141°C.

Tert-butyl(4-(4-nitrophenylsulfonamido)-4-oxobutyl)carbamate (6b)

Yield: 85%. ¹H-NMR (300 MHz, CDCl₃): δ (ppm) = 12.4 (s, 1H), 8.41-8.46 (d, 2H), 8.14-8.19 (d, 2H), 6.74-6.78 (t, 1H), 2.77-2.84 (q, 2H), 2.21-2.26 (t, 2H), 1.45-1.54 (m, 2H), 1.35 (s, 9H). ¹³C-NMR (300 MHz, DMSO): δ = 171.6, 155.5, 150.2, 144.5, 129.1, 124.1, 77.5, 56.0, 32.7, 28.2, 24.2. HRMS (ESI): calcd. for C₁₅H₂₀N₃O₇S⁻ 386.1027, found 386.1040 [M - H]⁻. Melting point: 163-165°C.

Tert-butyl (4-(4-chloro-3-nitrophenylsulfonamido)-4-oxobutyl)carbamate (6c)

Yield: 79%. ¹H-NMR (300 MHz, CDCl₃): δ (ppm) = 10.93 (s, 1H), 8.56 (s, 1H), 8.25-8.28 (dd, *J* = 8.4 Hz, *J* = 2.1 Hz, 1H), 7.72-7.75 (d, *J* = 8.4 Hz, 1H), 4.84 (s, 1H), 3.10-3.17 (q, 2H), 2.285-2.328 (t, 2H), 1.714-1.80 (m, 2H), 1.47 (s, 9H). ¹³C-NMR (300 MHz, CDCl₃): δ = 171.6, 157.6, 147.6, 139.0, 132.7, 125.7, 80.6, 39.0, 33.5, 28.3, 26.3. HRMS (ESI): calcd. for C₁₅H₁₉ClN₃O₇S⁻ 420.0638, found 420.0643 [M - H]⁻. Melting point: 92-95°C.

In silico ligand based design of indolylpiperidinyl derivatives as novel histamine H₁ receptor antagonists

Sarvesh Paliwal*, Supriya Singh, Mahima Pal

Department of Pharmacy, Banasthali University, Banasthali, Rajasthan, India.

ABSTRACT: Histamine H₁ receptor antagonists play a vital role in the first line treatment of a broad range of allergic diseases. Frequent dosing of the antagonist results in side effects like sedation and cardiovascular toxicity. The present study highlights the important structural requirement and mechanistic interpretation of novel indolylpiperidinyl derivatives as H₁ receptor antagonists so as to facilitate the design of newer antihistaminics with increased duration of action and comparatively reduced side effects. The significance of the developed quantitative structure-activity relationship (QSAR) models were evaluated on the basis of statistical values of square of correlation coefficient (r^2); (multiple linear regression (MLR), 0.86; and partial least squares (PLS), 0.85). The predictive ability of the resulting QSAR models was evaluated with cross-validated correlation coefficient (r^2_{cv}) values (MLR, 0.82; PLS, 0.82) generated for the training set and r^2 values (MLR, 0.763; PLS, 0.855) derived for test set. The final models comprised of multidimensional steric (verloop length, verloop B₃), electronic (total dipole moment) and steric (KAlpha1 index) descriptors. The study indicates that antihistaminic activity is largely explained by steric and electronic parameters. In line with parameters entered in the model some indolylpiperidines derivatives were designed with good antihistaminic properties and pharmacokinetic profiles.

Keywords: Quantitative structure-activity relationship (QSAR), tools for structure activity relationship (TSAR), multiple linear regression (MLR), partial least square (PLS)

1. Introduction

Among a wide range of mediators which are involved in the pathophysiology of allergic diseases, histamine remains the principal one and plays a fundamental role in the genesis of these diseases, particularly rhinitis and urticaria (1). Chronically, histamine also affects inflammatory cells and causes cellular activation (mast cells, basophils, and eosinophils) and release of proinflammatory mediators *e.g.*, leukotrienes and cytokines and results in an increase in the expression of class II human histocompatibility molecules (HLA) and vascular endothelial adhesion molecules (2-4).

Antihistaminics prevent symptoms associated with histamine release such as rhinorrhea, nasal and conjunctival itching, and lacrimation, although they do not control symptoms of nasal congestion (5). Depending on their action on the central nervous system (CNS), they are classified as "classical", or first-generation, and "non-classical", or second-generation.

In general, first-generation H₁ antihistamines (for example dexchlorpheniramine and hydroxyzine) cross the blood brain barrier (BBB), bind with ease to the cerebral H₁ receptors and also possess anticholinergic properties (3,6). Their principal side effect is sedation, dry mouth, and lack of receptor specificity at therapeutic doses. This has led to the development of a second-generation of H₁-antagonists (7).

Second-generation H₁-antagonists exhibit high potency, long-lasting effects and minimal adverse effects. They are unlikely to cross the BBB and rarely cause sedation. Some findings suggest that second generation H₁ receptor antagonists produce CNS depressant effects due to their liability to penetrate into the CNS (8). Also, adverse cardiac effects have been reported with second-generation H₁ antihistamines namely astemizole and terfenadine (9,10).

In line to the above discussion we felt that there is a need to reevaluate the binding requirements of antihistaminics by employing a computational approach. One of the most promising techniques to get insight into the structural requirements is quantitative structure-activity relationship (QSAR), which came into existence in the 1960's for the first time. QSAR is

*Address correspondence to:

Dr. Sarvesh Paliwal, Department of Pharmacy, Banasthali University, Banasthali, Rajasthan-304022, India.
E-mail: paliwalsarvesh@yahoo.com

a mathematical relationship linking chemical structure and pharmacological activity in a quantitative manner for a series of compounds representing hydrophobic, electronic, steric and other effects using multiple regression correlation methodology. QSAR increases the probability of success and reduces the time and cost involved in the drug discovery process (11). The aim of this investigation was to develop QSAR models using the multivariate analysis derived from global descriptors with the purpose to elucidate the contribution of substitutions of antihistamine antagonists and the forces involved in drug receptor interaction. The study of *de novo* contributions of the groups helped us to design and predict activity of some newer analogs.

2. Materials and Methods

A series of 53 indolylpiperidinyl benzoic acid derivatives was obtained from the literature for the present QSAR studies (12). For the current QSAR investigation 51 compounds were used and the remaining two compounds (**8** and **39**) were excluded in view of uncertain activity data since such data cannot be used for model development using tools for structure activity relationship (TSAR) software. Experimentally determined biological activity of compounds in the series was reported as a half minimum inhibitory concentration (IC₅₀) value. Since biological activities are generally skewed and are measures of the free energy of binding, the reported inhibitory constant values were converted into a corresponding negative log value.

The negative log IC₅₀ values were used as the dependent variable and various quantifying parameters as the independent variable. All computational studies were performed using TSAR (version 3.3) software (13).

2.1. Drawing and optimization of structures

The organic structure of 51 indolylpiperidinyl benzoic acid derivatives selected for QSAR studies, were sketched using ChemDraw Ultra 10.0. All sketched chemical structures were imported to a TSAR 3.3 spread sheet *via* .mol files. Structure entry and substitutions defining is an important stage in QSAR methodology. The substituents of each chemical structure were defined into six substituents namely R₁, R₂, R₃, R₄, R₅, and R₆. All the substituents were numbered according to their position in molecules, and each molecule had a defined number of substituents attached to the nucleus by a single bond. The substituent pattern opted for is given in Supplemental Table S1 (<http://www.ddtjournal.com/getabstract.php?id=538>).

TSAR has a built in program CORINA, which was used to convert all molecular structures and substitutions to 3D structures. The 3D structure concept was developed by Hiller (14). The three dimensional structure of a molecule is closely related to a large variety of chemical, physical and biological properties.

The CORINA automatically generates 3D atomic co-ordinates from the constitution of a molecule as expressed by a connection table or linear string (15).

The Cosmic module was used to optimize the structure of compounds. Cosmic calculates molecular energies by summing bond length, bond angle, torsion angle, van der waals, and coulombic terms for all appropriate sets of atoms. These calculations involve the valence electrons of the atoms of the molecule. These lead to further development of semi-empirical molecular orbital (MO) calculations (16). The calculations were terminated when the energy difference or the energy gradient were smaller than 1×10^{-5} and 1×10^{-10} kcal/mol, respectively (17).

The data set consisting of compounds with molecular structures and their biological activities were divided into a training and test set. Twenty percent of the compounds were selected with a maximum dissimilarity algorithm and assigned to the test set; with the remaining 80% assigned to the training set (18). The training set comprised of 41 molecules was used for QSAR model development and the test set of 10 molecules was used for model validation.

2.2. Calculation of molecular descriptors

Descriptors can be defined as numerical quantities that have been generated to represent the molecular configuration. It also contributes toward better understanding of structural, steric, electronic and multidimensional properties responsible for activity. The aim of calculating molecular descriptors is to provide all useful information about all chemical structures and respective substituents to build a good and predictive QSAR model. The nature of descriptors used and the extent to which they encode structural features related to biological activity is a crucial part of a QSAR study. The success of the QSAR analysis is significantly dependent on the accurate definition and appropriate use of molecular descriptors. Molecular descriptors are terms that characterize a specific aspect of a molecule.

TSAR can calculate up to 500 descriptors (topological, geometrical and electrostatic) derived from whole structures as well as substitution of compounds under consideration. Since a large pool of descriptors was calculated, there is a significant requirement for data reduction to eliminate chance correlation. A correlation matrix was used to reduce the number of descriptors and to identify the best subset of descriptors with minimum intercorrelation. The goal was to remove redundancy among the descriptors and to detect chance effects during model development.

A correlation coefficient describes the degree of linear correlation between two variables. Pair wise correlation coefficients were calculated for all pairs of descriptors. If an intercorrelation coefficient > 0.5 was detected, the descriptor with high correlation with biological activity was kept and others were discarded. In the next

phase data reduction was performed on the remaining descriptors on the basis of *t*-values using a backward elimination technique. Stepwise regressions were developed and the descriptors having lower *t*-values were discarded from the data set (19).

The reduction process was repeated a number of times and finally four independent descriptors: Verloop L (Substituent 5), Verloop B₃ (Substituent 5), total dipole moment (whole molecule), and KAlpha1 index (whole molecule), which were highly correlated with biological activity and exhibited minimum intercorrelation with each other, were retrieved. The statistical values for the most relevant descriptors and their corresponding *t*-values used in QSAR development are shown in Table 1 and the correlation matrix for the four descriptors is depicted in Table 2.

2.3. Multivariate statistical analysis

Multivariate statistical analysis is a set of statistical tools used for modeling a set of dependent variables, such as biological activity, and molecular descriptors as the independent variables (20). The relationship between the structural parameters (global descriptors) and the biological activities was quantified by multiple linear regressions (MLR) and partial least squares (PLS). Values for F-to-enter and F-to-leave were set to 4. Outliers in QSAR can be very important and interesting, especially when the observed biological activity is higher than the predicted one by the developed model (higher residual value). Outliers may be present due to inappropriate calculation of the parameter values used. The mathematical model may not be appropriate. There may be a lack of certain descriptors or parameters to describe QSAR for entire compounds. A different mechanism mode may even be a reason (21). Four outliers (6, 7, 10, and 23) were detected with the help of a regression line equation. There could be various reasons for the observed outliers. The acceptable and robust QSAR model was selected on the basis of various

statistical significant parameters like correlation coefficient (*r*), square of correlation coefficient (*r*²), cross-validated correlation coefficient (*r*²_{cv}), Fisher ratio (*F*), and standard deviation (*SD*). The resulting models were validated by a leave-one out cross-validation procedure and a test set prediction to check their predictability and robustness.

In addition to MLR, PLS has also been performed to check the robustness of the developed MLR model. PLS was developed in the 1960's by Herman Wold as an econometric technique. PLS is a robust multivariate regression method suitable for overcoming general problems in MLR related to over-abundant descriptors and therefore comparable predictive models can be obtained by the PLS method (22). The results of PLS were evaluated on the basis of *r*², *r*²_{cv}, and statistical significance.

3. Results and Discussion

Multivariate regression analysis such as MLR and PLS were carried out in order to discover the contribution of the whole molecule and substituents for biological activity. More specifically, the understanding of the *de novo* contribution of the functional groups helped to understand interactions between substitution on the N- chain of the indole ring and the transmembrane region of the H₁-receptor active site. The set of 41 compounds were subjected to stepwise multiple linear regression analysis in order to develop the QSAR model, considering antihistaminic activity as dependent variables and all the reduced set of descriptors as independent variables. When the multiple regression analysis was performed without deleting any outlier, we retrieved a statistically insignificant model. In order to improve the predictability and reliability of the model the outliers were detected and it was found that four compounds (6, 7, 10, and 23) had high residual values and were too far away from the regression line. Various models developed after deleting the four compounds one by one and in combination exhibited a high value

Table 1. Statistical values for the most relevant descriptors used in QSAR

	Abbreviation	Coefficient	Jackknife	<i>t</i> -Value	Covariance SE
Verloop L (subs.5)	X ₁	-0.24	0.02	-9.86	0.02
Verloop B ₃ (subs.5)	X ₂	-0.30	0.02	-9.09	0.03
Total dipole moment (Whole molecule)	X ₃	0.12	0.01	7.71	0.01
KAlpha1 index (Whole molecule)	X ₄	0.06	0.02	3.72	0.02

Table 2. Correlation matrix of classical descriptors used in QSAR models

	Verloop L (subs.5)	Verloop B ₃ (subs.5)	Total dipole moment (Whole molecule)	KAlpha1 index (Whole molecule)	Log IC ₅₀
Verloop L (subs.5)	1				
Verloop B ₃ (subs.5)	-0.55	1			
Total dipole moment (Whole molecule)	0.36	-0.40	1		
KAlpha1 index (Whole molecule)	0.18	0.23	0.09	1	
Log IC ₅₀	-0.13	-0.51	0.61	-0.01	1

of r^2 (0.86) and r^2_{cv} (0.82) for MLR analysis as shown in Table 3. In addition to MLR, the data set was also subjected to PLS analysis to check soundness of results obtained from MLR analysis. The PLS model generated showed comparable results to that of MLR (23) as exhibited by the high value of r^2 (0.85) and r^2_{cv} (0.82) as shown in Table 4.

3.1. Validation of statistical output of multivariate equation (PLS and MLR)

The model developed using MLR and PLS were validated and checked for predictability and robustness on the basis of the r^2 , r^2_{cv} , F value and its standard error S value.

3.1.1. Squared correlation coefficient (r^2)

In statistics, the coefficient of determination r^2 is the proportion of variability in a data set that is accounted for by a statistical QSAR model. In this determination, the term "variability" is defined as the sum of squares. There are equivalent expressions for r^2 based on analysis of the fraction of total variance in the data, which is explained by the regression model (24). It can be calculated using the following formula.

$$r^2 = 1 - \frac{\sum \Delta^2}{S_{yy}}$$

Where, $S_{yy} = \sum (y_{obs} - y_{mean})$, $\sum \Delta^2 = \sum (y_{obs} - y_{cal})^2$. Where " y_{obs} " is observed biological activities, " y_{mean} " is mean of biological activities value, and " y_{cal} " is calculated biological activity used in the equation. Also r^2 is used to describe the goodness of fit of the data. Its value should be greater than 0.7 for a sound model. The statistical significance of the generated QSAR model was evaluated in terms of r^2 values (MLR = 0.8657 and PLS = 0.859) which explained a 86.57% and 85.90% variance in biological activity. Moreover the r^2 values for the test set (MLR = 0.76 and PLS = 0.85) were also found to be significant.

3.1.2. Cross validated regression coefficient (r^2_{cv})

Cross-validation is an important tool to avoid over fitting of data, as over-fitting will give low accuracy on validation. The predictive value of the models were evaluated by LOO cross validation (24). The cross validated coefficient r^2_{cv} was calculated using the formula for PLS analysis.

$$r^2_{cv} = 1 - \frac{\sum (Y_{pred} - Y_{obs})^2}{\sum (Y_{pred} - Y_{mean})}$$

Where Y_{pred} , Y_{obs} , and Y_{mean} are predicted, actual and mean values of the target property (pIC₅₀), respectively. $\sum (Y_{pred} - Y_{obs})^2$ is the predictive sum of squares (PRESS). And for MLR, it can be calculated using the following formula.

$$r^2_{cv} = SD - PRESS/SD$$

Where SD is standard deviation and predicted residual sum of square (PRESS) = $\sum (y_{obs} - y_{cal})^2$. This method is used to predict the property value for a compound from the data set, which in turn is predicted from the regression equation calculated from the data for all of the compounds. For evaluation, predicted values can be used for squared correlation coefficient criteria. The r^2_{cv} should be more than 0.6 and a small difference between r^2 and r^2_{cv} indicates a good internal predictive ability of developed model. A small difference in r^2 (0.86) and r^2_{cv} (0.82) for MLR values is indicative of the high predictive ability of the developed model. Similarly the r^2 (0.85) and r^2_{cv} (0.82) values generated by PLS were also very close.

3.1.3. S value (SD)

SD is measured as the error mean square, which expresses the variation of the residuals or the variation about the regression line. It indicates, how well the function derived by the QSAR analysis predicts the

Table 3. Various equations derived after removing of outliers by the MLR method

S. No.	Equation	r	r^2	r^2_{cv}	S value	F value	Name of outliers
1.	$Y = -0.23X_1 - 0.32X_2 + 0.11X_3 + 0.05X_4 - 1.49$	0.86	0.75	0.25	0.16	27.40	ND
2.	$Y = -0.24X_1 - 0.30X_2 + 0.12X_3 + 0.06X_4 - 1.64$	0.90	0.82	0.73	0.13	40.20	7
3.	$Y = -0.23X_1 - 0.29X_2 + 0.12X_3 + 0.06X_4 - 1.72$	0.92	0.84	0.76	0.13	44.47	7, 23
4.	$Y = -0.23X_1 - 0.32X_2 + 0.10X_3 + 0.05X_4 - 1.43$	0.89	0.79	0.70	0.15	32.29	23, 6
5.	$Y = -0.23X_1 - 0.30X_2 + 0.11X_3 + 0.06X_4 - 1.72$	0.93	0.86	0.82	0.12	51.58	6, 7, 10, 23

Table 4. Various equations derived after removing of outliers by the PLS method

S. No.	Equation	Statistical significance	Cross validation (r^2_{cv})	Fraction of variance (r^2)	Name of outliers
1.	$Y = -0.23X_1 - 0.30X_2 + 0.12X_3 + 0.06X_4 - 1.78$	1.07	0.65	0.75	ND
2.	$Y = -0.23X_1 - 0.28X_2 + 0.13X_3 + 0.06X_4 - 1.92$	0.99	0.77	0.82	7
3.	$Y = -0.23X_1 - 0.28X_2 + 0.12X_3 + 0.06X_4 - 1.95$	1.02	0.77	0.84	7, 23
4.	$Y = -0.22X_1 - 0.30X_2 + 0.12X_3 + 0.06X_4 - 1.73$	0.95	0.75	0.78	23, 6
5.	$Y = -0.22X_1 - 0.27X_2 + 0.12X_3 + 0.07X_4 - 2.03$	0.97	0.82	0.86	6, 7, 10, 23

observed biological activity. Its value considers the number of object 'n' and the number of variable 'k'. Hereby, SD depends not only on the quality of fit but also on the number of degrees of freedom. The low values for the standard error estimate (0.118) of the developed model further testify about the statistical significance of the developed model. It can be calculated using the following formula.

$$SD = \sqrt{\sum(y_{\text{obs}} - y_{\text{cal}})^2 / n - k - 1}$$

3.1.4. F value (Fischer value)

It is a measure of the statistical significance of the regression model. It can be calculated using the following formula.

$$F = r^2(n - k - 1) / k(1 - r^2)$$

A high value of F (51.584) indicates that the model is statistically significant and a lower S value also supported the quality of the model.

3.2. Test set prediction

3.2.1. Internal test set prediction

The internal predictive capability of the QSAR model was also checked using test sets of compounds that were excluded during model development. All the compounds in the test set were treated in a manner analogous to the compounds in the training set. The r^2 value of MLR = 0.763 and PLS = 0.855 derived for the test set illustrate the high predictive ability of the developed model. The actual and predicted activity obtained after MLR and PLS analysis for the training and test set of antihistamines are given in Supplemental Tables S2 and S3 (<http://www.ddtjournal.com/getabstract.php?id=538>) and their corresponding graphs are shown in Figures 1 and 2.

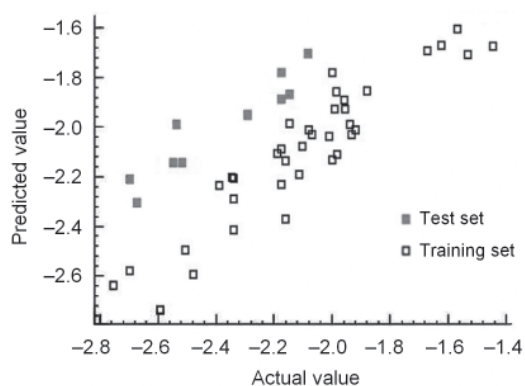


Figure 1. Plot of actual versus predicted values for the training set and test set molecules with the help of the MLR statistical method.

3.2.2. External test set prediction

A model is claimed to be validated when it is also able to predict the activities of external test set compounds. So, the generated model was further evaluated by an external test set comprising of H_1 receptor antagonists from the literature (25). Thirteen compounds were selected for the external test set showing diversity in an activity range as given in Table 5. The overall squared correlation coefficient was 0.68 (MLR) and 0.68 (PLS) for the external test set (Figures 3 and 4) testifying to the validity of the model.

3.3. Interpretation of the generated multivariate model

The highly predictive and robust MLR and PLS models were selected on the basis of statistical significance of the regression equations (Tables 3 and 4) obtained from training set compounds, which explains the relationship between biological activity and structures of molecules. Descriptors obtained from the final model (both MLR and PLS) were namely Verloop L (substitution R_5), Verloop B_3 (substitution R_5), Total dipole moment (whole molecule), and KAlphal index (whole molecule).

The Verloop L and Verloop B_3 parameters are steric parameters developed by Verloop and co-workers and are used to characterize geometry of substitution groups in the molecule. The length parameter, Verloop L, is defined as calculated length of the substituent along the axis of the bond connecting substituent with parent molecule (26). Width parameter Verloop B_3 characterizes distribution of atoms in the substituent with respect to the connecting bond. In addition, the Verloop B_3 parameter describes width of the substituent in the direction perpendicular to L (27). The equation clearly reveals that a decrease in length and width of substitution R_5 will increase binding affinity of compounds.

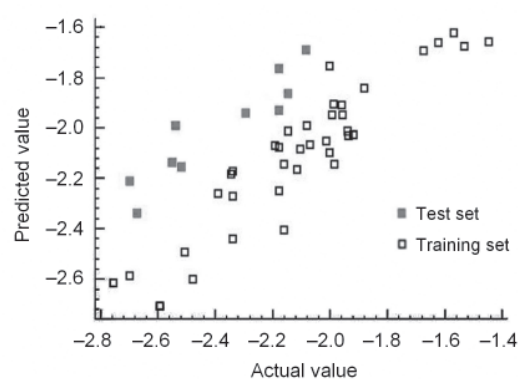
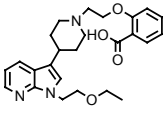
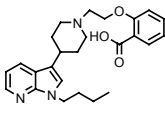
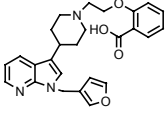
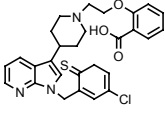
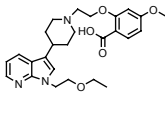
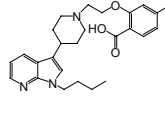
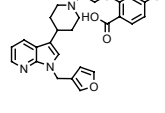
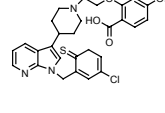
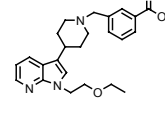
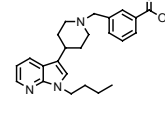
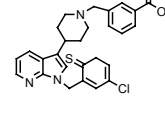
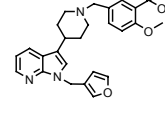
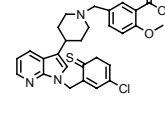


Figure 2. Plot of actual versus predicted values for the training set and test set molecules with the help of the PLS statistical method.

Table 5. Structures along with $-\log IC_{50}$ values and estimated value of the 13 piperidinylpyrrolopyridines and its derivatives as H_1 antagonists for external validation

Compound name	Structure of compound	Actual activity IC_{50} (nM)	Actual activity in $-\log IC_{50}$	Estimated activity by MLR	Estimated activity by PLS
1		190	-2.27875	-2.0532	-2.08818
2		235	-2.37107	-1.95353	-2.01655
3		225	-2.35218	-1.89567	-1.92184
4		295	-2.46982	-2.35658	-2.36357
5		185	-2.26717	-2.10389	-2.15123
6		215	-2.33244	-1.86682	-2.00285
7		170	-2.23045	-1.73856	-1.84707
8		240	-2.38021	-2.16555	-2.26474
9		403	-2.6053	-2.46071	-2.33642
10		275	-2.43933	-2.13215	-2.15197
11		330	-2.51851	-2.58772	-2.57525
12		205	-2.31175	-1.9529	-2.00152
13		365	-2.56229	-2.27669	-2.33247

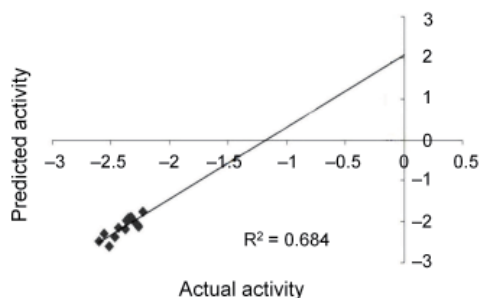


Figure 3. Plot of the correlation graph between experimental and estimated activities of the external test set molecules by MLR.

The equation in Tables 3 and 4 clearly shows that substitution on the N- chain of the indole ring is negatively correlated with H₁-antihistamine activity. This apparently explains the difference in activity of compounds **13** and **27** which differ only in substitution on the N- chain of the indole ring. Compound **13** exhibited a higher antihistaminic activity because it possesses a lower value for length and width parameters at this position when compared to compound **27**.

The decrease in H₁ antihistaminic activity with the length of substituents can be further demonstrated by the activity of compounds **1**, **26**, and **27**, which differ only in a single substitution. Compound **1** is more active than compounds **26**, and **27** as its R₅ substitution is shorter than the 2-[1,4]-dioxan-2-ylethyl of compound **26**, and the 2-pyridin-2-ylethyl of compound **27**. Compounds **26** and **27** have more or less the same length value. The above discussion reveals that while designing newer molecules care must be taken to keep the length and width of substitution at R₅ in a limited range because length and width of the substitution will cause steric hindrance between drug and receptor and consequently will decrease activity.

Total dipole moment for a whole molecule may be approximated as the vector sum of individual bond dipole moments. Moreover, dipole moment is a partial charge-dependent parameter calculated on the basis of center of charge over the substitution as the origin. The total dipole moment describes the electrostatic interaction between drug and receptor. It can be calculated using the following formula.

$$\mu = e \sum r_i q_i$$

Where r_i is the distance of the i th atom from the origin and q_i is the atomic charge of the i th atom. The descriptor uses Debye units. The total dipole moment is often considered as the direct characteristic of polarity of a molecule (28). The present series have an indolylpiperidine ring, the aromatic π system of which is formed by π electrons. Quantum mechanical calculations showed distribution of electron density among the atoms of the indole ring which results in a

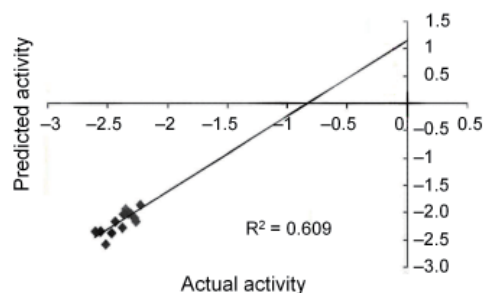


Figure 4. Plot of the correlation graph between experimental and estimated activities of the external test set molecules by PLS.

large molecular dipole moment which allows possibility of dipole-dipole interactions between the H₁ receptor and compounds under consideration. The basic nitrogen of the indole ring is confined to the region accessible to its counter ion on the histamine H₁-receptor, *i.e.*, the carboxylate group of aspartic acid (Asp116) (29).

In the regression equation total dipole moment of whole molecules is positively correlated with biological activity. It means that larger electronic properties of the compounds play a key role in the interaction between drug and receptor. Increasing total dipole moment of the whole molecule can increase binding between molecules and receptor and thus can increase interaction between molecules and the H₁ receptor. The above interpretation is in line with mutational studies done on cetirizine, a potent H₁ receptor antagonist. Cetirizine contains a COOH group which interacts with the protonated lysine (Lys200) present in the transmembrane domain V of the H₁ receptor (30). Likewise Indolylpiperidine derivatives containing a COOH group form an ionic bond/H bond with the positively charged amino group of lysine.

Another descriptor entering in the model was KAlpha1 which helps to differentiate the molecules according to their size, degree of branching, flexibility, and overall shape (31). The KAlpha1 index encodes information about several attributes of molecular shape, based upon atom count and path count of various orders. This index explains the elongated nature of molecules and their branches at the end. Each K index value would imply shape identity. Atoms other than Sp³ hybrids make a different size contribution to a molecule, thereby influencing its overall shape. Non-carbon Sp³ atoms should be counted more or less than one, the increment or decrement, called 'alpha' being based on the size contribution of the atom in question relative to a carbon Sp³. One basis of evaluating alpha is to use covalent radius of the atom. The quality of the equation and easy interpretation of the indices make this result useful for prediction of possible antihistaminic potency of some newer designed compounds (32).

The multivariate regression equation reveals that the KAlpha1 index of the whole molecule of the compound

is correlated positively with biological activity. It means that if we increase the shape and branching of the lead compound there will be an increase in H₁-antihistaminic activity because shape or steric configuration of a molecule have a potential influence on physical properties and biological activity. The QSAR studies suggested that the catalytic site of the protein and the steric requirements of the compounds play an important factor in the antagonist's potency.

This QSAR study clearly indicates that optimum steric and electronic properties of whole molecules are important for favorable interaction with the receptor. On the basis of the final multivariate regression model, some newer compounds were designed to find molecules with higher antihistaminic potencies than the existing series of indolylpiperidinyl benzoic acid derivatives.

4. Conclusion

On the basis of present study, it can be concluded that physicochemical descriptors have sufficient reliability to relate to the biological activity of indolylpiperidinyl benzoic acid molecules with their structural features. This physicochemical study suggests that the electronic and steric interaction between drug and receptors are dominant in whole molecules, whereas the multidimensional steric interaction is dominant due to substitution at R₅ in this series. It means that low length and width of substitution R₅ is important for interaction between drug and receptors. The study provides better understanding of the structural features and their binding affinities to the histamine H₁ receptor and helped in the design of orally active more potent H₁ receptor antagonists.

Acknowledgements

Computational resources were provided by Banasthali University, and the authors thank the Vice Chancellor, for extending all the necessary facilities.

References

1. Simons FE. H₁-Antihistamines: More relevant than ever in the treatment of allergic disorders. *J Allerg Clin Immunol.* 2003; 112:S42-S52.
2. Das AK, Yoshimura S, Mishima R, Fujimoto K, Mizuguchi H, Dev S, Wakayama Y, Kitamura Y, Horio S, Takeda N, Fukui H. Stimulation of histamine H₁ receptor up-regulates histamine H₁ receptor itself through activation of receptor gene transcription. *J Pharmacol Sci.* 2007; 103:374-382.
3. Bousquet J, Van Cauwenberge P, Khaltaev N; Aria Workshop Group; World Health Organization. Allergic rhinitis and its impact on asthma. *J Allergy Clin Immunol.* 2001; 108(Suppl 5):S147-S334.
4. Holgate ST, Canonica GW, Simons FE, Tagliaberto M, Tharp M, Timmerman H, Yanai K; Consensus Group on New-Generation Antihistamines. Consensus Group on New-Generation Antihistamines (CONGA): Present status and recommendations. *Clin Exp Allergy.* 2003; 33:1305-1324.
5. Scadding GK. Clinical assessment of antihistamines in rhinitis. *Clin Exp Allergy.* 1999; 29:77-81.
6. Simons FE, Simons KJ. The pharmacology and use of H₁-receptor-antagonist drugs. *N Engl J Med.* 1994; 330:1663-1670.
7. Kay GG. The effects of antihistamines on cognition and performance. *J Allergy Clin Immunol.* 2000; 105:S622-S627.
8. Shigemoto Y, Shinomiya K, Mio M, Azuma N, Kamei C. Effects of second-generation histamine H₁ receptor antagonists on the sleep-wakefulness cycle in rats. *Eur J Pharmacol.* 2004; 494:161-165.
9. Barbey JT, Anderson M, Ciprandi G, Frew AJ, Morad M, Priori SG. Cardiovascular safety of second-generation antihistamines. *Am J Rhinol.* 1999; 13:235-243.
10. DuBuske LM. Second-generation antihistamines: The risk of ventricular arrhythmias. *Clin Ther.* 1999; 21:281-295.
11. Hansch C, Verma RP. Overcoming tumor drug resistance with C2- modified 10-deacetyl 7-propionyl cephalomannines – A QSAR study. *Mol Pharmaceut.* 2009; 6:849-860.
12. Fonquerne S, Miralpeix M, Pagès L, *et al.* Synthesis and structure-activity relationships of novel histamine H₁ antagonists: Indolylpiperidinyl benzoic acid derivatives. *J Med Chem.* 2004; 47:6326-6337.
13. Tsar 3.3, Oxford Molecular Ltd., The Medawar Centre, Oxford Science Park, Oxford, 2000.
14. Hendrickson MA, Nicklaus MC, Milne GWA, Zaharevitz D. CONCORD and CAMBRIDGE: Comparison of computer-generated chemical structures with X-ray crystallographic data. *J Chem Inf Comput Sci.* 1993; 33:155-163.
15. Sadowski J, Gasteiger J. From atoms and bonds to three-dimensional atomic coordinates: Automatic model builders. *Chem Rev.* 1993; 93:2567-2581.
16. Molecular Modeling and Drug Design (Vinter JG, Gardner M, eds.). CRC Press Inc., Boca Raton, FL, USA, 1994.
17. Kovatcheva A, Buchbauer G, Golbraikh A, Wolschann P. QSAR modeling of r-campholenic derivatives with sandalwood odor. *J Chem Inf Comput Sci.* 2003; 43:259-266.
18. Kovatcheva A, Golbraikh A, Oloff S, Xiao Y, Zheng W, Wolschan P, Buchbauer G, Tropsha A. Combinatorial QSAR of ambergris fragrance compounds. *J Chem Inf Comput Sci.* 2004; 44:582-595.
19. Paliwal SK, Pal M, Siddiqui AA. Quantitative structure activity relationship analysis of angiotensin II AT1 receptor antagonists. *Med Chem Res.* 2010; 19:475-489.
20. Shen M, LeTiran A, Xiao Y, Golbraikh A, Kohn H, Tropsha A. Quantitative structure-activity relationship analysis of functionalized amino acid anticonvulsant agents using κ nearest-neighbor and simulated annealing PLS methods. *J Med Chem.* 2002; 7:2811-2823.
21. Kim KH. Outliers in SAR and QSAR: 2. Is a flexible binding site a possible source of outliers? *J Comput Aided Mol Des.* 2007; 21:421-435.
22. Paliwal S, Narayan A, Paliwal S. Quantitative structure activity relationship analysis of dicationic diphenylisoxazole as potent anti-trypanosomal agents. *QSAR Comb Sci.* 2009; 28:1367-1375.
23. Cramer RD. Partial least squares (PLS): Its strengths and limitations. *Perspect Drug Discov Des.* 1993; 1:269-278.
24. Hawkins DM, Basak SC, Mills D. Assessing model fit by

- cross-validation. *J Chem Inf Comput Sci.* 2003; 43:579-586.
25. Fonquerna S, Miralpeix M, Pagès L, Puig C, Cardús A, Antón F, Vilella D, Aparici M, Prieto J, Warreilow G, Beleta J, Ryder H. Synthesis and structure-activity relationships of piperidinylpyrrolopyridine derivatives as potent and selective H₁ antagonists. *Bio Med Chem Lett.* 2005; 15:1165-1167.
26. Paliwal S, Das S, Yadav D, Saxena M, Paliwal S. Quantitative structure activity relationship (QSAR) of N⁶-substituted adenosine receptor agonists as potential antihypertensive agents. *Med Chem Res.* 2011; 20:1643-1649.
27. *Molecular Descriptors in QSAR/QSPR* (Karelson M, ed.). Wiley Interscience, New York, NY, USA, 2000; pp. 220-221.
28. Paliwal S, Seth D, Yadav D, Yadav R, Paliwal S. Development of a robust QSAR model to predict the affinity of pyrrolidine analogs for dipeptidyl peptidase IV (DPP- IV). *J Enzyme Inhib Med Chem.* 2011; 26:129-140.
29. Ohta K, Hayashi H, Mizuguchi H, Kagamiyama H, Fujimoto K, Fukui H. Site-directed mutagenesis of the histamine H₁ receptor: Roles of aspartic acid 107, asparagine198 and threonine194. *Biochem Biophys Res Commun.* 1994; 203:1096-1101.
30. Gillard M, Van Der Perren C, Moguilevsky N, Massingham R, Chatelain P. Binding characteristics of cetirizine and levocetirizine to human H(1) histamine receptors: Contribution of Lys(191) and Thr(194). *Mol Pharmacol.* 2002; 61:391-399.
31. Kier LB. Shape indexes of orders one and three from molecular graphs. *Mol Inform.* 1986; 5:1-7.
32. Kier LB. Distinguishing atom differences in a molecular graph shape index. *Mol Inform.* 1986; 5:7-12.
- (Received December 5, 2011; Revised February 10, 2012; Re-revised March 16, 2012; Accepted April 3, 2012)*

Synthesis, analgesic, anti-inflammatory and ulcerogenic properties of some novel *N'*-((1-(substituted amino)methyl)-2-oxoindolin-3-ylidene)-4-(2-(methyl/phenyl)-4-oxoquinazolin-3(4*H*)-yl)benzohydrazide derivatives

Govindaraj Saravanan^{1,*}, Veerachamy Alagarsamy², Chinnasamy Rajaram Prakash³

¹ Medicinal Chemistry Research Laboratory, Bapatla College of Pharmacy, Jawaharlal Nehru Technological University, Hyderabad, Andhra Pradesh, India;

² Medicinal Chemistry Research Laboratory, M.N.R. College of Pharmacy, Sangareddy, Andhra Pradesh, India;

³ Department of Medicinal Chemistry, DCRM Pharmacy College, Inkollu, Andhra Pradesh, India.

ABSTRACT: A new series of *N'*-((1-(substituted amino)methyl)-2-oxoindolin-3-ylidene)-4-(2-(methyl/phenyl)-4-oxoquinazolin-3(4*H*)-yl)benzohydrazide derivatives 4a-4l were designed and synthesized from anthranilic acid. All the synthesized compounds were characterized by spectroscopic means and elemental analyses. The tail-flick technique and the carrageenan-induced foot paw edema test were performed for screening analgesic and anti-inflammatory activity, respectively. All of the compounds were also examined for their ulcerogenicity. Some of the compounds showed significant activity. Among the test compounds, 4b exhibited 53% and 69% analgesic activity at a dose of 10 and 20 mg/kg, respectively. It also displayed 47% (10 mg/kg) and 65% (20 mg/kg) anti-inflammatory activity with one-fourth of ulcer index of the reference drugs diclofenac and aspirin.

Keywords: Quinazolinone, isatin, schiff base, mannich base, analgesic, anti-inflammatory

1. Introduction

Inflammation is a defensive but exaggerated local tissue reaction in response to exogenous or endogenous insult. It is a fundamental physiological process that is not only essential for survival but at the same time is one of the major causes of human morbidity and mortality (1,2). A large number of non-steroidal anti-inflammatory drugs (NSAIDs) are available clinically to treat inflammatory

disorders. NSAIDs are one of the most widely used drug categories against inflammation, mild to moderate pain and fever. In the past decade, numerous advances have taken place in the understanding of pathogenesis and as a result, significant progress has been made and is still being explored for the development of novel NSAIDs (3). Prostaglandin synthetase or cyclooxygenase (COX) is an enzyme which catalyzes the rate limiting steps in the biosynthesis of cyclic endoperoxides from arachidonic acid to form prostaglandins (PGs). The most important mechanism of NSAIDs is considered to be primarily by inhibition of PGs synthesis; specifically competitive inhibition of COX (4). Generally, the NSAIDs inhibit both isoforms COX-1 and COX-2. Most NSAIDs are mainly COX-1 selective (e.g., indomethacin, aspirin, ketoprofen, piroxicam, and sulindac). The mechanism of action of celecoxib and rofecoxib is primarily selective inhibition of COX-2 (5). Others are considered to have mixed action on COX-1 and -2 (e.g., ibuprofen, naproxen, diclofenac, etodolac, nabumetone, and meloxicam). Other mechanisms that may contribute to NSAID mediated anti-inflammatory activity include the reduction of superoxide radicals, induction of apoptosis, inhibition of adhesion molecule expression, decrease of nitric oxide synthase, decrease of proinflammatory cytokine levels (tumor necrosis factor- α , interleukin-1), modification of lymphocyte activity, and alteration of cellular membrane functions (6). However, long term clinical usages of NSAIDs are associated with significant side effects such as severe gastrointestinal ulceration, bleeding, intolerance and nephrotoxicity (7,8). Therefore, investigation of new NSAIDs is still a major challenge and production of safer and more active NSAIDs and analgesic drugs are needed.

Quinazoline and quinazolinone nuclei have drawn great attention due to their wide range of chemotherapeutic activities (9-15). Additionally, different known anti-inflammatory drugs such as proquazone I, fluoroquazone II, and tryptanthrin III contain the quinazoline nucleus (Figure 1) (16-19). Also, it has been

*Address correspondence to:

Mr. Govindaraj Saravanan, Medicinal Chemistry Research Laboratory, Bapatla College of Pharmacy, Jawaharlal Nehru Technological University, Hyderabad, Andhra Pradesh, India.

E-mail: sarachem1981@gmail.com

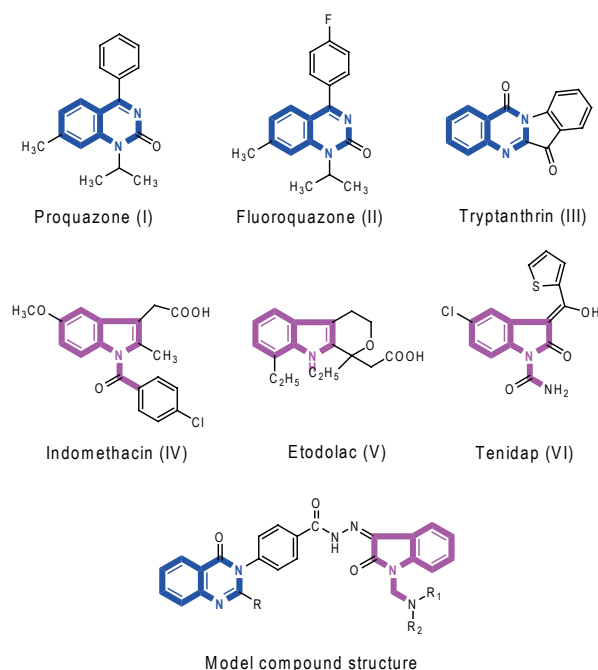


Figure 1. Some of the well established structures of NSAID and our model compound with its common pharmacophore features.

reported that the substitution pattern by different aryl or heteroaryl moieties at 2/3 position of the quinazolinone nucleus markedly influences analgesic and anti-inflammatory activity (20).

On the other hand the indole skeleton exists in a variety of natural products and is the precursor for many pharmaceuticals, such as indomethacin IV, etodolac V, and tenidap VI (Figure 1). In recent decades, the literature has been enriched with progressive findings about synthesis and pharmacological activities of isatin (oxidized form of indole) ring, which is a core structure in various synthetic pharmaceuticals displaying a wide variety of biological activities (21-27).

Based on the above observations and in continuation of our anti-inflammatory and analgesic drug research program (28,29), it was of interest to synthesize a novel series of quinazolinone derivatives with structure modifications involving incorporation of isatin moieties at the 3rd position and a methyl/phenyl group at the 2nd position of the quinazolinone ring as a trial to obtain safer and potent anti-inflammatory and analgesic agents. The ulcerogenic activity of the compounds was also determined.

2. Materials and Methods

2.1. Chemistry

The chemicals and reagents used were obtained from various chemical units Merck India Ltd., Qualigens, CDH, and SD Fine Chem. All solvents used were of laboratory research (LR) grade and purified before use.

All reaction steps were monitored until completion using thin layer chromatography (TLC). An iodine chamber and UV lamp were used for visualization of TLC spots. All melting points were performed in open glass capillary tubes and were uncorrected. ¹H-NMR spectra were performed on a Bruker ultra shield (300 MHz) NMR spectrometer in CDCl₃ using tetramethylsilane [(CH₃)₄Si] as an internal standard. Chemical shifts (δ) were expressed as parts per million (ppm). The multiplicities of the signals in the ¹H-NMR spectra were abbreviated by s (singlet), t (triplet), q (quartet), and m (multiplet). The *J* constant was given in Hz. Mass spectra were obtained on a JEOL-SX-102 instrument using electron impact ionization. All IR spectra were recorded in KBr pellets on a Jasco FT-IR 410 spectrometer. Elemental analyses were performed on a PerkinElmer model 240C analyzer and were within ± 0.4% of the theoretical values.

2.1.1. Synthesis of 2-(methyl/phenyl)-4H-benzo[1,3]oxazin-4-one (1a, 1b)

For the synthesis of the 2-methyl derivative: A mixture of anthranilic acid (1.37 g, 0.01 mol) and acetic anhydride (10.2 mL, 0.1 mol) was refluxed on a gentle flame for 1 h. The excess acetic anhydride was distilled off under reduced pressure and the residue was dissolved in petroleum ether and was kept aside for 1 h. The light brown solid **1a** obtained was filtered and dried (28).

For synthesis of the 2-phenyl derivative: To a solution of anthranilic acid 13.7 g (0.1 mol) dissolved in pyridine (60 mL), benzoyl chloride 28 g (0.2 mol) was added and the mixture was stirred for 30 min at room temperature followed by treatment with 5% NaHCO₃ (15 mL). The solid thus obtained **1b** was recrystallized from ethanol (29).

2.1.2. Synthesis of 4-(2-(methyl/phenyl)-4-oxoquinazolin-3(4H)-yl)benzohydrazide (2a, 2b)

A mixture of 2-(methyl/phenyl)-4H-benzo[1,3]oxazin-4-one **1a/1b** (1.61/2.23 g, 0.01 mol) and *p*-aminobenzohydrazide (1.51 g, 0.01 mol) was dissolved in anhydrous pyridine (50 mL) and heated on a sand bath for 10 h. The resulting solution was cooled in an ice bath and treated with dilute hydrochloric acid (100 mL). The product separated **2a/2b** was filtered, washed with water, and crystallized from ethanol.

2.1.3. Synthesis of 4-(2-(methyl/phenyl)-4-oxoquinazolin-3(4H)-yl)-N'-(2-oxoindolin-3-ylidene)benzohydrazide (3a, 3b)

Equimolar quantities of 4-(2-(methyl/phenyl)-4-oxoquinazolin-3(4H)-yl)benzohydrazide **2a/2b** (2.94/3.56 g, 0.01 mol) and isatin (1.47 g, 0.01 mol) were dissolved in warm ethanol (30 mL) and heated on

a steam bath for 1 h. After standing for approximately 24 h at room temperature, the crystalline products **3a/3b** were separated by filtration, dried under vacuum pressure and recrystallised from ethanol.

2.1.4. General procedure for the synthesis of *N'*-((1-(substituted amino)methyl)-2-oxoindolin-3-ylidene)-4-(2-(methyl/phenyl)-4-oxoquinazolin-3(4*H*)-yl)benzohydrazide (**4a-4l**)

To a solution of the derivative **3a/3b** (4.23/4.85 g, 0.01 mol) in glacial acetic acid (50 mL) containing 37% formalin (1 mL), the appropriate secondary amine derivative (0.02 mol) was added. The reaction mixture was refluxed on a water bath for 1-3 h. The reaction mixture was concentrated to approximately half the initial volume, and the resulting precipitate was recrystallized from ethanol to get a pure form of the product. The method used for the preparation and isolation of the compounds gave materials of good purity, as evidenced by their spectral analyses and by TLC. The spectral data for the title compounds **4a-4l** are presented in the appendix.

2.2. Animals

The animals used in the present study were Swiss albino mice weighing 20-25 g and Wistar rats weighing 150-200 g were procured from Bapatla College of Pharmacy, Bapatla, India. Animals were maintained in colony cages at $25 \pm 2^\circ\text{C}$, relative humidity of 45-55%, maintained under 12 h light and dark cycle and were fed standard animal feed (30) and water *ad libitum*. Animals were maintained under standard conditions in an animal house approved by the committee for the purpose of control and supervision on experiments on animals (CPCSEA). The protocol was approved by the Institutional Animal Ethics Committee. All animals were acclimatized to laboratory conditions for a week before use.

The synthesized compounds were evaluated for analgesic, anti-inflammatory and ulcerogenic activities. One-way analysis of variance (ANOVA) was performed to obtain significance for all exhibited activities. Test compounds and standard drugs were administered in the form of a suspension (1% carboxy methyl cellulose as a vehicle) by the oral route for analgesic and anti-inflammatory studies and as a suspension of 10% (v/v) Tween-80 by the intraperitoneal route of administration for ulcerogenicity studies.

2.3. Analgesic activity

The analgesic activity was performed by the tail-flick technique using Wistar albino mice (25-35 g) of either sex selected by a random sampling technique (31,32). Diclofenac sodium at a dose level of 10 and 20 mg/kg was administered orally as a reference drug for comparison. The test compounds at two dose levels (10 and 20 mg/kg) were

administered orally. The reaction times were recorded at 30 min, 1, 2, and 3 h after treatment and the cut-off time was 10 sec. The percent analgesic activity (PAA) was calculated by the following formula: $\text{PAA} = \frac{[T_2 - T_1/10 - T_1]}{T_1} \times 100$; where T_1 is the reaction time (sec) before treatment, and T_2 is the reaction time (sec) after treatment.

2.4. Anti-inflammatory activity

Anti-inflammatory activity was evaluated by the carrageenan-induced paw edema test in rats (33). Diclofenac sodium at 10 and 20 mg/kg was administered as a reference drug for comparison. The test compounds were administered at two dose levels (10 and 20 mg/kg). The paw volumes were measured using the mercury displacement technique with the help of a plethysmograph immediately before and 30 min, 1, 2, and 3 h after carrageenan injection. The percent inhibition of paw edema was calculated according to the following formula: percent inhibition $I = 100 \times [1 - (a - x)/(b - y)]$ where x is the mean paw volume of rats before the administration of carrageenan and the test compounds or the reference drug (test group), a is the mean paw volume of rats after the administration of carrageenan in the test group (drug treated), b is the mean paw volume of rats after the administration of carrageenan in the control group, y is the mean paw volume of rats before the administration of carrageenan in the control group.

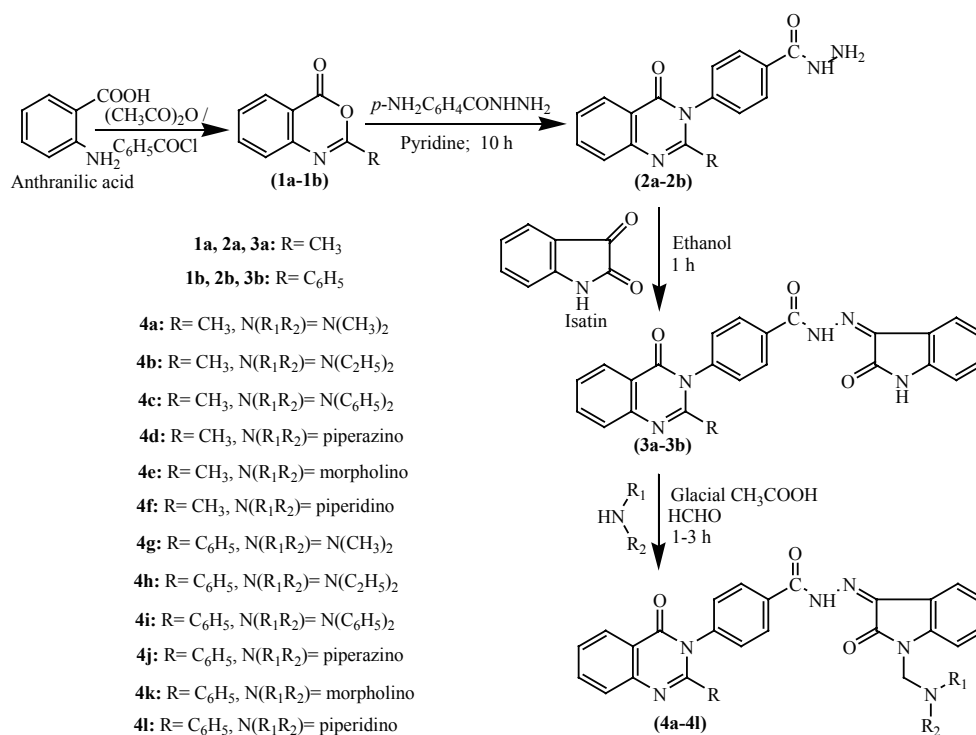
2.5. Ulcerogenicity

Ulceration in rats was induced as reported by Goyal *et al.* (34). Albino Wistar rats weighing 150-200 g of either sex were divided into various groups of six animals each. The control group of animals was only given 10% (v/v) Tween-80 suspension intraperitoneally. One group was administered with aspirin intraperitoneally at a dose of 200 mg/kg once daily for three days. Diclofenac was also administered as a standard drug at 20 mg/kg once daily for three days to another group of animals by the same route. The remaining group of animals was given the test compounds intraperitoneally at a dose of 20 mg/kg. On the fourth day, the pylorus was ligated using the method of Shay *et al.* (35). Animals were fasted for 36 h before the pylorus ligation procedure. The animals were sacrificed four hours post ligation. The stomach was removed and opened along with the greater curvature. Ulcer index was determined by the method of Ganguly and Bhatnagar (36).

3. Results and Discussion

3.1. Chemistry

The synthetic pathway giving access to the titled compounds **4a-4l** is represented in Scheme 1. Initially, 2-(methyl/phenyl)-4*H*-benzo[1,3]oxazin-



Scheme 1. Synthetic protocol of title compounds.

4-one **1a/1b** were synthesized from anthranilic acid using acetic anhydride/benzoyl chloride by a simple acetylation/benzoylation followed by a ring closure reaction. In the subsequent step, 4-(2-(methyl/phenyl)-4-oxoquinazolin-3(4*H*)-yl)benzohydrazide **2a/2b** were synthesized by a simple reaction of compounds **1a/1b** with *p*-aminobenzohydrazide with elimination of a water molecule. Before the final step, Schiff bases **3a/3b** were synthesized by nucleophilic addition of the amino derivatives **2a/2b** with the carbonyl compound isatin in ethanol. This reaction was followed by dehydration to generate compounds **3a/3b** by forming a stable imine. In the last step, the title compounds **4a-4l** were synthesized through a Mannich reaction by treating compound **3a/3b** with formaldehyde and secondary amines like dimethylamine, diethylamine, diphenylamine, piperazine, morpholine, and piperidine. The physicochemical parameters of all the synthesized compounds are summarized in Table 1. The structures of the synthesized compounds were confirmed by spectral (IR, ¹H-NMR, and Mass) and elemental analyses data.

3.2. Analgesic activity

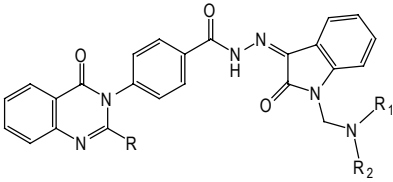
Using Wistar albino mice analgesic activity for title compounds **4a-4l** was carried out by the tail-flick technique. The results obtained from the above study are summarized in Table 2. The results of analgesic activity indicate that all the test compounds exhibited a graded dose response and not all of them are significant but some of them gave significant activity. Moreover, this study revealed that test compounds showed moderate

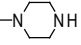
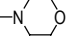
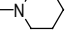
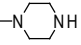
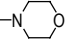
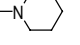
analgesic activity at 30 min of reaction time; the activity increased at 1 h, further it reached to peak level at 2 h and it decreased again at 3 h. Compound **4a** and **4g** with dimethyl substitution showed good activity. With the increased lipophilicity (diethyl group), compounds **4b** and **4h** showed an increase in activity. Substitution with alicyclic amine (piperidine) in **4f** and **4l** further increases the lipophilicity and retains the activity of diethyl substitution. The presence of an additional hetero atom such as nitrogen and oxygen in the alicyclic amine rings such as: (piperazine and morpholine) in **4d**, **4e**, **4j**, and **4k** led to a decrease in activity which might be due to a fall in lipophilicity. Aromatic substitution (diphenyl group) in **4c** and **4i** showed lower activity. The compounds with aliphatic substitution **4a**, **4b**, **4g**, and **4h** had shown better activity than the rest of the compounds **4c-4f** and **4i-4l** with alicyclic amine or aromatic substitution. Compounds **4b**, **4f**, **4h**, and **4l** were found to be the most active analgesic agents and they are almost equal or moderately more potent when compared to the reference standard diclofenac sodium.

3.3. Anti-inflammatory activity

Anti-inflammatory activity was performed by the carrageenan-induced paw edema test in rats. The anti-inflammatory activity results (Table 3) showed that all test compounds protected rats from carrageenan-induced inflammation reasonably at 30 min of reaction time; the activity increased at 1 h and it reached the maximum level at 2 h. Declining activity was observed at 3 h. The compounds possessing dimethyl amino substituents **4a**

Table 1. Synthesized compounds 4a-4l



Compound	-R	-N(R ₁ R ₂)	Mol. formula	% Yield	Mp (°C)	R _f ^a
4a	-CH ₃	-N(CH ₃) ₂	C ₂₇ H ₂₄ N ₆ O ₃	75	223-225	0.65
4b	-CH ₃	-N(C ₂ H ₅) ₂	C ₂₉ H ₂₈ N ₆ O ₃	72	256-258	0.72
4c	-CH ₃	-N(C ₆ H ₅) ₂	C ₃₇ H ₂₈ N ₆ O ₃	78	280-282	0.49
4d	-CH ₃		C ₂₉ H ₂₇ N ₇ O ₃	70	237-239	0.84
4e	-CH ₃		C ₂₉ H ₂₆ N ₆ O ₄	74	244-246	0.58
4f	-CH ₃		C ₃₀ H ₂₈ N ₆ O ₃	81	219-221	0.78
4g	-C ₆ H ₅	-N(CH ₃) ₂	C ₃₂ H ₂₆ N ₆ O ₃	78	265-268	0.68
4h	-C ₆ H ₅	-N(C ₂ H ₅) ₂	C ₃₄ H ₃₀ N ₆ O ₃	72	252-254	0.61
4i	-C ₆ H ₅	-N(C ₆ H ₅) ₂	C ₄₂ H ₃₀ N ₆ O ₃	71	229-231	0.70
4j	-C ₆ H ₅		C ₃₄ H ₂₉ N ₇ O ₃	75	286-288	0.45
4k	-C ₆ H ₅		C ₃₄ H ₂₈ N ₆ O ₄	77	248-251	0.54
4l	-C ₆ H ₅		C ₃₅ H ₃₀ N ₆ O ₃	70	212-214	0.80

^a Solvent system used was ethylacetate/hexane/formic acid (4:2:4, v/v).

Table 2. Analgesic activity of the synthesized compounds (Tail-flick method)

Compound	Dose (mg/kg)	Analgesic activity (%)			
		30 min	1 h	2 h	3 h
4a	10	35 ± 0.93*	41 ± 1.36*	45 ± 0.90*	33 ± 0.26*
	20	46 ± 0.51*	54 ± 0.51**	62 ± 0.33**	39 ± 0.62*
4b	10	40 ± 1.07**	48 ± 1.16*	53 ± 0.71*	37 ± 1.42**
	20	53 ± 0.90*	62 ± 0.48***	69 ± 0.79**	46 ± 1.53*
4c	10	25 ± 1.64*	29 ± 0.26*	34 ± 1.45*	24 ± 1.72*
	20	32 ± 1.55*	41 ± 1.21*	44 ± 1.86*	25 ± 1.89*
4d	10	30 ± 0.78*	36 ± 0.79*	41 ± 1.74*	29 ± 1.40*
	20	41 ± 1.22*	52 ± 1.37*	56 ± 1.42**	33 ± 1.19*
4e	10	28 ± 1.63*	35 ± 0.56*	39 ± 1.21*	27 ± 1.82*
	20	38 ± 0.81*	46 ± 1.16*	50 ± 1.64*	28 ± 1.36**
4f	10	37 ± 0.96***	47 ± 1.52*	49 ± 0.58**	33 ± 1.18*
	20	50 ± 1.94*	58 ± 2.02*	66 ± 1.22**	44 ± 0.61**
4g	10	33 ± 1.69**	38 ± 0.56*	44 ± 0.95*	32 ± 1.29*
	20	45 ± 0.67*	54 ± 1.27**	60 ± 0.74*	36 ± 1.62**
4h	10	38 ± 1.60*	47 ± 1.52**	50 ± 1.61*	35 ± 1.18*
	20	51 ± 0.51**	59 ± 1.41**	68 ± 1.73***	44 ± 1.10*
4i	10	22 ± 2.12*	27 ± 0.68*	30 ± 1.09*	20 ± 1.76*
	20	30 ± 1.39*	38 ± 1.67*	43 ± 1.28*	23 ± 0.61*
4j	10	29 ± 0.67*	34 ± 2.43*	38 ± 1.46*	27 ± 1.39*
	20	40 ± 0.52*	49 ± 1.16**	53 ± 0.87*	29 ± 1.67*
4k	10	27 ± 1.38*	33 ± 1.38*	36 ± 0.56**	26 ± 1.57*
	20	37 ± 1.09*	48 ± 0.69*	51 ± 2.10*	28 ± 0.75*
4l	10	34 ± 0.81**	45 ± 1.47*	49 ± 1.35**	31 ± 1.80*
	20	48 ± 0.64*	55 ± 1.59**	65 ± 0.57**	40 ± 1.52*
Control	--	3 ± 0.39	6 ± 0.52	5 ± 0.63	4 ± 0.43
Diclofenac	10	36 ± 1.52**	43 ± 1.31*	47 ± 1.87**	34 ± 1.16*
	20	48 ± 0.68*	57 ± 1.47***	63 ± 0.55*	39 ± 0.74**

Each value represents the mean ± SEM (n = 6).

Significance levels * p < 0.5, ** p < 0.01, *** p < 0.001 as compared with the respective control.

Table 3. Antiinflammatory activity (Carrageenan induced paw edema test in rats) and ulcer index of the synthesized compounds

Compound	Dose (mg/kg)	Anti-inflammatory activity (%)				Ulcer index
		30 min	1 h	2 h	3 h	
4a	10	31 ± 0.91*	38 ± 0.64**	42 ± 1.41*	30 ± 1.53*	0.55 ± 0.32
	20	42 ± 1.62*	50 ± 1.35*	61 ± 1.25**	39 ± 0.58*	
4b	10	36 ± 1.78*	44 ± 1.05*	47 ± 1.64**	39 ± 1.39*	0.46 ± 0.24
	20	47 ± 0.63*	58 ± 0.79***	65 ± 1.57*	48 ± 1.27**	
4c	10	16 ± 1.53*	20 ± 1.28*	29 ± 1.24*	19 ± 1.65*	0.64 ± 0.29
	20	25 ± 0.39*	36 ± 0.62*	41 ± 1.66*	25 ± 1.14*	
4d	10	24 ± 1.50*	30 ± 1.64*	34 ± 1.51*	25 ± 0.73*	0.88 ± 0.57
	20	33 ± 1.07**	42 ± 1.90*	50 ± 0.74*	31 ± 1.45*	
4e	10	21 ± 0.72*	26 ± 0.77*	32 ± 1.73*	24 ± 1.41*	0.70 ± 0.44
	20	31 ± 0.59*	39 ± 1.26*	46 ± 1.29*	28 ± 1.27*	
4f	10	25 ± 0.96*	33 ± 1.39*	36 ± 1.41*	27 ± 1.55**	0.76 ± 0.50
	20	36 ± 1.35**	45 ± 1.71*	54 ± 1.78**	34 ± 0.65*	
4g	10	28 ± 1.72**	36 ± 1.42***	39 ± 1.65*	28 ± 1.03*	0.56 ± 0.39
	20	40 ± 0.61*	49 ± 1.89*	58 ± 1.93**	39 ± 2.07**	
4h	10	34 ± 1.46**	40 ± 0.51*	42 ± 0.83*	38 ± 1.28*	0.49 ± 0.27
	20	45 ± 1.22*	54 ± 1.31**	63 ± 1.26***	48 ± 1.19*	
4i	10	15 ± 0.37*	18 ± 1.54*	26 ± 1.52*	17 ± 1.75*	0.68 ± 0.24
	20	23 ± 0.72*	32 ± 1.82*	39 ± 1.18*	20 ± 0.71*	
4j	10	22 ± 1.55*	27 ± 1.71**	33 ± 1.47*	23 ± 1.19*	0.92 ± 0.60
	20	30 ± 0.44*	41 ± 0.94*	48 ± 1.82*	28 ± 1.42*	
4k	10	19 ± 0.80*	23 ± 1.65*	30 ± 1.44*	21 ± 1.51*	0.72 ± 0.41
	20	28 ± 1.45*	37 ± 1.37**	42 ± 1.34*	26 ± 1.64*	
4l	10	24 ± 0.71*	31 ± 1.84*	34 ± 1.62*	26 ± 1.36*	0.77 ± 0.35
	20	34 ± 1.52*	44 ± 1.13**	51 ± 0.93*	30 ± 1.15**	
Control	--	4.1 ± 0.62	6.4 ± 0.95	4.9 ± 0.43	3.2 ± 0.58	0.13 ± 0.07
Diclofenac	10	30 ± 0.82**	36 ± 0.99*	40 ± 1.40**	32 ± 1.62*	1.61 ± 0.53
	20	42 ± 1.27*	52 ± 1.28***	59 ± 1.28**	41 ± 1.29*	
Aspirin	200	--	--	--	--	1.79 ± 0.65

Each value represents the mean ± SEM ($n = 6$).

Significance levels * $p < 0.5$, ** $p < 0.01$, *** $p < 0.001$ as compared with the respective control.

and **4g** exhibited equipotent anti-inflammatory activity to the reference standard diclofenac sodium. With increased lipophilicity, compounds with diethyl amino substituents **4b** and **4h** showed moderately more potent activity than that of diclofenac sodium. Unlike analgesic activity, the replacement of these alkyl groups with the alicyclic amine (piperidine) in **4f** and **4l** led to a sharp decrease in activity. Placement of an additional hetero atom such as nitrogen and oxygen with the alicyclic amine (piperazine and morpholine) in **4d**, **4e**, **4j**, and **4k** showed a further decrease in activity. Among all the synthesized compounds, **4c** and **4i** with aromatic substitution (diphenyl amino group) exhibited the least activity. Moreover among the tested compounds, 2-methyl quinazolinone derivatives showed greater analgesic and anti-inflammatory activity than the corresponding 2-phenyl quinazolinone analogs.

3.4. Ulcerogenicity

In addition all test compounds were examined for ulcerogenicity and the results are summarized in Table 3. All test compounds exhibited ulcer indexes less than those obtained with the standard diclofenac and aspirin. Results of the ulcer index revealed that compounds bearing alkyl substituents **4a**, **4b**, **4g**, and **4h** showed a

negligible ulcer index, whereas the replacement of the methyl group with a phenyl group at the 2nd position of the quinazolinone ring led to a slight increase in the ulcer index. The other test compounds, **4d-4f** and **4j-4l** possessing alicyclic amines exhibited a higher ulcer index. The test compounds exhibited 29-57% and 26-51% of the ulcer index when compared to the reference drug diclofenac (1.61 ± 0.53) and aspirin (1.79 ± 0.65), respectively. Among the tested compounds, *N'*-(1-((diethylamino) methyl)-2-oxoindolin-3-ylidene)-4-(2-methyl-4-oxoquinazolin-3(4*H*)-yl)benzohydrazide **4b** exhibited the least ulcer index (0.46 ± 0.24) which is about one-fourth of the ulcer index of the reference standards. Out all of the tested compounds, *N'*-(2-oxo-1-(piperazin-1-ylmethyl)indolin-3-ylidene)-4-(4-oxo-2-phenylquinazolin-3(4*H*)-yl)benzohydrazide **4j** was found to possess the highest ulcer index (0.92 ± 0.60) which is about 54% of the ulcer index of diclofenac and aspirin.

4. Conclusion

In summary, a series of *N'*-(1-(substituted amino)methyl)-2-oxoindolin-3-ylidene)-4-(2-(methyl/phenyl)-4-oxoquinazolin-3(4*H*)-yl)benzohydrazide derivatives **4a-4l** were synthesized and characterized

by IR, ¹H-NMR, mass spectroscopy and elemental analyses. Some of the test compounds exhibited significant analgesic and anti-inflammatory activity with a mild to moderate ulcer index. In general, it was found that 2-methyl quinazolinone analogs showed more potent activity than corresponding 2-phenyl quinazolinone derivatives. Also, quinazolinone derivatives bearing alkyl amino groups exhibited the best activity followed by derivatives bearing alicyclic amines whereas derivatives having aryl amino groups showed the least activity. Among all test compounds, *N*'-(1-((diethylamino)methyl)-2-oxoindolin-3-ylidene)-4-(2-methyl-4-oxoquinazolin-3(4*H*)-yl)benzohydrazide **4b** showed the most potent analgesic and anti-inflammatory activity which is more potent than that of the reference diclofenac. From this study we concluded that incorporation of an isatin moiety at the 3rd position and a methyl group at the 2nd position of the quinazolinone ring resulted in potent analgesic and anti-inflammatory activity with a minimal ulcer index. Hence, this analog could be developed as a new class of analgesic and anti-inflammatory agents. However, further structural modification should be planned to enhance their analgesic and anti-inflammatory activities with the low ulcerogenic index.

Acknowledgements

The authors gratefully acknowledge the management of Bapatla College of Pharmacy for providing infrastructure facilities to carry out this research work. The authors also want to thank the Central Instrumentation Facility, IIT Chennai, India for the spectral analysis of the compounds used in this study.

References

- O'Neill LA. Targeting signal transduction as a strategy to treat inflammatory diseases. *Nat Rev Drug Discov.* 2006; 5:549-563.
- Cheeseright TJ, Holm M, Lehmann F, Luik S, Gottert M, Melville JL, Laufer S. Novel lead structures for p38 MAP kinase *via* field screen virtual screening. *J Med Chem.* 2009; 52:4200-4209.
- Bhandari SV, Dangre SC, Bothara KG, Patil AA, Sarkate AP, Lokwani DK, Gore ST, Deshmane BJ, Raparti VT, Khachane CV. Design, synthesis and pharmacological screening of novel nitric oxide donors containing 1,5-diarylpyrazolin-3-one as nontoxic NSAIDs. *Eur J Med Chem.* 2009; 44:4622-4636.
- Chao EY, Caravella JA, Watson MA, *et al.* Structure-guided design of *N*-phenyl tertiary amines as trans repression-selective liver X receptor modulators with anti-inflammatory activity. *J Med Chem.* 2008; 51:5758-5765.
- Laufer SA, Hauser DRJ, Domeyer DM, Kinkel K, Liedtke AJ. Design, synthesis and biological evaluation of novel tri and tetra substituted imidazoles as highly potent and specific ATP-mimetic inhibitors of p38 MAP kinase: Focus on optimized interactions with the enzyme's surface-exposed front region. *J Med Chem.* 2008; 51:4122-4149.
- Hynes JJ, Dyckman AJ, Lin S, *et al.* Design, synthesis and anti-inflammatory properties of orally active 4-(phenylamino)-pyrrolo[2,1-*f*][1,2,4]triazine p38 α mitogen-activated protein kinase inhibitors. *J Med Chem.* 2008; 51:4-16.
- Anre RV, Cendilkumar A, Goli D, Anahale GS, Oswal RJ. Microwave assisted synthesis of novel pyrazolone derivatives attached to a pyrimidine moiety and evaluation of their anti-inflammatory, analgesic and antipyretic activities. *Saudi Pharma Journal.* 2011; 19:233-243.
- Amin KM, Kamel MM, Anwar MM, Khedr M, Syam YM. Synthesis, biological evaluation and molecular docking of novel series of spiro [(2*H*,3*H*)-quinazolin-2,1'-cyclohexan]-4(1*H*)-one derivatives as anti-inflammatory and analgesic agents. *Eur J Med Chem.* 2010; 45:2117-2131.
- Kumar P, Shrivastava B, Pandeya SN, Stables JP. Design, synthesis and potential 6 Hz psychomotor seizure test activity of some novel 2-(substituted)-3-([substituted] amino)quinazolin-4(3*H*)-one. *Eur J Med Chem.* 2011; 46:1006-1018.
- Abdel Gawad NM, Georgey HH, Youssef RM, El-Sayed NA. Synthesis and antitumor activity of some 2,3-disubstituted quinazolin-4(3*H*)-ones and 4,6-disubstituted-1,2,3,4-tetra hydroquinazolin-2*H*-ones. *Eur J Med Chem.* 2010; 45:6058-6067.
- Pattan SR, Krishna Reddy VV, Manvi FV, Desai BG, Bhat AR. Synthesis of *N*-3[4(4-chlorophenylthiazol-2-yl)-2-aminomethyl]quinazolin-4(3*H*)-one and their derivatives for antitubercular activity. *Indian J Chem.* 2006; 45B:1778-1781.
- Dinakaran M, Selvam P, Declercq E, Sridhar SK. Synthesis, antiviral and cytotoxic activity of 6-bromo-2,3-disubstituted-4(3*H*)-quinazolinones. *Biol Pharm Bull.* 2003; 26:1278-1282.
- Mohamed MS, Kamel MM, Kassem EMM, Abotaleb N, Abd El-moez SI, Ahmed MF. Novel 6,8-dibromo-4(3*H*)-quinazolinone derivatives of antibacterial and antifungal activities. *Eur J Med Chem.* 2010; 45:3311-3319.
- Shukla JS, Shukla R. Synthesis of 4-(5-substituted arylidene-4-thiazolidinone-2-thione)-6,8-substituted quinazolines as potential antihelmintic agents. *J Indian Chem Soc.* 1989; 66:209-210.
- Alagarsamy V, Rajasolomon V, Meena R, Ramseshu KV. Synthesis, analgesic, anti-inflammatory and antibacterial activities of some novel 2-butyl-3-substituted quinazolin-4(3*H*)-ones. *Biol Pharmac Bull.* 2005; 28:1091-1094.
- Vanryzin RJ, Trpold JH. The toxicology profile of the anti-inflammatory drug proquazone in animals. *Drug Chem Toxicol.* 1980; 3:361-379.
- Wheatly D. Analgesic properties of fluproquazone. *Rheumatol Rehabil.* 1982; 21:98-100.
- Fankhauser S, Laube W, Marti HR, Schultheis HR, Vogtlin J, Graf-fenried BV. Antipyretic activity of fluproquazone in man. *Arzneimittelforschung.* 1981; 31:934-935.
- Oberthur C, Hamburger M. Tryptanthrin content in *Isatis tinctoria* leaves – A comparative study of selected strains and post harvest treatments. *Planta Med.* 2004; 70:642-645.
- Kumar A, Verma RS, Jaju BP, Sinha JN. Quinazolinylypyrazolines as anti-inflammatory agents. *J Indian Chem Soc.* 1990; 67:920-921.

21. Muthukumar VA, George S, Vaidhyalingam V. Synthesis and pharmacological evaluation of 1-(1-((substituted)methyl)-5-methyl-2-oxoindolin-3-ylidene)-4-(substitutedpyridin-2-yl)thio semicarbazide. *Biol Pharm Bull.* 2008; 31:1461-1464.
22. Sridhar SK, Ramesh A. Synthesis and pharmacological activities of Schiff bases and hydrazones of Isatin derivatives. *Indian Drugs.* 2001; 38:174-180.
23. Kang IJ, Wang LW, Hsu TA, Yueh A, Lee CC, Lee YC, Lee CY, Chao YS, Shih SR, Chern JH. Isatin- β -thiosemicarbazones as potent herpes simplex virus inhibitors. *Bioorg Med Chem Lett.* 2011; 21:1948-1952.
24. Gudipati R, Anreddy RNR, Sarangapani M. Synthesis, characterization and anticancer activity of certain 3-{4-(5-mercapto-1,3,4-oxadiazole-2-yl)phenylimino}indolin-2-one derivatives. *Saudi Pharma Journal.* 2011; 19:153-158.
25. Banerjee D, Yogeewari P, Bhat P, Thomas A, Srividya M, Sriram D. Novel isatinyl thiosemicarbazones derivatives as potential molecule to combat HIV-TB co-infection. *Eur J Med Chem.* 2011; 46:106-121.
26. Singh DP, Kumar K, Sharma C. New 14-membered octaazamacrocyclic complexes: Synthesis, spectral, antibacterial and antifungal studies. *Eur J Med Chem.* 2010; 45:1230-1236.
27. Hans RH, Wiid IJF, Van Helden PD, Wan B, Franzblau SG, Gut J, Rosenthal PJ, Chibale K. Novel thiolactone-isatin hybrids as potential antimalarial and antitubercular agents. *Bioorg Med Chem Lett.* 2011; 21:2055-2058.
28. Alagarsamy V, Muruganatham G, Venkateshaperumal R. Synthesis, analgesic, anti-inflammatory and antibacterial activities of some novel 2-methyl-3-substituted quinazolin-4(3H)-ones. *Biol Pharm Bull.* 2003; 26:1711-1714.
29. Alagarsamy V, Rajasolomon V, Vanikavitha G, Paluchamy V, Ravichandran M, Arnoldsujin A, Thangathirupathi A, Amuthalakshmi S, Revathi R. Synthesis, analgesic, anti-inflammatory and anti-bacterial activities of some novel 2-phenyl-3-substituted quinazolin-4(3H)-ones. *Biol Pharm Bull.* 2002; 25:1432-1435.
30. Guide to the care and use of experimental animals (Olfert ED, Cross BM, McWilliam AA, eds.), Vol. 1. 2nd ed., Canadian Council of Animal Care, 1993.
31. Kulkarni SK. Heat and other physiological stress-induced analgesia: Catecholamine mediated and naloxone reversible response. *Life Sci.* 1980; 27:185-188.
32. D'Amour FE, Smith DL. A method for determining loss of pain sensation. *J Pharmacol Exp Ther.* 1941; 72:74-79.
33. Winter CA, Risley EA, Nuss GW. Carrageenin induced edema in hind paw of the rat as an assay for anti-inflammatory drugs. *Proc Soc Exp Biol Med.* 1962; 111:544-547.
34. Goyal RK, Chakrabarti A, Sanyal AK. The effect of biological variables on the anti ulcerogenic effect of vegetable plantain banana. *Planta Med.* 1985; 29:85-88.
35. Shay M, Komarov SA, Fels D, Meranze D, Grunstein H, Siple H. A simple method for the uniform production of gastric ulceration in the rats. *Gastroenterology.* 1945; 5:43-61.
36. Ganguly AK, Bhatnagar OP. Effect of bilateral adrenalectomy on production of restraint ulcers in the stomach of albino rats. *Can J Physiol Pharmacol.* 1973; 51:748-750.

(Received January 7, 2012; Revised February 20, 2012; Re-revised April 16, 2012; Accepted April 16, 2012)

Appendix

Characterization data of the synthesized compounds in the current study

2-Methyl-4H-benzo[1,3]oxazin-4-one (1a). Yield: 71%; mp = 182°C; IR (KBr) ν_{\max} cm^{-1} : 3,096 (Ar-CH_{str}), 2,882 (CH₃-CH_{str}), 1,712 (C=O), 1,636 (C=N), 1,055 (C-O-Cstr); ¹H-NMR (300 MHz, CDCl₃): δ ppm: 2.38 (s, 3H, CH₃), 6.92-7.40 (m, 4H, Ar-H); MS (EI) m/z : 161 [M⁺]; Anal. Calcd. for C₉H₇NO₂: C, 67.07; H, 4.38; N, 8.69. Found: C, 67.16; H, 4.40; N, 8.66.

2-Phenyl-4H-benzo[1,3]oxazin-4-one (1b). Yield: 80%; mp = 120°C; IR (KBr) ν_{\max} cm^{-1} : 3,077 (Ar-CH_{str}), 1,751 (C=O), 1,625 (C=N), 1,038 (C-O-Cstr); ¹H-NMR (300 MHz, CDCl₃): δ ppm: 6.95-7.78 (m, 9H, Ar-H); MS (EI) m/z : 223 [M⁺]; Anal. Calcd. for C₁₄H₉NO₂: C, 75.33; H, 4.06; N, 6.27. Found: C, 75.42; H, 4.05; N, 6.29.

4-(2-Methyl-4-oxoquinazolin-3(4H)-yl)benzohydrazide (2a). Yield: 74 %; mp = 174-176°C; IR (KBr) ν_{\max} cm^{-1} : 3,363 (NH_{str}), 3,038 (Ar-CH_{str}), 2,932 (CH₃-CH_{str}), 1,725 (C=O of quinazoline), 1,650 (C=O of amide); ¹H-NMR (300 MHz, CDCl₃): δ ppm: 2.53 (s, 3H, CH₃), 3.86 (s, 2H, NH₂), 6.85-7.92 (m, 8H, Ar-H), 9.82 (s, 1H, CONH); MS (EI) m/z : 294 [M⁺]; Anal. Calcd. for C₁₆H₁₄N₄O₂: C, 65.30; H, 4.79; N, 19.04. Found: C, 65.54; H, 4.78; N, 18.97.

4-(4-Oxo-2-phenylquinazolin-3(4H)-yl)benzohydrazide (2b). Yield: 77%; mp = 159-161°C; IR (KBr) ν_{\max} cm^{-1} : 3,384 (NH_{str}), 3,077 (Ar-CH_{str}), 1,751 (C=O of quinazoline), 1,669 (C=O of amide); ¹H-NMR (300 MHz, CDCl₃): δ ppm: 3.74 (s, 2H, NH₂), 7.13-8.09 (m, 13H, Ar-H), 9.85 (s, 1H, CONH); MS (EI) m/z : 356 [M⁺]; Anal. Calcd. for C₂₁H₁₆N₄O₂: C, 70.77; H, 4.53; N, 15.72. Found: C, 70.99; H, 4.52; N, 15.67.

4-(2-Methyl-4-oxoquinazolin-3(4H)-yl)-N'-(2-oxoindolin-3-ylidene)benzohydrazide (3a). Yield: 70%; mp = 190-192°C; IR (KBr) ν_{\max} cm^{-1} : 3,368 (NH_{str}), 3,045 (Ar-CH_{str}), 2,940 (CH₃-CH_{str}), 1,733 (C=O of quinazoline), 1,647 (C=O of amide), 1,592 (C=N_{str}); ¹H-NMR (300 MHz, CDCl₃): δ ppm: 2.60 (s, 3H, CH₃), 7.06-8.20 (m, 12H, Ar-H), 8.94 (s, 1H, NH of isatin), 9.90 (s, 1H, CONH); MS (EI) m/z : 423 [M⁺]; Anal. Calcd. for C₂₄H₁₇N₅O₃: C, 68.08; H, 4.05; N, 16.54. Found: C, 67.90; H, 4.06; N, 16.60.

4-(4-Oxo-2-phenylquinazolin-3(4H)-yl)-N'-(2-oxoindolin-3-ylidene)benzohydrazide (3b). Yield: 75%; mp = 203-205°C; IR (KBr) ν_{\max} cm^{-1} : 3,390 (NH_{str}), 3,034 (Ar-CH_{str}), 1,747 (C=O of quinazoline), 1,662 (C=O of amide), 1,605 (C=N_{str}); ¹H-NMR (300 MHz, CDCl₃): δ ppm: 7.28-8.31 (m, 17H, Ar-H), 9.02 (s, 1H, NH of isatin), 9.97 (s, 1H, CONH); MS (EI) m/z : 485

[M⁺]; Anal. Calcd. for C₂₉H₁₉N₅O₃: C, 71.74; H, 3.94; N, 14.43. Found: C, 71.95; H, 3.93; N, 14.39.

N'-(1-((dimethylamino)methyl)-2-oxoindolin-3-ylidene)-4-(2-methyl-4-oxoquinazolin-3(4H)-yl)benzohydrazide (**4a**). IR (KBr) ν_{\max} cm⁻¹: 3,361 (NH_{str}), 3,047 (Ar-CH_{str}), 2,935 (CH₃-CH_{str}), 1,738 (C=O of quinazoline), 1,672 (C=O of amide); ¹H-NMR (300 MHz, CDCl₃): δ ppm: 2.36 (s, 3H, CH₃ of quinazoline), 2.95 (s, 6H, N(CH₃)₂), 4.51 (s, 2H, NCH₂N), 6.98-7.83 (m, 12H, Ar-H), 9.87 (s, 1H, CONH); MS (EI) *m/z*: 480 [M⁺]; Anal. Calcd. for C₂₇H₂₄N₆O₃: C, 67.49; H, 5.03; N, 17.49. Found: C, 67.25; H, 5.05; N, 17.54.

N'-(1-((diethylamino)methyl)-2-oxoindolin-3-ylidene)-4-(2-methyl-4-oxoquinazolin-3(4H)-yl)benzohydrazide (**4b**). IR (KBr) ν_{\max} cm⁻¹: 3,388 (NH_{str}), 3,020 (Ar-CH_{str}), 2,942 (CH₃-CH_{str}), 1,745 (C=O of quinazoline), 1,649 (C=O of amide); ¹H-NMR (300 MHz, CDCl₃): δ ppm: 1.62 (t, *J* = 5.4 Hz, 6H, CH₃ of C₂H₅), 2.55 (s, 3H, CH₃ of quinazoline), 4.49 (q, *J* = 5.8 Hz, 4H, CH₂ of C₂H₅), 4.79 (s, 2H, NCH₂N), 7.06-8.11 (m, 12H, Ar-H), 9.94 (s, 1H, CONH); MS (EI) *m/z*: 508 [M⁺]; Anal. Calcd. for C₂₉H₂₈N₆O₃: C, 68.49; H, 5.55; N, 16.52. Found: C, 68.71; H, 5.54; N, 16.46.

N'-(1-((diphenylamino)methyl)-2-oxoindolin-3-ylidene)-4-(2-methyl-4-oxoquinazolin-3(4H)-yl)benzohydrazide (**4c**). IR (KBr) ν_{\max} cm⁻¹: 3,355 (NH_{str}), 3,066 (Ar-CH_{str}), 2,938 (CH₃-CH_{str}), 1,720 (C=O of quinazoline), 1,654 (C=O of amide); ¹H-NMR (300 MHz, CDCl₃): δ ppm: 2.28 (s, 3H, CH₃ of quinazoline), 4.35 (s, 2H, NCH₂N), 6.85-7.97 (m, 22H, Ar-H), 9.81 (s, 1H, CONH); MS (EI) *m/z*: 604 [M⁺]; Anal. Calcd. for C₃₇H₂₈N₆O₃: C, 73.50; H, 4.67; N, 13.90. Found: C, 73.67; H, 4.66; N, 13.86.

4-(2-Methyl-4-oxoquinazolin-3(4H)-yl)-*N'*-(2-oxo-1-(piperazin-1-ylmethyl)indolin-3-ylidene)benzohydrazide (**4d**). IR (KBr) ν_{\max} cm⁻¹: 3,376 (NH_{str}), 3,052 (Ar-CH_{str}), 2,947 (CH₃-CH_{str}), 1,741 (C=O of quinazoline), 1,645 (C=O of amide); ¹H-NMR (300 MHz, CDCl₃): δ ppm: 2.40 (s, 3H, CH₃ of quinazoline), 3.09-3.53 (m, 1H, NH of piperazine), 3.81-4.25 (m, 8H, CH₂ of piperazine), 4.47 (s, 2H, NCH₂N), 6.82-8.01 (m, 12H, Ar-H), 9.99 (s, 1H, CONH); MS (EI) *m/z*: 521 [M⁺]; Anal. Calcd. for C₂₉H₂₇N₇O₃: C, 66.78; H, 5.22; N, 18.80. Found: C, 66.96; H, 5.21; N, 18.74.

4-(2-Methyl-4-oxoquinazolin-3(4H)-yl)-*N'*-(1-(morpholinomethyl)-2-oxoindolin-3-ylidene)benzohydrazide (**4e**). IR (KBr) ν_{\max} cm⁻¹: 3,409 (NH_{str}), 3,041 (Ar-CH_{str}), 2,936 (CH₃-CH_{str}), 1,728 (C=O of quinazoline), 1,662 (C=O of amide), 1,065 (C-O-C_{str}); ¹H-NMR (300 MHz, CDCl₃): δ ppm: 2.32 (t, *J* = 6.0 Hz, 4H, C₃, C₅-CH₂ of morpholine), 2.69 (s, 3H, CH₃ of quinazoline), 3.45 (t, *J* = 5.2 Hz, 4H, C₂, C₆-CH₂ of morpholine), 4.38 (s, 2H, NCH₂N), 7.04-8.15 (m, 12H,

Ar-H), 9.82 (s, 1H, CONH); MS (EI) *m/z*: 522 [M⁺]; Anal. Calcd. for C₂₉H₂₆N₆O₄: C, 66.66; H, 5.02; N, 16.08. Found: C, 66.87; H, 5.01; N, 16.03.

4-(2-Methyl-4-oxoquinazolin-3(4H)-yl)-*N'*-(2-oxo-1-(piperidin-1-ylmethyl)indolin-3-ylidene)benzohydrazide (**4f**). IR (KBr) ν_{\max} cm⁻¹: 3,364 (NH_{str}), 3,039 (Ar-CH_{str}), 2,950 (CH₃-CH_{str}), 1,732 (C=O of quinazoline), 1,657 (C=O of amide); ¹H-NMR (300 MHz, CDCl₃): δ ppm: 1.24-1.78 (m, 6H, C₃, C₄, C₅-CH₂ of piperidine), 2.22 (s, 3H, CH₃ of quinazoline), 2.57 (t, *J* = 5.6 Hz, 4H, C₂, C₆-CH₂ of piperidine), 4.63 (s, 2H, NCH₂N), 7.15-8.29 (m, 12H, Ar-H), 9.76 (s, 1H, CONH); MS (EI) *m/z*: 520 [M⁺]; Anal. Calcd. for C₃₀H₂₈N₆O₃: C, 69.22; H, 5.42; N, 16.14. Found: C, 69.05; H, 5.44; N, 16.18.

N'-(1-((dimethylamino)methyl)-2-oxoindolin-3-ylidene)-4-(4-oxo-2-phenylquinazolin-3(4H)-yl)benzohydrazide (**4g**). IR (KBr) ν_{\max} cm⁻¹: 3,352 (NH_{str}), 3,074 (Ar-CH_{str}), 2,945 (CH₃-CH_{str}), 1,723 (C=O of quinazoline), 1,640 (C=O of amide); ¹H-NMR (300 MHz, CDCl₃): δ ppm: 2.81 (s, 6H, N(CH₃)₂), 4.55 (s, 2H, NCH₂N), 6.90-8.07 (m, 17H, Ar-H), 9.85 (s, 1H, CONH); MS (EI) *m/z*: 542 [M⁺]; Anal. Calcd. for C₃₂H₂₆N₆O₃: C, 70.84; H, 4.83; N, 15.49. Found: C, 70.59; H, 4.84; N, 15.55.

N'-(1-((diethylamino)methyl)-2-oxoindolin-3-ylidene)-4-(4-oxo-2-phenylquinazolin-3(4H)-yl)benzohydrazide (**4h**). IR (KBr) ν_{\max} cm⁻¹: 3,393 (NH_{str}), 3,038 (Ar-CH_{str}), 2,957 (CH₃-CH_{str}), 1,742 (C=O of quinazoline), 1,676 (C=O of amide); ¹H-NMR (300 MHz, CDCl₃): δ ppm: 1.75 (t, *J* = 5.8 Hz, 6H, CH₃ of C₂H₅), 4.32 (q, *J* = 5.2 Hz, 4H, CH₂ of C₂H₅), 4.70 (s, 2H, NCH₂N), 7.12-8.34 (m, 17H, Ar-H), 10.03 (s, 1H, CONH); MS (EI) *m/z*: 570 [M⁺]; Anal. Calcd. for C₃₄H₃₀N₆O₃: C, 71.56; H, 5.30; N, 14.73. Found: C, 71.78; H, 5.28; N, 14.69.

N'-(1-((diphenylamino)methyl)-2-oxoindolin-3-ylidene)-4-(4-oxo-2-phenylquinazolin-3(4H)-yl)benzohydrazide (**4i**). IR (KBr) ν_{\max} cm⁻¹: 3,358 (NH_{str}), 3,024 (Ar-CH_{str}), 1,750 (C=O of quinazoline), 1,665 (C=O of amide); ¹H-NMR (300 MHz, CDCl₃): δ ppm: 4.52 (s, 2H, NCH₂N), 6.99-8.03 (m, 27H, Ar-H), 9.97 (s, 1H, CONH); MS (EI) *m/z*: 666 [M⁺]; Anal. Calcd. for C₄₂H₃₀N₆O₃: C, 75.66; H, 4.54; N, 12.60. Found: C, 75.40; H, 4.55; N, 12.64.

N'-(2-oxo-1-(piperazin-1-ylmethyl)indolin-3-ylidene)-4-(4-oxo-2-phenylquinazolin-3(4H)-yl)benzohydrazide (**4j**). IR (KBr) ν_{\max} cm⁻¹: 3,370 (NH_{str}), 3,058 (Ar-CH_{str}), 1,736 (C=O of quinazoline), 1,643 (C=O of amide); ¹H-NMR (300 MHz, CDCl₃): δ ppm: 2.81-3.38 (m, 1H, NH of piperazine), 3.65-4.24 (m, 8H, CH₂ of piperazine), 4.34 (s, 2H, NCH₂N), 6.87-7.80 (m, 17H, Ar-H), 10.09 (s, 1H, CONH); MS (EI) *m/z*: 583 [M⁺]; Anal. Calcd. for C₃₄H₂₉N₇O₃: C, 69.97; H, 5.01; N, 16.80. Found: C, 70.22; H, 4.99; N, 16.75.

N'-(1-(morpholinomethyl)-2-oxoindolin-3-ylidene)-4-(4-oxo-2-phenylquinazolin-3(4H)-yl)benzohydrazide (**4k**). IR (KBr) ν_{\max} cm^{-1} : 3,385 (NH_{str}), 3,028 ($\text{Ar-CH}_{\text{str}}$), 1,739 (C=O of quinazoline), 1,652 (C=O of amide), 1,053 ($\text{C-O-C}_{\text{str}}$); $^1\text{H-NMR}$ (300 MHz, CDCl_3): δ ppm: 2.56 (t, $J = 5.6$ Hz, 4H, $\text{C}_3, \text{C}_5\text{-CH}_2$ of morpholine), 3.32 (t, $J = 6.0$ Hz, 4H, $\text{C}_2, \text{C}_6\text{-CH}_2$ of morpholine), 4.46 (s, 2H, NCH_2N), 7.05-8.09 (m, 17H, Ar-H), 9.90 (s, 1H, CONH); MS (EI) m/z : 584 [M^+]; Anal. Calcd. for $\text{C}_{34}\text{H}_{28}\text{N}_6\text{O}_4$: C, 69.85; H, 4.83; N, 14.38. Found: C, 69.64; H, 4.84; N, 14.43.

N'-(2-oxo-1-(piperidin-1-ylmethyl)indolin-3-ylidene)-4-(4-oxo-2-phenylquinazolin-3(4H)-yl)benzohydrazide (**4l**). IR (KBr) ν_{\max} cm^{-1} : 3,367 (NH_{str}), 3,033 ($\text{Ar-CH}_{\text{str}}$), 1,724 (C=O of quinazoline), 1,670 (C=O of amide); $^1\text{H-NMR}$ (300 MHz, CDCl_3): δ ppm: 1.12-1.67 (m, 6H, $\text{C}_3, \text{C}_4, \text{C}_5\text{-CH}_2$ of piperidine), 2.30 (t, $J = 5.2$ Hz, 4H, $\text{C}_2, \text{C}_6\text{-CH}_2$ of piperidine), 4.61 (s, 2H, NCH_2N), 7.22-8.38 (m, 17H, Ar-H), 9.85 (s, 1H, CONH); MS (EI) m/z : 582 [M^+]; Anal. Calcd. for $\text{C}_{35}\text{H}_{30}\text{N}_6\text{O}_3$: C, 72.15; H, 5.19; N, 14.42. Found: C, 72.41; H, 5.18; N, 14.38.

Evaluation of innate immune stimulating activity of polysaccharides using a silkworm (*Bombyx mori*) muscle contraction assay

Tomoko Fujiyuki¹, Hiroshi Hamamoto¹, Kenichi Ishii¹, Makoto Urai¹, Keiko Kataoka², Tadahiro Takeda³, Shoji Shibata¹, Kazuhisa Sekimizu^{1,2,*}

¹ Graduate School of Pharmaceutical Sciences, The University of Tokyo, Tokyo, Japan;

² Genome Pharmaceuticals Institute Co., Ltd., Tokyo, Japan;

³ Department of Sports Health, Nagoya Gakuin University, Seto, Aichi, Japan.

ABSTRACT: In silkworm larvae, the mature form of paralytic peptide (PP), an insect cytokine, is produced from pro-PP in association with activation of innate immune responses, resulting in slow muscle contraction. We utilized this reaction, muscle contraction in silkworms coupled with innate immunity stimulation, to quantitatively measure the innate immune stimulating activity of various natural polysaccharides. β -Glucan of *Gyrophora esculenta* (GE-3), fucoidan from sporophyll of *Undaria pinnatifida*, and curdlan induced silkworm muscle contraction. We further demonstrated that GE-3 had therapeutic effects on silkworms infected by baculovirus. Based on these findings, we propose that the silkworm muscle contraction assay is useful for screening substances that stimulate innate immunity before evaluating therapeutic effectiveness in mammals.

Keywords: Silkworm, innate immunity, polysaccharide

1. Introduction

Innate immunity is the first line of defense against microbe infection. Recent studies indicate that molecular mechanisms of innate immunity are highly conserved among invertebrates and vertebrates (1,2). Because innate immunity mechanisms are activated in response to various pathogens, stimulation of innate immunity may be an effective therapy against infectious disease. For example, interferon stimulates the innate immune system and is currently used for hepatitis C antiviral therapy. *In vitro* screening for innate immunity

stimulants using immune cells from mammalian animals has been developed (3-5). Serious problems, however, are associated with *in vitro* assays using cultured cells to evaluate innate immunity stimulants. For example, most compounds from natural sources are contaminated with lipopolysaccharides (LPS) from Gram-negative bacteria, which stimulate innate immunity at very low concentrations. Further, most candidate compounds obtained by *in vitro* screening are not therapeutically effective because of problems of pharmacokinetics in animal bodies. Various issues with the so-called ADME (absorption, distribution, metabolism, and excretion) properties complicate this process. Therefore, for drug development it is necessary to perform quantitative measurement of therapeutic effects *in vivo*. Efficient methods of evaluating the innate immune stimulating activity of agents *in vivo*, however, are quite limited. To overcome the problems in screening systems of innate immune stimulants, we established an assay using the silkworm *Bombyx mori* based on muscle contraction, which is associated with activation of innate immunity (6,7).

Recently, we reported that injection of yeast β -glucans and bacterial peptidoglycans into the silkworm *Bombyx mori* induces maturation of the insect cytokine paralytic peptide (PP), which results in muscle contraction of the larvae (6,7). Because the muscle contraction, induced by macromolecules that exist in the outer membrane of the bacteria or cell wall of fungi, is a slow reaction requiring over 5 min (6,7), it very clearly differs from the rapid muscle contraction induced by neurotransmitters. Pre-PP is present in the hemolymph of the silkworm larvae (8), then processed to mature PP, which causes paralysis of the silkworm larvae (9). PP induces activation of cellular and humoral immunity (7,10), thus it is likely that the silkworm muscle contraction by PP reflects activation of the innate immune system. The advantages of using the silkworm muscle contraction assay to evaluate immunostimulants include the following: *i*) the system does not respond to LPS due to presence of LPS-absorbing proteins in the

*Address correspondence to:

Dr. Kazuhisa Sekimizu, Graduate School of Pharmaceutical Sciences, The University of Tokyo, 7-3-1 Hongo, Bunkyo-ku, Tokyo 113-0033, Japan.
E-mail: sekimizu@mol.f.u-tokyo.ac.jp

hemolymph; *ii*) as the method is based on bioassay using the silkworm body, it can be used to exclude compounds with pharmacokinetic problems; and *iii*) compounds that are toxic can be excluded using the bioassay with silkworm muscle specimens (11-14).

We previously purified a polysaccharide with innate immune-stimulating activity from green tea extracts that induces silkworm muscle contraction (15). In the present study, we evaluated the innate immune stimulating activities of various polysaccharides using the silkworm muscle contraction assay system. To further establish the usefulness of this system for screening therapeutically effective materials, we examined the therapeutic effect of β -glucans from *Gyrophora esculenta* (GE-3) in a silkworm baculovirus infection model (16).

2. Materials and Methods

2.1. Polysaccharides

GE-3 (17), an acid-hydrolyzed product of GE-3, a sulfate of GE-3 (18), lichenan (19), isolichenan (19), and ukonan (20,21) were prepared as previously described. Fucoidan (Riken Vitamin, Tokyo, Japan), yeast β -glucans (Sigma-Aldrich, St. Louis, MO, USA or Oriental Yeast Co. Ltd, Tokyo, Japan), curdlan (Sigma-Aldrich), laminarin (Sigma-Aldrich), lentinan (Ajinomoto, Tokyo, Japan), and schizophyllan (Kaken Pharmaceutical Co. Ltd, Tokyo, Japan) were purchased from the indicated vendors. The polysaccharides were dissolved in 0.9% NaCl (2-20 mg/mL). LPS derived from *Escherichia coli*, *Vibrio cholerae* Inaba 569B, *Pseudomonas aeruginosa* 10, *Klebsiella pneumoniae*, and *Shigella flexneri* 1A were purchased from Sigma-Aldrich and dissolved in 0.9% NaCl (250 μ g/mL).

2.2. Evaluation of silkworm larvae muscle contraction

We measured the muscle contraction activity of various samples as previously reported (6,7). Briefly, the head of the silkworm larvae (5th instar) was cut off, tied with a string with a weight, and stabilized until autonomous vibration terminated. Samples (50 μ L) were injected into the body fluid of decapitated silkworms with a 1-mL syringe attached to a 27-gauge needle (Terumo). The maximum length of each specimen before and after the injection was measured to calculate the contraction ratio (Contraction value; C value). One unit was defined as the activity inducing 15% contraction of the specimen at maximal contraction.

2.3. Detection of activated PP

The hemolymph of the silkworm fifth instar larva was collected and an aliquot (75 μ L) was mixed with 25 μ L of GE-3 suspension (80, 250, 800, or 2,500 μ g/mL in

0.9% NaCl). The samples were incubated at 25°C for 3 min, heated at 100°C for 5 min, and then centrifuged at 10,000 \times g for 10 min. The proteins in the supernatant were separated by sodium dodecyl sulfate-polyacrylamide gel electrophoresis. Immunoblot analysis was performed with anti-PP antibody (a kind gift from Dr. Kamimura (8)) as previously described (7). Although this antibody also reacts to pre-PP, it can be discriminated from mature PP as their molecular weights differ. Chemically synthesized mature PP (8) was used as a positive control.

2.4. Examination of therapeutic effects of GE-3 in a silkworm nucleopolyhedrosis virus (NPV) infection model

Bombyx mori nucleopolyhedrosis virus (NPV; 1.28 \times 10⁵ pfu/50 μ L) (16) was injected into the hemolymph of the silkworm larvae (5th instar), and then GE-3 solution or ganciclovir (250 μ g/larva) was injected into the hemolymph or into the midgut. Surviving larvae were counted for 5 days post-inoculation. A survival curve was prepared using the Kaplan-Mayer method (GraphPad Prism3, MDF Co. Ltd., Tokyo, Japan).

3. Results

3.1. Activity of polysaccharides that induce silkworm muscle contraction

β -Glucans are pathogen cell wall components and are well known to induce activation of innate immunity (1, 22). Here, we first examined whether these materials induce silkworm muscle contraction. Curdlan of *Alcaligenes faecalis*, GE-3, and fucoidan from the sporophyll of *Undaria pinnatifida* induced muscle contraction (Table 1). On the other hand, lentinan

Table 1. Induction of silkworm muscle contraction by polysaccharides from natural origins

Polysaccharide	Structure	Activity (unit/mg)
Curdlan	β -1,3 Glucan	100
GE-3	β -1,6 Glucan	38
Fucoidan	Sulfated polysaccharide	36
Yeast β -glucan (Sigma)	β -1,3 Glucan (+ β -1,6 glucan)	33
Yeast β -glucan (Oriental yeast)	β -1,3 Glucan (+ β -1,6 glucan)	20
Lichenan	β -1,3; 1,4 Glucan	6
Isolichenan	α -1,3; 1,4 Glucan	6
Laminaran	β -1,3 Glucan	< 1
Lentinan	β -1,3 Glucan (+ β -1,6 glucan)	< 10
Schizophyllan	β -1,3 Glucan (+ β -1,6 glucan)	< 2
Ukonan A	Acidic polysaccharide	< 19
Ukonan B	Acidic polysaccharide	< 10
Ukonan C	Acidic polysaccharide	< 10
Ukonan D	Neutral polysaccharide	< 17

Activity (1 unit) was defined as that causing muscle contraction with the value of 0.15 (15% contraction). The inequality sign (<) indicates that the activity was lower than the limits of detection (*i.e.*, the maximum dose tested did not induce 15% muscle contraction).

and schizophyllan, which are reported to activate mammalian immune cells (23,24), did not induce muscle contraction. Laminarin, a β -1,3 glucan with low molecular weight, shows little activity for inducing TNF- α production in macrophages (25). Laminarin also showed no activity in the silkworm muscle contraction assay. Other plant polysaccharides, such as ukonan A-D (26,27), showed little activity to induce silkworm muscle contraction. Thus, various polysaccharides that stimulate mammalian immune cells also stimulated muscle contraction in silkworms.

Activity of immunostimulants for innate immunity has been evaluated based on the induction of cytokine production and phagocytosis by mammalian macrophages (28,29). Because LPS from Gram-negative bacteria are active in these assays at extremely low concentrations, the effects of LPS derived from contaminated bacteria in samples is a serious problem for evaluating immunostimulation. We previously reported that *E. coli* LPS do not induce silkworm muscle contraction (15). Here, we further examined whether other bacterial LPS fractions induce silkworm muscle contraction. LPS fractions derived from *Vibrio cholerae*, *Pseudomonas aeruginosa*, *Klebsiella pneumoniae*, and *Shigella flexneri* did not induce silkworm muscle contraction, even with administration of up to 12.5 μ g (data not shown). These findings indicate that the effects of LPS derived from contaminated bacteria in the samples can be ignored in the muscle contraction assay.

We then examined the mechanism of the GE-3 induced silkworm muscle contraction. We previously reported that yeast β -glucan convert pro-PP into mature PP in the silkworm hemolymph, resulting in muscle contraction (7). Silkworm hemolymph was incubated with GE-3 and immunoblot analysis was performed to detect mature PP. The increase in mature PP was dependent on the GE-3 concentration (Figure 1), indicating that GE-3 induced PP activation in the silkworm hemolymph. This finding suggests that the observed muscle contraction induced by GE-3

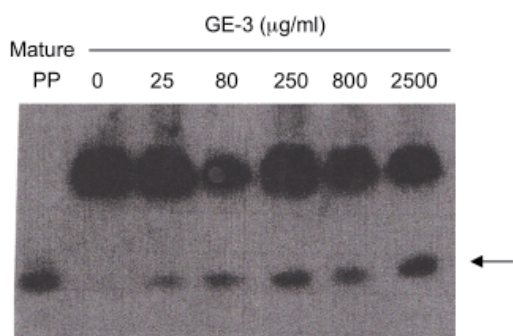


Figure 1. Production of the active form of PP by GE-3 in isolated hemolymph. The silkworm hemolymph (75 μ L) and GE-3 solution (25 μ L) were incubated and then PP was detected by immunoblotting. The final concentration of GE-3 is shown at the top of each lane. Arrow indicates the band position corresponding to mature PP.

administration was mediated by PP production from pro-PP in the hemolymph of the silkworm sample.

To identify the structural determinants of GE-3 necessary for silkworm muscle contraction, we tested the activity of acid-hydrolyzed or sonicated GE-3. These treatments resulted in decreased muscle contraction (Table 2), suggesting that the high molecular mass of β -1,6 glucans is necessary to induce muscle contraction.

3.2. Therapeutic effect of GE-3 against viral infection

We previously reported that the innate immune response activated by PP contributes to defend silkworms from *Staphylococcus aureus* infection (7). Microarray analysis revealed that injection of PP alters gene expression patterns in the silkworm hemocytes and fat body cells, resulting in the induction of genes involved in innate immunity (10). Stimulants of innate immunity are therapeutically effective against viral infection (30-34). Thus, we hypothesized that activation of PP by GE-3 would contribute to the defense against viral infection in the silkworm. To test this, we first searched for genes induced by both PP and baculovirus (*Bombyx mori* nucleopolyhedrosis virus) infection (35,36) using microarray analysis. Expression of *Ka11761* (*integrin*), *Ka07712* (*MMP*), *arylphorin*, *promoting protein*, and *actin A3* was induced in the hemocytes, and expression of *Ka07075* (*BmEts*) was induced in the fat body cells by both PP and baculovirus (Supplemental Table 1, <http://www.ddtjournal.com/getabstract.php?id=540>). *Ka05805*, whose function is unknown, was induced in the two types of cells by both PP and baculovirus infection. In addition, defensin, which is induced during viral infection in *Drosophila* (37), was also induced by PP injection in the silkworm fat body cells. Therefore, PP induces the expression of a set of genes whose expression is also induced during viral infection.

We next tested whether GE-3 administration contributes to host defense against viral infection using a silkworm NPV infection model (16). Intra-hemolymph administration of GE-3 delayed the NPV killing effect (Figure 2A). The therapeutic effects of GE-3 for NPV-infected silkworms were dose-dependent (Figure 2B). These results suggest that GE-3 contributes to host resistance against viral infection through the activation of innate immunity induced by PP. The extent of the therapeutic effect by GE-3 was comparable to that by ganciclovir, which was used as a positive control (Figure 2C).

Table 2. Structure of GE-3 necessary for inducing silkworm muscle contraction

Treatment to GE-3	Activity (units/mg)
None	38 \pm 6 (n = 23)
Sonication	11 \pm 4 (n = 3)
Hydrolysis by sulfuric acid	< 2 (n = 5)

n: number of experiments.

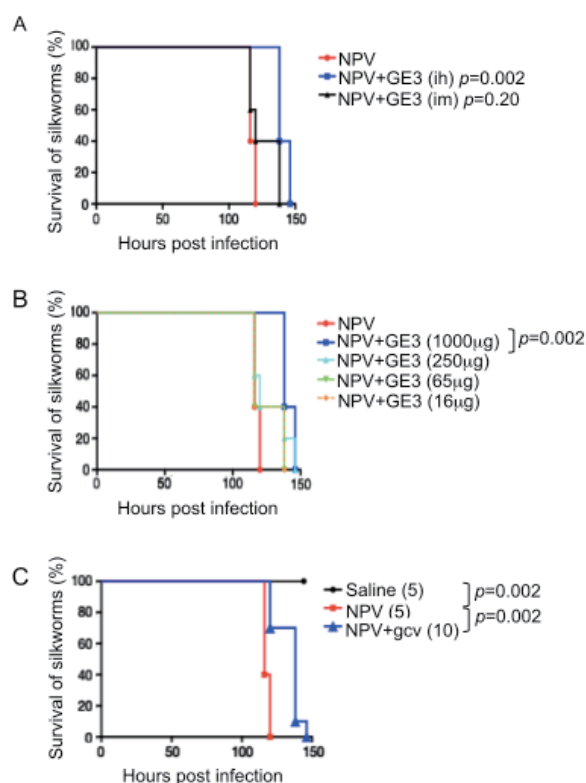


Figure 2. Therapeutic effects of GE-3 on silkworm larvae survival after NPV infection. (A) GE-3 (1 mg/larva) was injected into the hemolymph (ih) or midgut (im) of NPV-infected larvae. Survival curves were compared between non-treated and GE-3 injected groups using the log-rank test. N = 5 for each group. (B) Various concentrations of GE-3 solution were injected into the hemolymph of NPV-infected larvae. N = 5 for each group. p; log-rank test. (C) NPV or saline was injected into the hemolymph and then ganciclovir (250 µg/larva) was injected into the hemolymph. Silkworm larvae survival rate was examined. Number of tested larvae is shown in parentheses.

4. Discussion

The findings of the present study demonstrated that yeast β -1,6 glucans, GE-3 from *Gyrophora esculenta*, fucoidan, and curdlan (β -1,3 glucan) induced silkworm muscle contraction. These polysaccharides may activate immune cells in the hemolymph to produce mature PP, resulting in silkworm muscle contraction (7). Some β -glucans, such as laminarin, lentinan, and schizophyllan showed little activity in the silkworm muscle contraction system. One possible explanation for this is that receptors for silkworm muscle contraction have different specificities from those of immune cells in mammals. Another possibility is that β -glucans that did not induce silkworm muscle contraction may have ADME problems in the animal body. Further evaluation is needed to address these possibilities.

LPS does not induce silkworm muscle contraction. Therefore, contamination by LPS in the samples can be ignored in this screening system. The limited action of LPS in the silkworm muscle specimen can be explained by the presence of LPS binding proteins that neutralize LPS in the insect hemolymph (38,39).

Furthermore, using the silkworm model, ADMET (absorption, distribution, metabolism, excretion, and toxicity) of compounds can be easily evaluated (13,14, 40). We propose that screening substances that activate innate immune systems using the silkworm muscle contraction assay system is an efficient method for identifying therapeutically effective compounds for infectious diseases, as a pre-screening system prior to more advanced stages of evaluation with mammals.

In the present study, we examined the therapeutic effectiveness of β -1,6 glucans from GE-3 in a silkworm model of NPV infection. Whereas several lines of evidence suggest the effectiveness of polysaccharides in the treatment for viral infectious diseases (30-32, 41), evidence for a relationship between therapeutic effectiveness and stimulation of immunity by polysaccharides is limited. Our results provide new evidence for this relationship. We showed that genes induced during NPV infection (35,36) were also induced in the hemocytes and fat body cells of the silkworm when PP was activated. These findings suggest that various molecules involved in the defense system against NPV infection may be induced by PP activation. For example, tetraspanin and integrin, which are induced in hemocytes after PP activation, are induced during NPV infection (35). Association of these molecules contributes to the cellular immune response (42), suggesting that they are involved in cellular immune responses to exclude virus-infected cells during NPV infection. Mechanism of which PP induces these gene expressions will be interesting subjects for future.

Acknowledgements

This study was supported by the Hokuto Foundation for Bioscience; a Grant-in-Aid for Challenging Exploratory Research (23659074); the Program for the Promotion of Fundamental Studies in Health Sciences of NIBIO; and grants from Genome Pharmaceuticals Co. Ltd. TF was the recipient of a Grant-in-Aid from Japan Society for the Promotion of Science for young scientists (21-40175).

References

1. Kimbrell DA, Beutler B. The evolution and genetics of innate immunity. *Nat Rev Genet.* 2001; 2:256-267.
2. Vilmos P, Kurucz E. Insect immunity: Evolutionary roots of the mammalian innate immune system. *Immunol Lett.* 1998; 62:59-66.
3. Tam PE, Hindsill RD. Evaluation of immunomodulatory chemicals: Alteration of macrophage function *in vitro*. *Toxicol Appl Pharmacol.* 1984; 76:183-194.
4. Miller RL, Tomai MA, Harrison CJ, Bernstein DI. Immunomodulation as a treatment strategy for genital herpes: Review of the evidence. *Int Immunopharmacol.* 2002; 2:443-451.

5. Mizumoto N, Gao J, Matsushima H, Ogawa Y, Tanaka H, Takashima A. Discovery of novel immunostimulants by dendritic-cell-based functional screening. *Blood*. 2005; 106:3082-3089.
6. Sekimizu K, Larranaga J, Hamamoto H, Sekine M, Furuchi T, Katane M, Homma H, Matsuki N. D-Glutamic acid-induced muscle contraction in the silkworm, *Bombyx mori*. *J Biochem*. 2005; 137:199-203.
7. Ishii K, Hamamoto H, Kamimura M, Sekimizu K. Activation of the silkworm cytokine by bacterial and fungal cell wall components *via* a reactive oxygen species-triggered mechanism. *J Biol Chem*. 2008; 283:2185-2191.
8. Kamimura M, Nakahara Y, Kanamori Y, Tsuzuki S, Hayakawa Y, Kiuchi M. Molecular cloning of silkworm paralytic peptide and its developmental regulation. *Biochem Biophys Res Commun*. 2001; 286:67-73.
9. Ha SD, Nagata S, Suzuki A, Kataoka H. Isolation and structure determination of a paralytic peptide from the hemolymph of the silkworm, *Bombyx mori*. *Peptides*. 1999; 20:561-568.
10. Ishii K, Hamamoto H, Kamimura M, Nakamura Y, Noda H, Imamura K, Mita K, Sekimizu K. Insect cytokine paralytic peptide (PP) induces cellular and humoral immune responses in the silkworm *Bombyx mori*. *J Biol Chem*. 2010; 285:28635-28642.
11. Hamamoto H, Kamura K, Razanajatovo IM, Murakami K, Santa T, Sekimizu K. Effects of molecular mass and hydrophobicity on transport rates through non-specific pathways of the silkworm larva midguts. *Int J Antimicrob Agents*. 2005; 26:38-42.
12. Hamamoto H, Kurokawa K, Kaito C, Kamura K, Manitra Razanajatovo I, Kusahara H, Santa T, Sekimizu K. Quantitative evaluation of the therapeutic effects of antibiotics using silkworms infected with human pathogenic microorganisms. *Antimicrob Agents Chemother*. 2004; 48:774-779.
13. Hamamoto H, Tonoike A, Narushima K, Horie R, Sekimizu K. Silkworm as a model animal to evaluate drug candidate toxicity and metabolism. *Comp Biochem Physiol C*. 2009; 149:334-339.
14. Fujiyuki T, Imamura K, Hamamoto H, Sekimizu K. Evaluation of therapeutic effects and pharmacokinetics of antibacterial chromogenic agents in a silkworm model of *Staphylococcus aureus* infection. *Drug Discov Ther*. 2010; 4:349-354.
15. Dhital S, Hamamoto H, Urai M, Ishii K, Sekimizu K. Purification of innate immunostimulant from green tea using a silkworm muscle contraction assay. *Drug Discov Ther*. 2011; 5:18-25.
16. Orihara Y, Hamamoto H, Kasuga H, Shimada T, Kawaguchi Y, Sekimizu K. A silkworm-baculovirus model for assessing the therapeutic effects of antiviral compounds: Characterization and application to the isolation of antivirals from traditional medicines. *J Gen Virol*. 2008; 89:188-194.
17. Shibata S, Nishikawa Y, Takeda T, Tanaka M. Polysaccharide in lichens and fungi. I. Antitumor active polysaccharides of *Gyrophora esculenta* Miyoshi and *Lasallia papulosa* (Ach.) Lano. *Chem Pharm Bull (Tokyo)*. 1968; 16:2362-2369.
18. Hirabayashi K, Iwata S, Ito M, Shigeta S, Narui T, Mori T, Shibata S. Inhibitory effect of a lichen polysaccharide sulfate, GE-3-S, on the replication of human immunodeficiency virus (HIV) *in vitro*. *Chem Pharm Bull (Tokyo)*. 1989; 37:2410-2412.
19. Fukuoka F, Nakanishi M, Shibata S, Nishikawa Y, Takeda T, Tanaka M. Polysaccharides in lichens and fungi. II. Antitumor activities on sarcoma-180 of the polysaccharide preparations from *Gyrophora esculenta* Miyoshi, *Cetraria islandica* (L.) Ach. var. *orientalis* Asahina, and some other lichens. *Gann*. 1968; 59:421-432.
20. Gonda R, Tomoda M, Shimizu N, Kanari M. Characterization of polysaccharides having activity on the reticuloendothelial system from the rhizome of *Curcuma longa*. *Chem Pharm Bull (Tokyo)*. 1990; 38:482-486.
21. Gonda R, Takeda K, Shimizu N, Tomoda M. Characterization of a neutral polysaccharide having activity on the reticuloendothelial system from the rhizome of *Curcuma longa*. *Chem Pharm Bull (Tokyo)*. 1992; 40:185-188.
22. Brown GD, Gordon S. Fungal beta-glucans and mammalian immunity. *Immunity*. 2003; 19:311-315.
23. Kupfahl C, Geginat G, Hof H. Lentinan has a stimulatory effect on innate and adaptive immunity against murine *Listeria monocytogenes* infection. *Int Immunopharmacol*. 2006; 6:686-696.
24. Mizuno T, Sakai T, Chihara G. Health foods and medical usages of mushrooms. *Food Rev Int*. 1995; 11:69-81.
25. Adachi Y, Okazaki M, Ohno N, Yadomae T. Leukocyte activation by (1→3)-β-D glucans. *Mediators Inflamm*. 1997; 6:251-256.
26. Gonda R, Tomoda M, Ohara N, Takada K. Arabinogalactan core structure and immunological activities of ukonan C, an acidic polysaccharide from the rhizome of *Curcuma longa*. *Biol Pharm Bull*. 1993; 16:235-238.
27. Gonda R, Tomoda M, Takada K, Ohara N, Shimizu N. The core structure of ukonan A, a phagocytosis-activating polysaccharide from the rhizome of *Curcuma longa*, and immunological activities of degradation products. *Chem Pharm Bull*. 1992; 40:990-993.
28. Koide S, Steinman RM. Induction of murine interleukin 1: Stimuli and responsive primary cells. *Proc Natl Acad Sci U S A*. 1987; 84:3802-3806.
29. Cooper PH, Mayer P, Baggiolini M. Stimulation of phagocytosis in bone marrow-derived mouse macrophages by bacterial lipopolysaccharide: Correlation with biochemical and functional parameters. *J Immunol*. 1984; 133:913-922.
30. Chang CF, Su MS, Chen HY, Liao IC. Dietary β-1,3-glucan effectively improves immunity and survival of *Penaeus monodon* challenged with white spot syndrome virus. *Fish Shellfish Immunol*. 2003; 15:297-310.
31. Davis JM, Murphy EA, Brown AS, Charmichael MD, Ghaffar A, Mayer EP. Effects of moderate exercise and oat β-glucan on innate immune function and susceptibility to respiratory infection. *Am J Physiol Regul Integr Comp Physiol*. 2004; 286:R366-372.
32. Murphy EA, Davis JM, Carmichael MD, Mayer EP, Ghaffar A. Benefits of oat β-glucan and sucrose feedings on infection and macrophage antiviral resistance following exercise stress. *Am J Physiol Regul Integr Comp Physiol*. 2009; 297:R1118-1194.
33. Wakabayashi H, Kurokawa M, Shin K, Teraguchi S, Tamura Y, Shiraki K. Oral lactoferrin prevents body weight loss and increases cytokine responses during herpes simplex virus type 1 infection of mice. *Biosci Biotechnol Biochem*. 2004; 68:537-544.
34. Shin K, Wakabayashi H, Yamauchi K, Teraguchi S,

- Tamura Y, Kurokawa M, Shiraki K. Effects of orally administered bovine lactoferrin and lactoperoxidase on influenza virus infection in mice. *J Med Microbiol.* 2005; 54:717-723.
35. Sagisaka A, Fujita K, Nakamura Y, Ishibashi J, Noda H, Imanishi S, Mita K, Yamakawa M, Tanaka H. Genome-wide analysis of host gene expression in the silkworm cells infected with *Bombyx mori* nucleopolyhedrovirus. *Virus Res.* 2010; 147:166-175.
36. Bao YY, Tang XD, Lv ZY, Wang XY, Tian CH, Xu YP, Zhang CX. Gene expression profiling of resistant and susceptible *Bombyx mori* strains reveals nucleopolyhedrovirus-associated variations in host gene transcript levels. *Genomics.* 2009; 94:138-145.
37. Zambon RA, Nandakumar M, Vakharia VN, Wu LP. The Toll pathway is important for an antiviral response in *Drosophila*. *Proc Natl Acad Sci U S A.* 2005; 102:7257-7262.
38. Koizumi N, Morozumi A, Imamura M, Tanaka E, Iwahana H, Sato R. Lipopolysaccharide-binding proteins and their involvement in the bacterial clearance from the hemolymph of the silkworm *Bombyx mori*. *Eur J Biochem.* 1997; 248:217-224.
39. Kato Y, Motoi Y, Taniai K, Kadono-Okuda K, Yamamoto M, Higashino Y, Shimabukuro M, Chowdhury S, Xu J, Sugiyama M, Hiramatsu M, Yamakawa M. Lipopolysaccharide-lipophorin complex formation in insect hemolymph: A common pathway of lipopolysaccharide detoxification both in insects and in mammals. *Insect Biochem Mol Biol.* 1994; 24:547-555.
40. Asami Y, Horie R, Hamamoto H, Sekimizu K. Use of silkworms for identification of drug candidates having appropriate pharmacokinetics from plant sources. *BMC Pharmacol.* 2010; 10:7.
41. Hayashi K, Nakano T, Hashimoto M, Kanekiyo K, Hayashi T. Defensive effects of a fucoidan from brown alga *Undaria pinnatifida* against herpes simplex virus infection. *Int Immunopharmacol.* 2008; 8:109-116.
42. Zhuang S, Kelo L, Nardi JB, Kanost MR. An integrin-tetraspanin interaction required for cellular innate immune responses of an insect, *Manduca sexta*. *J Biol Chem.* 2007; 282:22563-22572.

(Received April 6, 2012; Accepted April 20, 2012)

Regulation of Janus-activated kinase-2 (JAK2) by diindolylmethane in ovarian cancer *in vitro* and *in vivo*

Prabodh K. Kandala, Sanjay K. Srivastava*

Department of Biomedical Sciences and Cancer Biology Center, Texas Tech University Health Sciences Center, Amarillo, TX, USA.

ABSTRACT: Janus-activated kinase-2 (JAK2) plays an important role in the activation of signal transducer and activation of transcription 3 (STAT3), which is over expressed in majority of ovarian tumors. We have reported previously that diindolylmethane (DIM) induces apoptosis in ovarian cancer cells by inhibiting STAT3. However, the role of JAK2 in our model was not yet understood and hence evaluated in this report. SKOV-3 human ovarian cancer cells were used to evaluate concentration and time dependent effects of DIM. Interleukin 3 (IL-3) and epidermal growth factor (EGF) were used to activate JAK2. Tumor xenograft studies were used to determine modulation of JAK2 *in vivo*. DIM treatment blocked the phosphorylation of JAK2 at Tyr-1007 in a concentration-dependent manner. In a time-dependent study, inhibition of JAK2 by DIM was as early as 1 h, which was followed by the inhibition of STAT3 and survivin. IL-3-induced phosphorylation of JAK2 and STAT3 was significantly blocked by DIM. IL-3 treatment blocked DIM-induced apoptosis. EGF treatment resulted in the activation of JAK2 and STAT3 but suppressed by DIM. These results indicate the involvement of cytokines and growth factors in the activation of JAK2/STAT3 and that DIM suppress their activation. Furthermore, DIM in combination with cisplatin drastically reduced the phosphorylation of JAK2 when compared to cisplatin alone. Western blot analysis of tumors from DIM treated mice showed significant inhibition of JAK2 activation as compared with controls. These findings provide a rationale for further clinical investigation of DIM for its potential use alone or in combination with chemotherapy of ovarian cancer.

Keywords: Diindolylmethane, JAK2, STAT3, apoptosis, EGF, cisplatin

*Address correspondence to:

Dr. Sanjay K. Srivastava, Department of Biomedical Sciences, Texas Tech University Health Sciences Center, Suite 1103, 1406 Coulter, Amarillo, Texas 79106, USA.

E-mail: sanjay.srivastava@ttuhsc.edu

1. Introduction

Ovarian cancer still remains a leading gynecological malignancy not only in western countries, but all over the world (1). It is the fifth leading cause of cancer related deaths, has the highest mortality rate among gynecologic cancers and is the most lethal malignancy of the female reproductive system (2). Greater than 90% of ovarian cancers arise from the surface epithelium. Ovarian tumorigenesis is associated with ovulation-associated wound repair and inflammation (1,3). Janus activated kinase/signal transducer and activation of transcription (JAK/STAT) is a major pathway that is activated during inflammation (4).

JAK/STAT pathway is pivotal in transducing multitude of signals for development and homeostasis in mammals (5). JAK activation plays an important role in cell proliferation, differentiation, migration and apoptosis (5-7). These cellular events are critical in growth and development of various organs. Mutations such as JAK2V617F that constitutively activates or fails to regulate JAK signaling confer oncogenic properties to a cell (6,8). JAK family comprises of four members, JAK1, JAK2, JAK3, and TYK2 (9). Activation of JAKs occurs by ligand receptor mediated multimerization (10). Activated JAKs subsequently auto-phosphorylate their receptors and additionally phosphorylate STATs (11). Phosphorylated STATs dimerize and translocate to nucleus, where they bind to specific regulatory sequences to activate or repress transcription of target genes such as *Mcl-1* and *survivin* (12,13). Thus, JAK/STAT signaling provides a direct mechanism to translate an extracellular signal into a transcriptional response and hence an important target for therapeutic intervention.

Accumulating epidemiological studies strongly indicate an inverse relation between intake of cruciferous vegetables and ovarian cancer (14). 3,3'-Diindolylmethane (DIM, Figure 1) is an important indole compound present in cruciferous vegetables (15). DIM was shown to possess anti-cancer properties against several cancers (15). Our laboratory previously demonstrated that DIM inhibits proliferation of ovarian cancer by inducing apoptosis in ovarian cancer cells by targeting STAT3 and epidermal growth factor receptor (EGFR) (16,17). However, whether these effects are mediated through JAK2 was not clear.

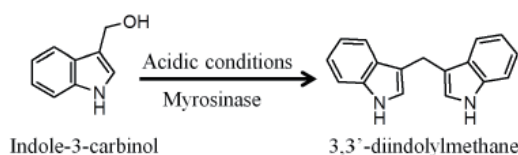


Figure 1. Formation of 3,3'-diindolylmethane (DIM) from indole-3-carbinol (I3C).

In the current study, we show that JAK2 is a mediator of STAT3 activation in our model. We also show that JAK2 is an important downstream signal transducer of EGFR.

2. Materials and Methods

2.1. Chemicals

BR-DIM was a kind gift from Dr. Michael Zeligs (Bio Response, Boulder, CO, USA). Antibodies against p-JAK2 (Tyr-1007), p-STAT3 (Tyr-705), survivin, Cl-caspase 3, and Cl-PARP were procured from Cell Signaling Technology (Danvers, MA, USA). Actin antibody, EGF, and IL-3 were procured from Sigma Aldrich (St. Louis, MO, USA). McCoy's 5A medium was purchased from Mediatech (Manassas, VA, USA). Cisplatin was obtained from Novaplus (Bedford, OH, USA).

2.2. Cell lines and cell culture

SKOV-3 cells were procured from American Type Culture Collection (ATCC, Manassas, VA, USA). SKOV-3 cells were maintained in McCoy's 5A medium supplemented with 10% fetal bovine serum (FBS) and 1% antibiotic mixture. Cells were maintained at 37°C in a humidified incubator circulated with 5% CO₂/95% air. Normal ovarian surface epithelium (NOSE) cells were kind gift from Dr. Jinsong Liu (M.D. Anderson Cancer Center, TX, USA) were cultured in 1:1 mixture of MCD105 and medium 199 supplemented with 15% FBS and 1% PSN as described previously (17).

2.3. Western blotting

SKOV-3 cells were exposed to varying concentrations of DIM alone or in combination with cisplatin. In another experiment cells were exposed to 10 ng/mL IL-3 or 50 ng/mL EGF prior to treating with 75 μM DIM. Cells were collected, lysed, and 20-80 μg of protein was subjected to SDS gel electrophoresis and proteins were blotted onto PVDF membrane. After blocking with 10% nonfat dry milk in Tris buffered saline (TBS), the membrane was incubated overnight with corresponding primary antibodies. Subsequently, the membrane was incubated with appropriate secondary antibody, and the immunoreactive bands were visualized using enhanced chemiluminescence kit (Thermo Scientific, Rockford, IL, USA) according to manufacturer's instructions as described by us previously (18).

2.4. Annexin V apoptosis assay

SKOV-3 cells were plated at a density of 0.3×10^6 cells per well in a six-well plate and allowed to attach overnight. Cells were exposed to IL-3 an hour before treatment with DIM. After 24 h, cells were washed, suspended in binding buffer and incubated for 15 min with annexin V-FITC (BD Biosciences, San Jose, CA, USA). Fluorescence was measured using C6 Accuri flow cytometer (Ann Arbor, MI, USA) with a minimum of 10,000 events per sample as described by us previously (19).

2.5. EGF and IL-3 treatment

SKOV-3 cells were exposed to 50 ng/mL EGF or 10 ng/mL IL-3 for 15 min followed by treatment with 75 μM DIM for 24 h. Cells were then processed for apoptosis assay or Western blotting as described above.

2.6. Analysis of tumors from control and DIM treated mice

Four to six week old female athymic nude mice were purchased from Charles River Laboratories (Wilmington, MA, USA). The use of mice and their treatment was approved by Institutional Animal Care and Use Committee (IACUC), Texas Tech University Health Sciences Center, and all experiments were carried out in strict compliance with regulations. Mice were fed with antioxidant-free AIN-76A special diet for a week before starting the experiment. About 5×10^6 SKOV-3 cells were injected subcutaneously into both right and left flanks. Mice were randomly arranged in each group. Control group received PBS whereas mice in the treatment group received 3 mg DIM suspended in PBS by oral gavage every day. Tumors from female athymic nude mice that received PBS or 3 mg DIM suspended in PBS by oral gavage every day were excised, snap frozen and lysed as explained by us previously (18). Tumor lysates were subjected to Western blotting for monitoring the activation of JAK2 as explained above.

2.7. Quantitation and statistical analysis

Densitometric analysis and quantitation was analyzed using UNSCAN-IT (Orem, UT, USA). All the statistical analysis was performed using Prism 5.0 (GraphPad Software Inc., San Diego, CA, USA). The data represents mean \pm S.D. Student's *t*-test was used to compare the control and treated groups. All statistical tests were two sided. Differences were considered statistically significant when the *p* value was less than 0.05.

3. Results

3.1. DIM inhibits activation of JAK2 in ovarian cancer cells

JAK2/STAT3 is aberrantly expressed in ovarian tumors (20). Therefore targeting JAK2-STAT3 may inhibit the

growth of ovarian cancer cells. We previously identified STAT3 as a critical target of DIM in ovarian cancer cells (17). However, the role of JAK2 in DIM mediated inhibition of STAT3 was not clear. Hence to determine the effect of DIM on JAK2, SKOV-3 ovarian cancer cells were treated with various concentrations of DIM for 24 h. Our Western blotting results reveal that DIM inhibits the activation of JAK2 by blocking its phosphorylation at Tyrosine 1007 (Figure 2A). The effect of DIM on JAK2 was concentration dependent with about 80% inhibition of p-JAK2 (Tyr-1007) by exposure to 75 μ M DIM (Figure 2B). We had previously shown that DIM was least effective on normal ovarian surface epithelial (NOSE) cells (17). Interestingly, our current results exhibit that normal ovarian cells do not show any constitutive activation of JAK2 as indicated by the absence of phosphorylation at Tyr-1007 (Figure 2C). These studies clearly suggest that JAK2 is a target of DIM in ovarian cancer cells.

3.2. Early inhibition of JAK-2 by DIM

Since we observed remarkable inhibition of JAK2 phosphorylation by DIM, we next determined the kinetics of JAK2 inhibition. SKOV-3 cells were treated with 75 μ M DIM for desired time points and the cell lysates were evaluated by Western blotting. Our results indicate that

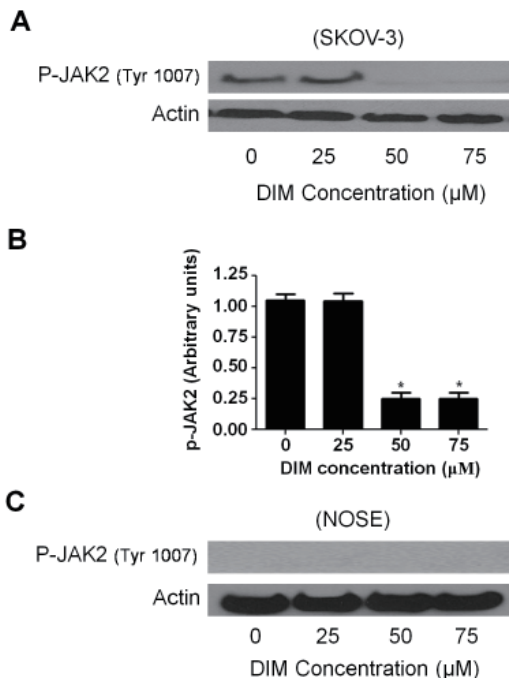


Figure 2. DIM treatment inhibits the activation of JAK2 in ovarian cancer cells but not in normal ovarian surface epithelial cells. SKOV-3 cells or normal ovarian surface epithelial cells (NOSE) were treated with various concentrations of DIM or treated with 75 μ M DIM for desired time intervals. Cells were collected, lysed and subjected to Western blotting. (A) Representative blots of p-JAK2 (Tyr-1007) and its (B) quantitation showing the concentration-dependent effect of DIM in SKOV-3 cell. (C) Representative blot of p-JAK2 (Tyr-1007) showing that DIM has least effect on NOSE cells. Actin was used as loading control.

inhibition of JAK2 activation by DIM was as early as 1 h (Figure 3). Since recent literature suggests that STAT3 was down stream of JAK2, we also looked for p-STAT3. DIM treatment substantially blocked the activation of STAT3 by suppressing its phosphorylation at Tyr-705 in SKOV-3 cells, and this inhibition started 1 h after treatment. Inhibition of STAT3 activation correlated with inhibition of JAK2 activation (Figure 3). Similarly, survivin, a downstream target of JAK2-STAT3 was substantially downregulated by 1 h of DIM treatment (Figure 3). These results not only substantiate that JAK2 is a target of DIM, but also indicate that STAT3 and survivin were regulated by JAK2 in our model.

3.3. DIM regulates STAT3 pathway via JAK2 activation

Our above observations demonstrate a link between JAK2, STAT3, and survivin in our model. To firmly establish the association between these molecules, SKOV-3 cells were stimulated with IL-3. IL-3 is a cytokine that phosphorylates JAK2 at Tyr-1007 and activates it. Our results show that treatment of SKOV-3 cells with 10 ng/mL IL-3 not only increased the activation of JAK2 by 2-fold but also increased the phosphorylation of STAT3 at Tyr-705 and expression of survivin by approximately 2.3- and 2-fold, respectively (Figure 4). To determine the effect of DIM on IL-3 induced activation/expression of these molecules, cells were treated with IL-3 for 15 min followed by treatment with DIM for 24 h. Our interesting results show that DIM treatment significantly blocked IL-3 induced phosphorylation of JAK2 (Tyr-1007), p-STAT3 (Tyr-705) and expression of survivin (Figure 4). These results confirm that STAT3 and survivin were regulated by JAK2 in our model.

3.4. IL-3 treatment blocks DIM-induced apoptosis in SKOV-3 cells

We further questioned ourselves, whether activating

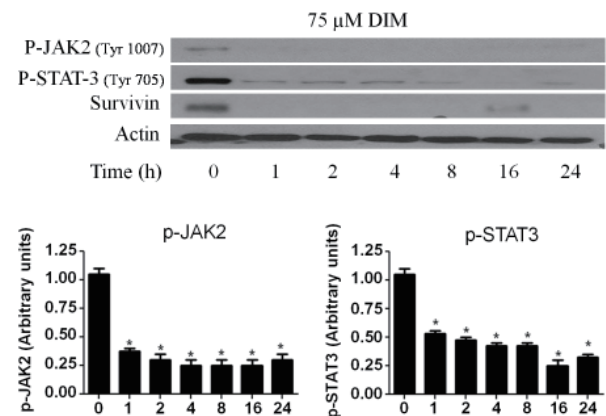


Figure 3. DIM treatment inhibits activation of JAK2 as early as one hour. Representative blots and their quantitation showing the time dependent effect of 75 μ M DIM on p-JAK2 (Tyr-1007), p-STAT3 (Tyr-705) and survivin. Actin was used as loading control. * $p < 0.05$ compared to control.

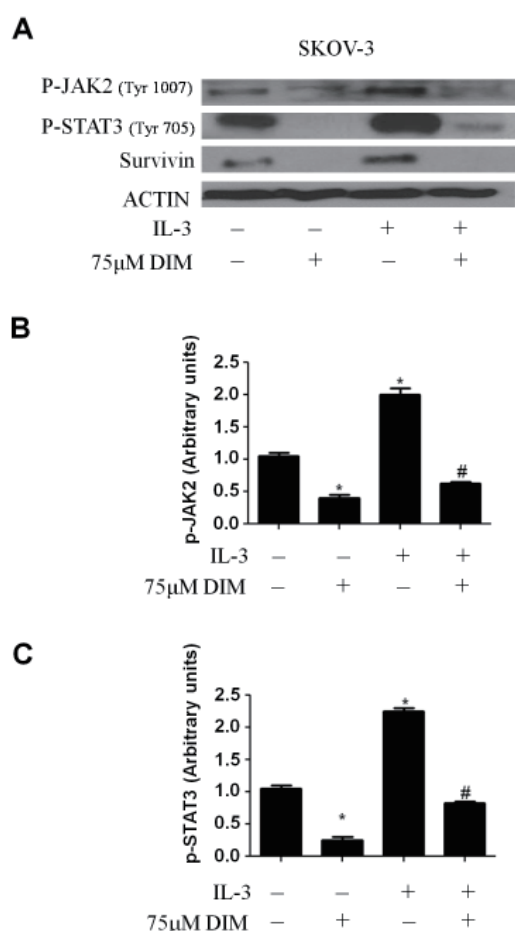


Figure 4. JAK2 is a critical target in DIM mediated apoptosis. SKOV3 cells were stimulated with 10 ng/mL IL-3 for 15 min followed by treatment with 75 µM DIM for 24 h. (A) Whole cell lysates were resolved on 10% SDS-PAGE for the analysis of phosphorylation of JAK2 at Tyr-1007, phosphorylation of STAT3 at Tyr-705 and expression of survivin. Actin was used as loading control. Quantitation of (B) p-JAK2 and (C) p-STAT3 were represented as bar diagram.

JAK2 would abrogate DIM mediated apoptosis. To answer this question, SKOV-3 cells were treated with IL-3 followed by 75 µM DIM for 24 h and apoptosis was determined. As expected, IL-3 treatment reduced the apoptosis induced by DIM in SKOV-3 cells (Figure 5A). For example, apoptosis mediated by 75 µM DIM alone was approximately 2.5-fold over control whereas in presence of IL-3, DIM-induced apoptosis was only 1.2-fold over control suggesting that IL-3 substantially blocked DIM-induced apoptosis (Figure 5B). Accordingly, IL-3 treatment significantly reduced the cleavage of caspase-3 and PARP induced by DIM treatment in SKOV-3 ovarian cancer cells (Figure 5C).

3.5. EGFR regulates JAK2-STAT3 pathway in our model

EGFR is activated in around 70% of ovarian tumors. Several studies demonstrated the possibility that EGFR activation in ovarian cancer would lead to phosphorylation of JAK2/STAT3 (20). Interestingly,

our published studies indicated that EGFR is a target of DIM in ovarian cancer cells both *in vitro* and *in vivo* (16). We hypothesized that regulation of JAK2/STAT3 by DIM in ovarian cancer cells was mediated through EGFR. To test our hypothesis, SKOV-3 ovarian cancer cells were treated with EGF before treatment with DIM. EGF is a ligand of EGFR, subsequent binding of which leads to the activation of EGFR. Figure 6A clearly demonstrates that EGF treatment lead to the activation of JAK2 and STAT3 in SKOV-3 cells. Activation of JAK2 and STAT3 was approximately 2.5- and 2-fold, respectively by EGF as compared to constitutive expression in SKOV-3 cells (Figures 6B and 6C). Interestingly, DIM treatment significantly suppressed EGF mediated phosphorylation of JAK2 and STAT3 (Figures 6A-6C), confirming the role of EGF in the activation of JAK2 and STAT3.

3.6. JAK2 inhibition potentiates the effect of cisplatin

Cisplatin is a drug used clinically to treat patients with ovarian cancer. However, cisplatin has several side effects including systemic toxicity. DIM was previously shown by us to potentiate the effect of cisplatin in ovarian cancer cells (17). To determine the involvement of JAK2 in the effect of DIM with cisplatin combination, SKOV-3 cells were treated with 50 µM DIM for 24 h followed by treatment with 10 µM cisplatin for 24 h. As expected, our results indicate that DIM treatment alone and in combination with cisplatin remarkably reduced the phosphorylation of JAK2 at Tyr-1007 (Figure 7A). Approximately 70% reduction in the expression of p-JAK2 (Tyr-1007) was observed in DIM treated SKOV-3 cells (Figure 7B). The decrease in the phosphorylation of JAK2 in combination treatment (DIM and cisplatin) was further reduced when compared with cisplatin treatment alone (Figure 7B). These results suggest that DIM treatment can potentiate the effect of cisplatin in ovarian cancer cells by targeting JAK2.

3.7. DIM treatment suppresses the growth of ovarian tumors by inhibiting JAK2 phosphorylation

In our previously published studies, we have shown that oral administration of 3 mg DIM per day for 48 days significantly suppressed the growth of SKOV-3 ovarian tumor xenografts in athymic nude mice (16,17). To further establish whether JAK2 activation play any role in the growth of ovarian tumors, the tumors from control and DIM treated mice were analyzed by Western blotting. Our results reveal that JAK2 phosphorylation in tumors from the mice that received DIM was approximately 50% lesser than in the tumors from mice from control group (Figure 8). Based on these observations, it can be concluded that reduced tumor growth in DIM treated mice was associated with reduced activation of JAK2.

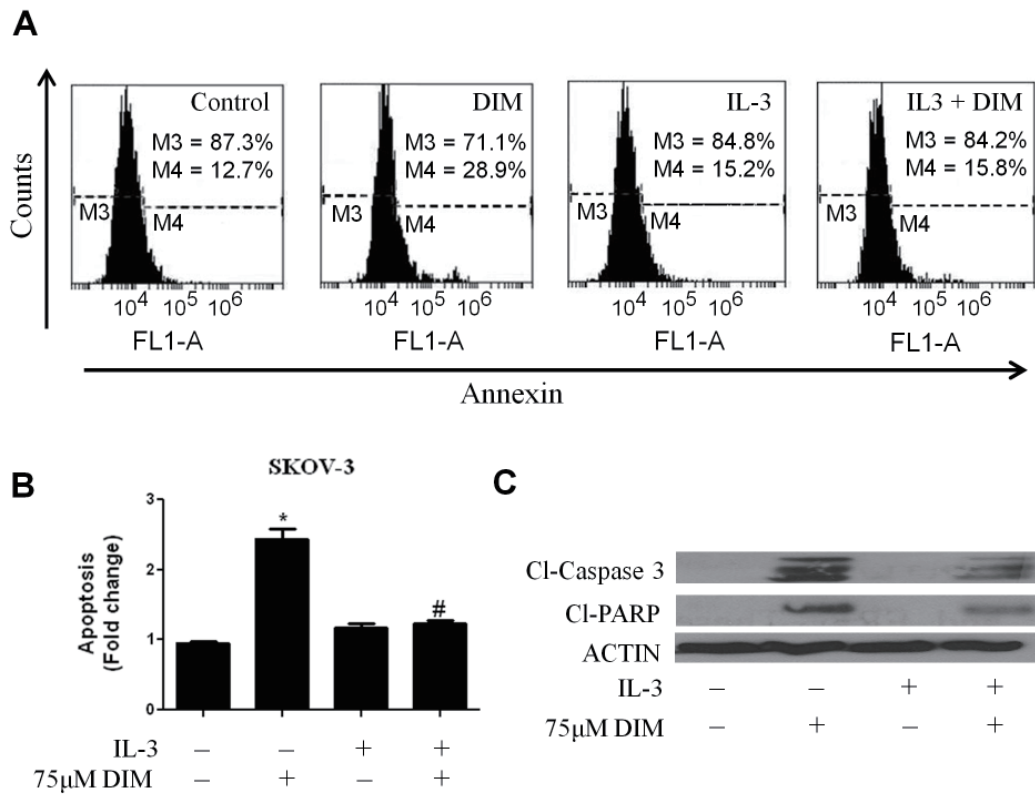


Figure 5. IL-3 treatment abrogates DIM induced apoptosis. (A) Effect of IL-3 on DIM induced apoptosis in SKOV-3 cells as detected by annexin V staining. (B) Bar graphs representing the apoptosis as indicated by annexin positive cells. * $p < 0.05$ compared to control. # $p < 0.05$ when compared to IL-3 treatment. (C) SKOV3 cells were stimulated with 10 ng/mL IL-3 for 15 min followed by treatment with 75 µM DIM for 24 h. Whole cell lysates were resolved on 10% SDS-PAGE for the analysis for cleavage of caspase-3 and PARP.

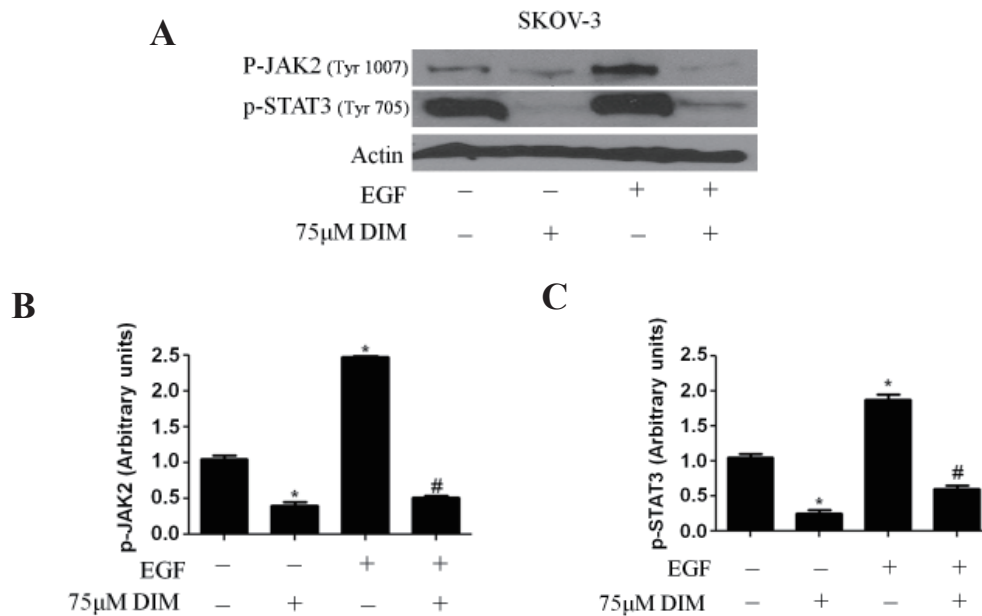


Figure 6. EGFR regulates JAK2/STAT3. SKOV3 cells were stimulated with 50 ng/mL EGF for 15 min and then treated with 75 µM DIM for 24 h. (A) Whole cell lysates were resolved on 10% SDS-PAGE to detect the phosphorylation of JAK2 at Tyr-1007 and phosphorylation of STAT3 at Tyr-705. Actin was used as loading control. Quantitation of (B) p-JAK2 and (C) p-STAT3 blots was also represented in bottom panel.

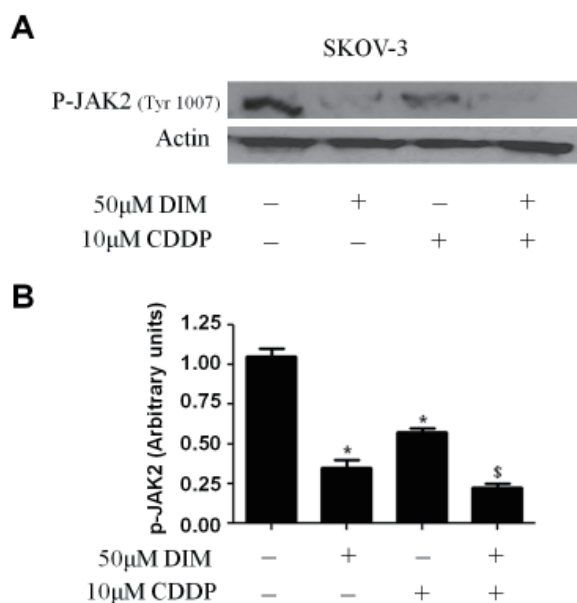


Figure 7. DIM potentiates the effect of cisplatin by inhibiting JAK2 phosphorylation. (A) Representative blots and (B) quantitation of p-JAK2 showing the effect of 50 µM DIM, 10 µM cisplatin or combination of both in SKOV-3 ovarian cancer cells. * $p < 0.05$ when compared to control. # $p < 0.05$ when compared to IL-3 treatment. \$ $p < 0.05$ when compared to cisplatin treatment.

4. Discussion

The primary objective of the current study was to test whether the anti-cancer effects of DIM were mediated by inhibition of JAK2. JAK2 is an important therapeutic target in ovarian cancer. Its activation has been observed in a large fraction of human ovarian tumors compared with normal ovarian tissues (20). Moreover JAK2 signaling regulates gene expression of various pro-survival and anti-apoptotic molecules (5). Inhibition of JAK2 signaling triggers cell death in human cancer cells (20,21). Our results show that SKOV-3 cells, which come from high grade ovarian tumors, have higher constitutive phosphorylation of JAK2, whereas normal ovarian surface epithelial (NOSE) cells do not express JAK2 in its activated form. Our findings are in agreement with previously published study which reported that normal and benign ovaries lack activated JAK2 and it is aberrantly expressed only in low and high grade ovarian carcinomas (6).

Various cytokines and growth factors can activate JAK2. IL-3, a pleiotropic cytokine is well known to activate JAK2 by phosphorylation at Tyr-1007 (22). DIM treatment not only eliminated constitutive activation of JAK2, but also blocked IL-3 mediated activation of JAK2. Interestingly, IL-3 treatment abrogated DIM-induced apoptosis as shown by reduced cleavage of caspase 3 and PARP as well as by annexin V staining of treated cells. Interestingly, AG490 a JAK2 inhibitor was shown to induce apoptosis in various cancer cells suggesting that JAK2 is required for cell survival and

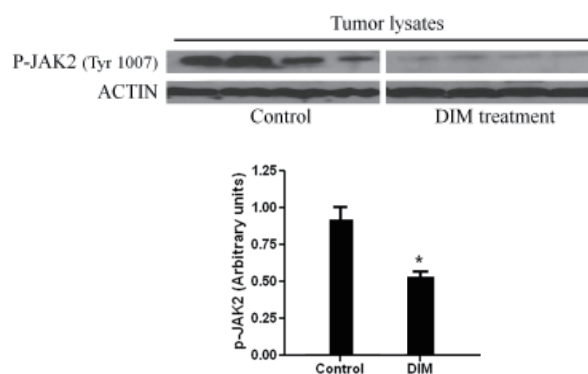


Figure 8. DIM suppresses ovarian tumor growth by inhibiting p-JAK2. Tumors from control and DIM treated mice were excised, lysed and analyzed by Western blot for p-JAK2 (Tyr-1007). Actin was used as loading control. Densitometric quantitation was represented. * $p < 0.05$ compared to control.

hence a target in cancer cells (14,20).

One of the major downstream effector of JAK2 is STAT3 (6,14,20). Activated JAK2 subsequently auto-phosphorylates its receptors and additionally phosphorylates STAT3. Phosphorylated STAT3 dimerizes and translocates to nucleus, where it binds to specific regulatory sequences to activate or repress transcription of target genes (23). Hence, JAK2 and thereby STAT3 play an important role in various stages of cancer progression. Our results demonstrate a relationship between JAK2 and STAT3 in ovarian cancer cells. The inhibition of STAT3 activation was consistent with inhibition of JAK2 activation in our time dependent study. Importantly, IL-3 treatment not only activated JAK2, but subsequently increased the phosphorylation of STAT3 but inhibited by DIM. Our results also demonstrate a link between JAK2/STAT3 and survivin. Expression of survivin was increased by IL-3 treatment and reduced by DIM. It is noteworthy that the gene expression profiling of a previous study showed that survivin is a target of DIM in breast cancer (24). Our results establish that JAK2 causes STAT3 activation in ovarian cancer cells and the apoptotic effects of DIM were due to inhibition of JAK2/STAT3 activation. These results are in agreement with previous studies which demonstrated that inhibition of JAK2/STAT3 pathway induced apoptosis and inhibited cell growth (21,25).

Over expression of EGFR occurs in almost 70% of ovarian cancers (26). Activation of EGFR has been associated with poor progression and increase in survival of ovarian cancer cells. Our previous studies showed that EGFR as a target of DIM (16). Our current study established a cross-talk between EGFR and JAK2/STAT3 pathway. EGF, a ligand known to activate EGFR, significantly activated JAK2 and STAT3 by phosphorylation. Nevertheless, DIM treatment substantially suppressed the phosphorylation of JAK2 and STAT3 mediated by EGF. Our studies indicate that

perhaps DIM targets EGFR-JAK2-STAT3 signaling axis to inhibit the growth of ovarian cancer. Our results are in agreement with the findings of previous study which indicated a link between EGFR and JAK2/STAT3 in carcinomas (5).

Our previously published results showed that administration of 3 mg DIM/day substantially retarded the growth of ovarian tumors *in vivo* (17). The tumor suppressive effects were mediated by reduction in JAK2 phosphorylation in the present study. DIM is a major phytochemical present in cruciferous vegetables (3). We showed that DIM is minimally toxic to normal cells. For example, 120 μ M DIM inhibited 75% proliferation of cancer cells whereas affected only 25% of NOSE cells, showing selectivity towards cancer cells (17). A recent clinical study showed that dose of up to 300 mg DIM was well tolerated in humans (27). Importantly, DIM is in clinical trials to treat cervical neoplasia and prostate carcinomas (28,29). Our current results also established that inhibition of JAK2 activation by DIM potentiates the effects of cisplatin, a clinically used drug with several side effects. Hence, this gives a possibility of using low non-toxic doses of cisplatin if DIM is administered concomitantly with cisplatin. Nevertheless, further clinical evaluations are required to confirm the safety of DIM alone or in combination with cisplatin in patients with ovarian cancer.

Taken together, our current study demonstrates the rationale for further clinical investigation of DIM for its potential use alone or in combination with chemotherapy of ovarian cancer.

Acknowledgements

This work was supported in part by RO1 grants CA 106953 and CA 129038 (to S.K.S) awarded by National Cancer Institute, NIH. We thank Dr. Jinsong Liu (M.D. Anderson Cancer Center, Houston, TX) for providing NOSE cells. The technical help of Srinivas Reddy Boreddy, Kartick Pramanik and Parul Gupta with the *in vivo* experiment is greatly appreciated.

References

- Cannistra SA. Cancer of the ovary. *N Engl J Med.* 2004; 351:2519-2529.
- Solomon LA, Ali S, Banerjee S, Munkarah AR, Morris RT, Sarkar FH. Sensitization of ovarian cancer cells to cisplatin by genistein: The role of NF-kappaB. *J Ovarian Res.* 2008; 1:9.
- Mehrotra R, Tyagi G, Jangir DK, Dawar R, Gupta N. Analysis of ovarian tumor pathology by Fourier Transform Infrared Spectroscopy. *J Ovarian Res.* 2010; 3:27.
- Campbell IL. Cytokine-mediated inflammation, tumorigenesis, and disease-associated JAK/STAT/SOCS signaling circuits in the CNS. *Brain Res Brain Res Rev.* 2005; 48:166-177.
- Rawlings JS, Rosler KM, Harrison DA. The JAK/STAT signaling pathway. *J Cell Sci.* 2004; 117:1281-1283.
- Igaz P, Toth S, Falus A. Biological and clinical significance of the JAK-STAT pathway; lessons from knockout mice. *Inflamm Res.* 2001; 50:435-441.
- O'Shea JJ, Gadina M, Schreiber RD. Cytokine signaling in 2002: New surprises in the Jak/Stat pathway. *Cell.* 2002; 109:S121-S131.
- Levine RL, Gilliland DG. JAK-2 mutations and their relevance to myeloproliferative disease. *Curr Opin Hematol.* 2007; 14:43-47.
- Aaronson DS, Horvath CM. A road map for those who don't know JAK-STAT. *Science.* 2002; 296:1653-1655.
- Heinrich PC, Behrmann I, Haan S, Hermanns HM, Müller-Newen G, Schaper F. Principles of interleukin (IL)-6-type cytokine signalling and its regulation. *Biochem J.* 2003; 374:1-20.
- Kisseleva T, Bhattacharya S, Braunstein J, Schindler CW. Signaling through the JAK/STAT pathway, recent advances and future challenges. *Gene.* 2002; 285:1-24.
- Epling-Burnette PK, Liu JH, Catlett-Falcone R, Turkson J, Oshiro M, Kothapalli R, Li Y, Wang JM, Yang-Yen HF, Karras J, Jove R, Loughran TP Jr. Inhibition of STAT3 signaling leads to apoptosis of leukemic large granular lymphocytes and decreased Mcl-1 expression. *J Clin Invest.* 2001; 107:351-362.
- Gritsko T, Williams A, Turkson J, *et al.* Persistent activation of stat3 signaling induces survivin gene expression and confers resistance to apoptosis in human breast cancer cells. *Clin Cancer Res.* 2006; 12:11-19.
- Bosetti C, Negri E, Franceschi S, Pelucchi C, Talamini R, Montella M, Conti E, La Vecchia C. Diet and ovarian cancer risk: A case-control study in Italy. *Int J Cancer.* 2001; 93:911-915.
- Banerjee S, Kong D, Wang Z, Bao B, Hillman GG, Sarkar FH. Attenuation of multi-targeted proliferation-linked signaling by 3,3'-diindolylmethane (DIM): From bench to clinic. *Mutat Res.* 2011; 728:47-66.
- Kandala PK, Wright SE, Srivastava SK. Blocking epidermal growth factor activation by 3,3'-diindolylmethane suppresses ovarian tumor growth *in vitro* and *in vivo*. *J Pharmacol Exp Ther.* 2012; 341:24-32.
- Kandala PK, Srivastava SK. Diindolylmethane suppresses ovarian cancer growth and potentiates the effect of cisplatin in tumor mouse model by targeting signal transducer and activator of transcription 3 (STAT3). *BMC Med.* 2012; 10:9.
- Kandala PK, Srivastava SK. Activation of checkpoint kinase 2 by 3,3'-diindolylmethane is required for causing G2/M cell cycle arrest in human ovarian cancer cells. *Mol Pharmacol.* 2010; 78:297-309.
- Boreddy SR, Pramanik KC, Srivastava SK. Pancreatic tumor suppression by benzyl isothiocyanate is associated with inhibition of PI3K/AKT/FOXO pathway. *Clin Cancer Res.* 2011; 17:1784-1795.
- Colomiere M, Ward AC, Riley C, Trenerry MK, Cameron-Smith D, Findlay J, Ackland L, Ahmed N. Cross talk of signals between EGFR and IL-6R through JAK2/STAT3 mediate epithelial-mesenchymal transition in ovarian carcinomas. *Br J Cancer.* 2009; 100:134-144.
- Li F, Rajendran P, Sethi G. Thymoquinone inhibits proliferation, induces apoptosis and chemosensitizes human multiple myeloma cells through suppression of signal transducer and activator of transcription 3 activation pathway. *Br J Pharmacol.* 2010; 161:541-554.
- Natarajan C, Sriram S, Muthian G, Bright JJ. Signaling through JAK2-STAT5 pathway is essential for IL-3-

- induced activation of microglia. *Glia*. 2004; 45:188-196.
23. Bromberg JF, Wrzeszczynska MH, Devgan G, Zhao Y, Pestell RG, Albanese C, Darnell JE, Jr. Stat3 as an oncogene. *Cell*. 1999; 98:295-303.
 24. Rahman KW, Li Y, Wang Z, Sarkar SH, Sarkar FH. Gene expression profiling revealed survivin as a target of 3,3'-diindolylmethane-induced cell growth inhibition and apoptosis in breast cancer cells. *Cancer Res*. 2006; 66:4952-4960.
 25. Wang WZ, Zhang BY, Yuan J, Mao JW, Mei WJ. Effect of curcumin on JAK-STAT signaling pathway in hepatoma cell lines. *Yao Xue Xue Bao*. 2009; 44:1434-1439. (in Chinese)
 26. Alper O, Bergmann-Leitner ES, Bennett TA, Hacker NF, Stromberg K, Stetler-Stevenson WG. Epidermal growth factor receptor signaling and the invasive phenotype of ovarian carcinoma cells. *J Natl Cancer Inst*. 2001; 93:1375-1384.
 27. Reed GA, Sunega JM, Sullivan DK, Gray JC, Mayo MS, Crowell JA, Hurwitz A. Single-dose pharmacokinetics and tolerability of absorption-enhanced 3,3'-diindolylmethane in healthy subjects. *Cancer Epidemiol Biomarkers Prev*. 2008; 17:2619-2624.
 28. Del Priore G, Gudipudi DK, Montemarano N, Restivo AM, Malanowska-Stega J, Arslan AA. Oral diindolylmethane (DIM): Pilot evaluation of a nonsurgical treatment for cervical dysplasia. *Gynecol Oncol*. 2010; 116:464-467.
 29. Heath EI, Heilbrun LK, Li J, Vaishampayan U, Harper F, Pemberton P, Sarkar FH. A phase I dose-escalation study of oral BR-DIM (BioResponse 3,3'-diindolylmethane) in castrate-resistant, non-metastatic prostate cancer. *Am J Transl Res*. 2010; 2:402-411.

(Received February 10, 2012; Revised March 21, 2012; Accepted March 26, 2012)

Analyzing global trends of biomarker use in drug interventional clinical studies

Kunihiko Hayashi^{1,2,*}, Sachiko Masuda¹, Hiromichi Kimura¹

¹Pharmaco-Business Innovation Laboratory, Graduate School of Pharmaceutical Science, The University of Tokyo, Tokyo, Japan;

²Office of Pharmaceutical Industry Research, Japan Pharmaceutical Manufacturers Association, Tokyo, Japan.

ABSTRACT: The trend of biomarker use in drug interventional clinical studies was analyzed using *ClinicalTrials.gov* to provide an overview of how biomarkers are used to streamline clinical studies and to examine regional differences. A total of 3,383 clinical study data was analyzed according to phase, region, sponsor, and therapeutic class. The number of clinical studies using biomarkers has been increasing constantly and is dependent on the number of Phase I and II studies. The majority of studies (58.5%) were sponsored by the United States, with the studies being conducted mainly in the sponsor's home region (80.3%). The use of biomarkers was prominent in the oncology area (37.1%). Although current data indicates some bias in the clinical use of biomarkers, it is expected that their use will increase in later phase studies or other therapeutic areas as biomarker development proceeds. In addition, limited regional use of biomarkers may lead to differences in biomarker use in drug development and in combination with political support may result in differences in competitiveness of drug development. Biomarkers would be a powerful tool against deteriorating research and development productivity when used more in appropriate clinical study conditions.

Keywords: Drug development, clinical study efficiency, industrial policy

1. Introduction

Deterioration in drug research and development (R&D) productivity has occurred as a consequence of a dramatic increase in the cost of launching new drugs;

a trend that has had a major impact on pharmaceutical companies (1,2). Paul *et al.* had reported that the cost to launch one drug was \$1,778 million including capital costs (1). They showed that the cost incurred in clinical development (Phase I-III) was higher compared with that in the preclinical phase and accounted for 63% of the total cost for each new molecular entity launched. In addition, the cost of clinical studies increased in later phases, with the average out-of-pocket cost for Phase I, II, and III studies to launch one product being \$128 million, \$185 million, and \$235 million, respectively (1). Therefore, the impact of clinical study failure, particularly in later phases, is substantial for pharmaceutical companies.

Various methods and tools have been introduced to improve the efficiency and success rate of clinical studies. These approaches were included in the Critical Path Opportunities List published by the Food and Drug Administration (FDA) in 2006 (3). Seventy-six items were discussed in the List and were thought to improve the productivity of drug development when they became available. The List included various topics, such as clinical trial design, bioinformatics, and manufacturing, with the number of items related to biomarkers being the largest. Biomarkers are useful for precise diagnosis of diseases, predicting patient outcomes, monitoring disease status and response to treatment, excluding patients potentially vulnerable to drugs, selecting patients who would benefit from drugs, and selecting the appropriate dose for patients. Biomarkers may therefore contribute to the streamlining of R&D. As mentioned above, the cost of clinical studies and impact of study failure is considerable and biomarkers are used to mitigate such impacts. However, it remains unclear how biomarkers are used in clinical studies (*e.g.*, phase of studies, study sponsor, and therapeutic area).

Identifying the use of biomarkers in clinical studies may provide information on how biomarkers can contribute to streamlining of clinical studies and how they can be used to increase the effectiveness of these studies. In addition, cross-regional analysis of biomarker use also needs to be considered. As the number of clinical studies varies between regions, the number of clinical studies using biomarkers may also vary

*Address correspondence to:

Kunihiko Hayashi, Pharmaco-Business Innovation Laboratory, Graduate School of Pharmaceutical Science, The University of Tokyo, 7-3-1 Hongo, Bunkyo-ku, Tokyo 103-0023, Japan.
E-mail: hayashi-opir@jpma.or.jp

between regions. Precise analysis may provide future perspectives for drug development and identify strategic differences among regions (4).

2. Methods

ClinicalTrials.gov is the biggest clinical study registry, was developed by the US National Institutes of Health (NIH) in collaboration with FDA and was used as the clinical study database in this analysis. A keyword search using "biomarker" (including "marker") was used to obtain a set of data that identified biomarkers with research interest. The data of the studies identified were downloaded into a spread sheet with available field data. XML files of these studies that included more detailed information were also downloaded. To focus on the effects of biomarkers on drug/therapy development, clinical studies using drug (small molecule drugs and biologics for therapeutic use) as a study intervention were further selected using field data. These studies included not only interventional studies, but also a small number of observational studies. Observational studies were therefore eliminated. The selected studies were then stratified according to year (classified by start date), study phase, region of sponsor (US, European Union (EU), Japan or other), funding body (industry, US government, or other), and therapeutic group (classified by condition and intervention). For analysis, Phase I/II and II/III studies were regarded as Phase II and III, respectively. The sponsor's region was classified according to the location information provided. The therapeutic area was selected on the basis of the drug intervention using the therapeutic subgroup (2nd level) of the Anatomical Therapeutic Chemical (ATC) classification system (5).

3. Results

A search of clinical studies registered in *ClinicalTrials.gov* identified 40,172 drug interventional studies conducted between 2002 and 2009 (Figure 1). Of these studies, 3,383 studies were identified as the biomarker studies that used any type of biomarker, while the remaining 26,789 studies did not include a biomarker. Biomarker studies were further analyzed.

The number of clinical studies using biomarkers has been increasing year after year, with the proportion of such studies compared to the total number of registered

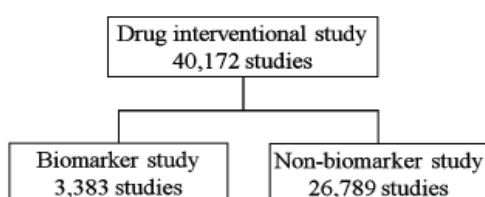


Figure 1. Flowchart showing disposition of biomarker studies for analysis.

studies also increasing (Figure 2). These studies were then stratified according to their phase. Information on phase was missing in 11.1% of studies, although more than two-thirds of these were considered to be early phase studies based on their study size (< 100 subjects). The number of Phase I and II studies using biomarkers increased steadily, producing 153 Phase I studies and 305 Phase II studies in 2009, and in parallel, the proportion of these studies compared to the total number of corresponding phase studies also increased with time, reaching 11.6% and 13.6% in Phase I and II in 2009, respectively. In contrast, the numbers of Phase III and IV studies using biomarkers increased slightly, producing 71 Phase III studies and 61 Phase IV studies in 2009, although the proportion of these studies compared to the total number of corresponding phase studies remained almost unchanged at around 6% (Figure 3).

When the studies were stratified according to location of the study sponsor it was observed that 58.5% were conducted by US sponsors, 31.5% by EU sponsors, 2.6% by Japanese sponsors, and 7.4% by other sponsors. The number of studies by US sponsor increased steadily,

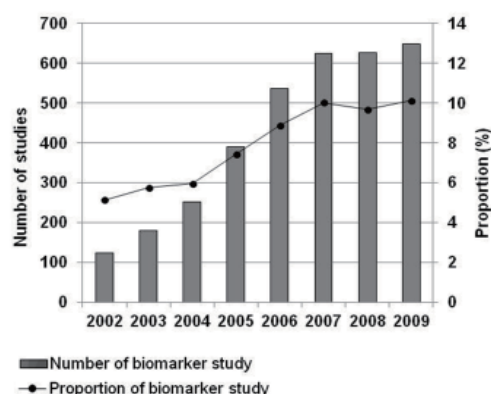


Figure 2. The number and proportion of biomarker studies.

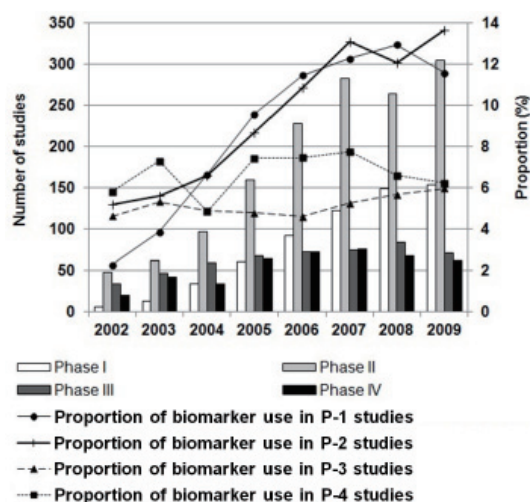


Figure 3. The number and proportion of biomarker studies grouped according to phase.

producing over 400 studies in 2009, while those from EU sponsors also increased until 2007 but slightly decreased in 2008 and 2009 (Figure 4). The number of studies by Japanese sponsors remained low (at most 20 studies) throughout the period. The relationship between sponsor region and study location was analyzed, although study site information was missing in 243 studies. It was found that 80.3% of clinical studies conducted by the US, EU, or Japanese sponsors were conducted in their home country, while 76.9% of biomarker studies were conducted in a single county and 16.1% as multinational studies (Table 1). When this figure was grouped according to sponsor region, different tendencies were observed between the regions, with 10.9%, 25.7%, and 17.0% of US-, EU- and Japanese-sponsored studies being multinational, respectively.

Regarding characteristics of study sponsors, the number of industry funded studies (total 1,620 studies) were more than that of the US government (*i.e.*, NIH, US National Institutes) (total 826 studies), whereas the proportion of biomarker use was higher in US government-funded studies (*e.g.* 13.4% in 2009) than industry-funded studies (*e.g.* 6.0% in 2009) (Figure 5).

Studies were classified into therapeutic subgroups of interventional drugs to analyze biomarker use according to therapeutic areas. As shown in Table 2, the number of clinical studies using biomarkers was notably high for antineoplastic agents (37.1%), followed by lipid modifying agents (6.1%), drugs used in diabetes (5.0%), and drugs for treatment of bone diseases (3.9%) (Table 2). These studies were then classified according to sponsor characteristics and the number of studies was

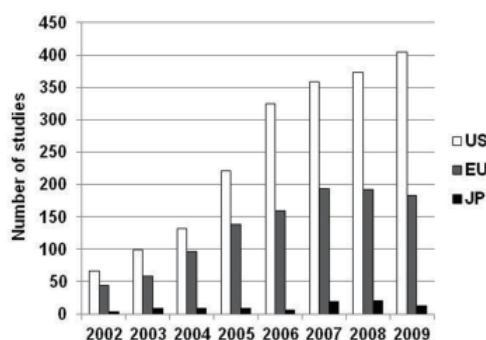


Figure 4. The number of biomarker studies grouped according to sponsor region.

grouped into four major therapeutic subclasses. The US government, US industry, and EU industry funded 826, 853, and 656 studies, respectively; however, when these numbers were divided into therapeutic areas, a different trend was observed (Table 3). The number of clinical studies on antineoplastic agents was high in US government-funded investigations. A similar trend was observed in US industry-funded studies, although the number was relatively low in EU industry-funded studies.

4. Discussion

Our analysis illustrated that researchers have shown an increasing interest in the use of biomarkers in clinical trials over time, with the proportion of such studies compared to total number of studies also rising. This trend may reflect the increase in Phase I and II studies and the fact that biomarkers are used extensively in oncology studies that are predominantly early phase investigations. It has been reported that development of antineoplastic/immunologic agents was the most active of all therapeutic classes (6), due to accumulation of knowledge in cancer biology and an associated increase in the number of molecular-targeted medicines. It has also been reported that biomarker use has increased in oncology Phase I studies, with pharmacodynamic markers being used most frequently for the study of the mechanism of action (7). Early phase studies tend to

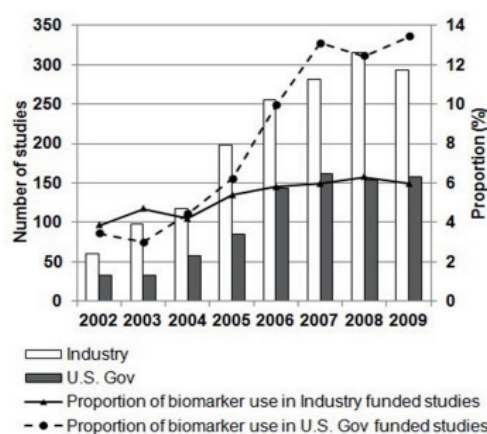


Figure 5. The number and proportion of biomarker studies grouped according to funding by industry or the US government.

Table 1. The number of studies grouped according to sponsor location and type of study

Sponsor location and type of clinical study	US sponsor	EU sponsor	JP sponsor	Total
Single country study in home region	1,522 (76.9%)	539 (50.6%)	31 (35.2%)	2,092 (66.8%)
Single country study outside home region	96 (4.9%)	187 (17.5%)	32 (36.4%)	315 (10.1%)
MNT including home region	190 (9.6%)	232 (21.8%)	1 (1.1%)	423 (13.5%)
MNT outside home region	25 (1.3%)	42 (3.9%)	14 (15.9%)	81 (2.6%)
No site information	145 (7.3%)	66 (6.2%)	10 (11.4%)	221 (7.1%)
	1,978 (total)	1,066 (total)	88 (total)	3,132 (total)

MNT: multinational trial.

Table 2. The number of studies grouped by therapeutic class

ATC2	Therapeutic class	Number of studies
A10	Drugs used in diabetes	168 (5.0%)
A11	Vitamins	79 (2.3%)
B01	Antithrombotic agents	64 (1.9%)
C09	Agents acting on the rennin-angiotensin system	82 (2.4%)
C10	Lipid modifying agents	205 (6.1%)
G03	Sex hormones and modulators of the genital system	83 (2.5%)
J05	Antivirals for systemic use	69 (2.0%)
J06	Immune sera and immunoglobulins	71 (2.1%)
L01	Antineoplastic agents	1,255 (37.1%)
L02	Endocrine therapy	74 (2.2%)
L03	Immunostimulants	92 (2.7%)
L04	Immunosuppressants	97 (2.9%)
M01	Antiinflammatory and antirheumatic products	63 (1.9%)
M05	Drugs for treatment of bone diseases	134 (3.9%)
N06	Psychoanaleptics	66 (2.0%)
R03	Drugs for obstructive airway diseases	82 (2.4%)

ATC classes with less than 50 studies were eliminated.

include biomarkers in oncology and other therapeutic areas, such as pharmacodynamics, pathology, or biomarker exploration, and these collectively contribute to the large number of biomarkers used in Phase I and II investigations. Although use of pharmacodynamic or pathological markers has increased, these markers were usually limited to secondary or exploratory endpoints. Clinical studies using a biomarker as a primary endpoint or patient stratification are still infrequent. This suggests that biomarkers useful for evaluating true endpoints or for selecting patients have not increased to a great extent, and therefore use of biomarkers in later phase studies has not increased. Considering the fact that later stage studies are more costly, development of biomarkers suitable for these studies is necessary to enhance efficiency of clinical studies. Although development of these biomarkers is difficult, FDA recognized the necessity of these biomarkers and efforts have been made to establish some surrogate markers through Critical Path Initiatives. The pharmaceutical industry also understands the importance of predictive markers for patient selection and investigational drugs, and there is now extensive development of these markers, primarily for antitumor agents. FDA also acted in concert with the pharmaceutical industry and released guidelines to support such development activities (8,9). The number of these markers is still insufficient, although the number of investigational drugs using patient stratification markers is increasing, mainly in antitumor drug studies. Therefore, the number of biomarkers will definitely increase with the development of pharmacogenomics technology and related regulations and guidelines. These regulations support use of biomarkers, not only in the area of oncology, but also other therapeutic areas and ultimately will help streamline drug development.

Table 3. The number of studies in major therapeutic classes grouped according to funding by industry or the US government

Therapeutic class	US Government	US Industry	EU Industry
Antineoplastic agents	470	333	171
Drugs used in diabetes	28	43	34
Lipid modifying agents	22	61	36
Drugs for treatment of bone disease	5	34	55
Total	826	853	656

The number of biomarker-related clinical studies was highest in the US. This may be due to the US being the largest pharmaceutical market. In addition, US government policies strongly support healthcare-related R&D (e.g., National Cancer Program and Critical Path research). In spite of the large number of clinical studies using biomarkers, the majority of studies were conducted in a single country. The proportion of single country studies is higher than the previously reported rate in North America (54.7%) or Western Europe (27.0%) (4). This is due to the majority of studies being relatively small Phase I or II investigations conducted at a small number of investigational sites. In addition, the large number of US government-funded studies conducted mainly in the US also affected this difference. A higher proportion of single country studies also indicates the lower proportion of global studies. The recent study globalization was led by cost constraints; however, it is known that there are ethnic differences in pharmacogenomics in certain cases, and therefore it is reasonable to conduct clinical studies and collect data in home countries to avoid such potential biases (10). To utilize biomarkers more efficiently, it is important to collect unbiased data within home countries, i.e., conducting clinical studies within home countries is important to streamline R&D that uses biomarkers. In this context, the situation in Japan is worrisome as the number of biomarker studies is quite small despite Japan being the second largest pharmaceutical market as a single country. As the Japanese regulatory authorities often require clinical data of Japanese patient populations for review and approval, the small number of biomarker studies may lead to a future lag in biomarkers being used in drug development studies, which would be similar to the problem of drug lag in the country (11). An example of such biomarker lag is the preclinical renal toxicity markers developed by the Critical Path Institute's Predictive Safety Testing Consortium. These markers were authorized by FDA and European Medicines Agency (EMA) in 2008, whereas Japanese Pharmaceuticals and Medical Devices Agency (PMDA) only authorized these in 2010 (12,13). There is a potential risk that biomarker lag may therefore occur in Japan. An increase in the number of clinical studies and use of biomarkers in Japan should be encouraged to avoid this situation.

Finally, while US and EU industries and the US government funded studies more or less equally, the US government funded more oncology studies. The number of oncology studies was substantial compared to other therapeutic areas, with this difference being related to the US healthcare-related policies. National Cancer Institute (NCI) gained the biggest share of the US NIH budget, with the budget for studies including biomarkers constituting almost half of its budget. This trend contributed to the considerable number of early stage oncology studies. In this way, the US government has led the development of biomarkers and the industry has followed. Combined with the aforementioned R&D concentration in home regions, it is likely that the US R&D competitiveness will increase led by the US government, particularly in the field of oncology.

The use of biomarkers has been increasing, although their use is still limited in early phase and oncology studies. Various strategic actions have been implemented to improve this situation, such as investment in the development of biomarkers and preparation of various guidelines for biomarker development. These actions will help biomarker development and streamline clinical studies using biomarkers.

It has also become evident that biomarker use is active in the US, particularly in the field of oncology, mainly due to the US government healthcare-related policies. Collecting data in home regions and implementing policies to support this together with the aforementioned strategies will strengthen the competitiveness of drug development in all countries.

As discussed above, the use of biomarkers has not been sufficient to date. When development of biomarkers proceeds, particularly patient selection markers, this could lead to segmentation of patient populations. Small patient populations could be an obstacle in drug development if streamlining of development is not achieved using biomarkers. Market segmentation may also be a disincentive for pharmaceutical companies even when drugs can be developed using small patient populations. In contrast, provision of safe and effective drugs to small patient populations is necessary from a national perspective of health, and therefore governments also need to play a role in the development and use of biomarkers. The roles of the pharmaceutical industry and government in biomarker development and use are mutually complementary and collaboration between these parties is important for the development of medicine using biomarkers.

Biomarkers would be powerful tools against deteriorating R&D productivity when used more in appropriate clinical study conditions.

Limitation. *ClinicalTrials.gov* was employed in this research, although due to the nature of this database it is possible that there may be a registration bias. As US is the largest pharmaceutical market and many industries

try to first launch their product in this market, many industry-funded studies are registered on this site. US academia and national institutes also register their studies under US Investigational New Drugs (IND), whereas clinical studies conducted by EU or Japanese academia or national institutes may not have been registered on this site. These studies may be covered by other registries such as the Japanese Pharmaceutical Information Center (JAPIC), University Hospital Medical Information Network (UMIN) (Japan), or EudraCT (Europe), although the format of these registries is not unified and therefore integration of this information was not possible. In addition, data before 2004 may be limited as clinical study registration was only encouraged by the International Committee of Medical Journal Editors in 2004 (14). Furthermore, there were some cases in which the contents of the study synopsis were not detailed. Therefore, our research could have underestimated the use of biomarkers due to limitations in the keyword search. Further detailed research on the purpose of biomarker use needs to be considered.

References

1. Paul SM, Mytelka DS, Dunwiddie CT, Persinger CC, Munos BH, Lindborg SR, Schacht AL. How to improve R&D productivity: The pharmaceutical industry's grand challenge. *Nat Rev Drug Discov.* 2010; 9:203-214.
2. DiMasi JA, Hansen RW, Grabowski HG. The price of innovation: New estimates of drug development costs. *J Health Econ.* 2003; 22:151-185.
3. US Department of Health and Human Services, Food and Drug Administration. Critical Path Opportunities List, March 2006. <http://www.fda.gov/downloads/ScienceResearch/SpecialTopics/CriticalPathInitiative/CriticalPathOpportunitiesReports/UCM077258.pdf> (accessed February 6, 2012).
4. Thiers FA, Sinskey AJ, Berndt ER. Trends in the globalization of clinical trials. *Nat Rev Drug Discov.* 2008; 7:13-14.
5. WHO Collaborating Centre for Drug Statistics Methodology. Guidelines for ATC classification and DDD assignment 2011. Oslo, 2010.
6. DiMasi JA, Feldman L, Secker A, Wilson A. Trends in risks associated with new drug development: Success rates for investigational drugs. *Clin Pharmacol Ther.* 2010; 87:272-277.
7. Goulart BHL, Clark JK, Pien HH, Roberts TG, Finkelstein SN, Chabner BA. Trends in the use and role of biomarkers in phase I oncology trials. *Clin Cancer Res.* 2007; 13:6719-6726.
8. US Department of Health and Human Services, Food and Drug Administration. Guidance for Industry, Qualification Process for Drug Development Tool, October 2010. <http://www.fda.gov/downloads/Drugs/GuidanceComplianceRegulatoryInformation/Guidances/UCM230597.pdf> (accessed February 6, 2012).
9. US Department of Health and Human Services, Food and Drug Administration. Draft Guidance for Industry and FDA Staff, *In Vitro* Companion Diagnostic Devices, July

2011. <http://www.fda.gov/downloads/MedicalDevices/DeviceRegulationandGuidance/GuidanceDocuments/UCM262327.pdf> (accessed February 6, 2012).
10. Yasuda SU, Zhang L, Huang SM. The role of ethnicity in variability in response to drugs: Focus on clinical pharmacology studies. *Clin Pharmacol Ther.* 2008; 84:417-423.
 11. Tsuji K, Tsutani K. Approval of new drugs 1999-2007: Comparison of the US, the EU and Japan situations. *J Clin Pharm Ther.* 2010; 35:289-301.
 12. US Department of Health and Human Services, Food and Drug Administration. FDA, EMA to Consider Additional Test Results When Assessing New Drug Safety, June 2008. <http://www.fda.gov/NewsEvents/Newsroom/PressAnnouncements/2008/ucm116911.htm> (accessed February 6, 2012).
 13. Pharmaceuticals and Medical Devices Agency. Record of the Consultation on Pharmacogenomics/Biomarkers, May 2010. <http://www.pmda.go.jp/operations/shonin/info/consult/file/pbm-kiroku-e.pdf> (accessed February 6, 2012).
 14. De Angelis C, Drazen JM, Frizelle FA, Haug C, Hoey J, Horton R, Kotzin S, Laine C, Marusic A, Overbeke AJ, Schroeder TV, Sox HC, Van Der Weyden MB. Clinical trial registration: A statement from the International Committee of Medical Journal Editors. *N Engl J Med.* 2004; 351:1250-1251.
- (Received February 10, 2012; Revised March 29, 2012; Accepted April 3, 2012)

Standardization of perioperative management on hepato-biliary-pancreatic surgery

Jianjun Gao^{1,2}, Peipei Song¹, Sumihito Tamura¹, Kiyoshi Hasegawa¹, Yasuhiko Sugawara¹, Norihiro Kokudo¹, Kanji Uchida³, Ryo Orii³, Fanghua Qi^{1,4}, Jiahong Dong^{5,*}, Wei Tang^{1,*}

¹ Department of Surgery, Graduate School of Medicine, The University of Tokyo, Tokyo, Japan;

² China-Japan Cooperation Center for Drug Discovery & Screening, Shandong University, Ji'nan, China;

³ Department of Anesthesiology, Faculty of Medicine, The University of Tokyo, Tokyo, Japan;

⁴ Provincial Hospital Affiliated to Shandong University, Ji'nan, China;

⁵ Hepato-Biliary-Pancreatic Surgery Division, The General Hospital of PLA, Beijing, China.

ABSTRACT: Japan-China Joint Medical Workshop (2012) on standardization of perioperative management on hepato-biliary-pancreatic surgery was held by the Center for Medical Standards Research, IRCA-BSSA Group in Japan on April 15-16, 2012. Experts in the fields of surgery, anesthesia, pharmacy, and public health from 21 health institutions from Japan and China presented their research achievements and shared their medical experience of perioperative management on hepato-biliary-pancreatic surgery, which should facilitate building of guidelines for hepatocellular carcinoma and be expected to promote standardized management of liver cancer in Asia.

Keywords: Guideline, standardized management, liver surgery, liver transplantation

From advocacy of evidence-based medicine to establishment of clinical pathways, the concept of "standardized management of care" has garnered substantial attention globally and has been fully implemented in several countries. Clinical practices prove that standardized management of care contributes to normalized medical practices, optimized health care programs, decreased medical risks, increased efficiency of medical services, and reduced health care costs (1,2). In this context, the Center for Medical Standards Research (CMSR) was established by the IRCA-BSSA Group in Japan in 2011, aiming to promote the advancement of evidence-based medicine, standardization

of medical care, and systematic cataloging of research findings in related disciplines. Many research programs on standardized management of diseases have been promoted by CMSR since the establishment, especially for the research between Japan and China. Concerning liver cancer, the Japan-China Joint Team for Medical Research and Cooperation on Hepatocellular Carcinoma was established in 2011 with the support of CMSR. The team carried out a retrospective study and analyzed the published guidelines for hepatocellular carcinoma (HCC) worldwide, and clarified principles of evidence-, resource-, and population-based guidelines that should be given a great deal of attention in constructing prospective guidelines for HCC, especially for China and other Asian countries (3,4).

As part of the standardized management of liver cancer, the Japan-China Joint Team for Medical Research and Cooperation on Hepato-Biliary-Pancreatic Surgery was also established with the support of CMSR. In order to promote information exchange between experts from Japan and China, the Japan-China Joint Medical Workshop (2012) on Standardization of Perioperative Management on Hepato-Biliary-Pancreatic Surgery was held by CMSR at the University of Tokyo, Tokyo, Japan on April 15-16, 2012. Experts in the fields of surgery, anesthesia, pharmacy, and public health from 21 health institutions from Japan and China presented their research achievements and shared their medical experience of perioperative management on hepato-biliary-pancreatic surgery.

In this workshop, experts from the Chinese PLA General Hospital, Peking Union Medical College Hospital, Peking University People's Hospital, and other institutes introduced the current Chinese research status and their experience on the topics of protection of remnant liver function, perioperative management for abdominal surgery, and so on. Specifically, the experts' research and experience on perioperative management of safe liver resection from the University

*Address correspondence to:

The "Japan-China Joint Team for Medical Research and Cooperation"

Dr. Jiahong Dong (E-mail: dongjh301@163.com) and Dr. Wei Tang (E-mail: tang-sur@h.u-tokyo.ac.jp)

of Tokyo Hospital (UTH) was impressive since the short-term mortality after hepatectomy in this hospital is nearly 0 which is far less than that in representative hospitals of other countries (ranges: approximate 4-6%) (5-11). Their research and experience are shared as the following. First, in preparation for safe hepatectomy, they thought that evaluation of liver function, volumetric analysis, and keeping sufficient functional liver volume were thought to be important, and asserted that *i*) the indocyanine green (ICG) test is a key method to estimate liver function (12-14); *ii*) volumetric analysis using preoperative simulation is useful (15-17), and *iii*) portal vein embolization (PVE) (16,18,19) and venous reconstruction can contribute to securing sufficient functional liver volume (20-22). Second, in intra-operative management, control of central vein pressure (CVP), transection technique, and inflow occlusion should be paid close attention to. They proposed that *i*) low CVP should be achieved by some techniques such as infusion restriction, reducing TV (23), and blood salvage (24); *ii*) clamp crushing remains the first choice (25-28); and *iii*) intermittent inflow occlusion is safe and useful (29,30). Third, in post-operative management, prevention of infection including proper placement and management of drainage tubes (31) administration of antibiotics, control of ascites including exact control of water balance and proper administration of diuretics should be considered (32). The experience of UTH on management of safe hepatectomy may provide a valuable reference for standardization of perioperative management of liver surgery (11).

Experts from UTH also introduced their research and experience in living donor liver transplantation (LDLT). They emphasized that most important in LDLT is safety of the living donor with good quality of life after donation (33-35). To assure this, a careful protocol based evaluation process under a multidisciplinary approach (36,37) and a tailored graft selection algorithm (38) have been established. As for the recipients, three important points in pre-operative examination have been stressed. First is exclusion of pulmonary hypertension. Specifically, when right ventricular systolic pressure (RVSP) is evaluated to be more than 50 mmHg by ultrasound imaging (US), the pressure must be measured directly. If the pressure is actually more than 50 mmHg, the patient should be contraindicated for LDLT. Second is exclusion of infectious disease that may seriously compromise survival. Bacterial, viral, and fungal checks are necessary for successful LDLT. Third is the check for esophageal varices and treatment, and endoscopic ligation if necessary. In postoperative care, four major complications including infection, acute cellular rejection (ACR), biliary stenosis, and thrombosis occur with rates of approximately 40%, 30%, 10%, and 8%, respectively. Close monitoring and early intervention is mandatory in every aspect for better survival of the recipient. In case of suspected infectious complications, treatment with

prophylactic administration of antibiotics, and antiviral or antifungal drugs may be justified (39-41). Of note is the novel approach with plasma (1 → 3) β -D-glucan measurement for preemptive treatment of fungal diseases that may often become fatal once becoming symptomatic (41). Meticulous adjustment of immunosuppressive drug levels (42), regularly performed US to confirm intact blood flow, in combination with adequate anticoagulation may further contribute to early sound recovery of the recipient. The experience of UTH on LDLT may also contribute to the standardization of liver surgery.

In conclusion, the Japan-China Joint Medical Workshop (2012) discussed the hot topic of standardization of perioperative management on hepato-biliary-pancreatic surgery, with information exchange from Japan and China. The experts' research and experience presented in this workshop should facilitate building of guidelines. Furthermore, these achievements are expected to promote standardized management of liver cancer in Asia.

Acknowledgements

This work was supported by the Center for Medical Standards Research, IRCA-BSSA Group. We are grateful to Dr. Takeaki Ishizawa, Dr. Yosuke Inoue, and Dr. Atsushi Shimizu (Department of Surgery, Graduate School of Medicine, The University of Tokyo) for their support of this conference.

References

1. Srinivasan C, Sachdeva R, Morrow WR, Gossett J, Chipman CW, Imamura M, Jaquiss RD. Standardized management improves outcomes after the Norwood procedure. *Congenit Heart Dis*. 2009; 4:329-337.
2. Brignole M, Ungar A, Bartoletti A, Ponassi I, Lagi A, Mussi C, Ribani MA, Tava G, Disertori M, Quartieri F, Alboni P, Raviele A, Ammirati F, Scivales A, De Santo T. Standardized-care pathway vs. usual management of syncope patients presenting as emergencies at general hospitals. *Europace*. 2006; 8:644-650.
3. Song P, Tang W, Tamura S, Hasegawa K, Sugawara Y, Dong J, Kokudo N. The management of hepatocellular carcinoma in Asia: A guideline combining quantitative and qualitative evaluation. *Biosci Trends*. 2010; 4:283-287.
4. Song P, Tobe RG, Inagaki Y, Kokudo N, Hasegawa K, Sugawara Y, Tang W. The management of hepatocellular carcinoma around the world: A comparison of guidelines from 2001 to 2011. *Liver Int*. 2012 Mar 20. doi: 10.1111/j.1478-3231.2012.02792.x.
5. Kishi Y, Abdalla EK, Chun YS, Zorzi D, Madoff DC, Wallace MJ, Curley SA, Vauthey JN. Three hundred and one consecutive extended right hepatectomies: Evaluation of outcome based on systematic liver volumetry. *Ann Surg*. 2009; 250:540-548.
6. Poon RT, Fan ST, Lo CM, Liu CL, Lam CM, Yuen WK, Yeung C, Wong J. Improving perioperative outcome expands the role of hepatectomy in management of benign and malignant hepatobiliary diseases: Analysis of

- 1222 consecutive patients from a prospective database. *Ann Surg.* 2004; 240:698-708; discussion 708-710.
7. Dimick JB, Cowan JA Jr, Knol JA, Upchurch GR Jr. Hepatic resection in the United States: Indications, outcomes, and hospital procedural volumes from a nationally representative database. *Arch Surg.* 2003; 138:185-191.
 8. Belghiti J, Kianmanesh R. Surgical treatment of hepatocellular carcinoma. *HPB (Oxford).* 2005; 7:42-49.
 9. Fong Y, Sun RL, Jarnagin W, Blumgart LH. An analysis of 412 cases of hepatocellular carcinoma at a Western center. *Ann Surg.* 1999; 229:790-799; discussion 799-800.
 10. Fuster J, Garcia-Valdecasas JC, Grande L, Tabet J, Bruix J, Anglada T, Taura P, Lacy AM, Gonzalez X, Vilana R, Bru C, Sole M, Visa J. Hepatocellular carcinoma and cirrhosis. Results of surgical treatment in a European series. *Ann Surg.* 1996; 223:297-302.
 11. Imamura H, Seyama Y, Kokudo N, Maema A, Sugawara Y, Sano K, Takayama T, Makuuchi M. One thousand fifty-six hepatectomies without mortality in 8 years. *Arch Surg.* 2003; 138:1198-1206; discussion 1206.
 12. Makuuchi M, Kosuge T, Takayama T, Yamazaki S, Kakazu T, Miyagawa S, Kawasaki S. Surgery for small liver cancers. *Semin Surg Oncol.* 1993; 9:298-304.
 13. Torzilli G, Makuuchi M, Inoue K, Takayama T, Sakamoto Y, Sugawara Y, Kubota K, Zucchi A. No-mortality liver resection for hepatocellular carcinoma in cirrhotic and noncirrhotic patients: Is there a way? A prospective analysis of our approach. *Arch Surg* 1999; 134:984-992.
 14. Ishizawa T, Hasegawa K, Aoki T, Takahashi M, Inoue Y, Sano K, Imamura H, Sugawara Y, Kokudo N, Makuuchi M. Neither multiple tumors nor portal hypertension are surgical contraindications for hepatocellular carcinoma. *Gastroenterology.* 2008; 134:1908-1916.
 15. Urata K, Kawasaki S, Matsunami H, Hashikura Y, Ikegami T, Ishizone S, Momose Y, Komiyama A, Makuuchi M. Calculation of child and adult standard liver volume for liver transplantation. *Hepatology.* 1995; 21:1317-1321.
 16. Kubota K, Makuuchi M, Kusaka K, Kobayashi T, Miki K, Hasegawa K, Harihara Y, Takayama T. Measurement of liver volume and hepatic functional reserve as a guide to decision-making in resectional surgery for hepatic tumors. *Hepatology.* 1997; 26:1176-1181.
 17. Kawasaki S, Makuuchi M, Matsunami H, Hashikura Y, Ikegami T, Chisawa H, Ikeno T, Noike T, Takayama T, Kawarazaki H. Preoperative measurement of segmental liver volume of donors for living related liver transplantation. *Hepatology.* 1993; 18:1115-1120.
 18. Makuuchi M, Thai BL, Takayasu K, Takayama T, Kosuge T, Gunvén P, Yamazaki S, Hasegawa H, Ozaki H. Preoperative portal embolization to increase safety of major hepatectomy for hilar bile duct carcinoma: A preliminary report. *Surgery.* 1990; 107:521-527.
 19. Imamura H, Shimada R, Kubota M, Matsuyama Y, Nakayama A, Miyagawa S, Makuuchi M, Kawasaki S. Preoperative portal vein embolization: An audit of 84 patients. *Hepatology.* 1999; 29:1099-1105.
 20. Mise Y, Hasegawa K, Satou S, Aoki T, Beck Y, Sugawara Y, Makuuchi M, Kokudo N. Venous reconstruction based on virtual liver resection to avoid congestion in the liver remnant. *Br J Surg.* 2011; 98:1742-1751.
 21. Hashimoto T, Kokudo N, Aoki T, Natori T, Arita J, Sano K, Imamura H, Sugawara Y, Makuuchi M. Reconstruction of middle hepatic vein using a rotating left hepatic vein flap. *J Am Coll Surg.* 2004; 199:656-660.
 22. Sakamoto Y, Yamamoto J, Kosuge T, Sugawara Y, Seki M, Kokudo N, Azekura K, Yamaguchi T, Muto T, Makuuchi M. Extended left hepatectomy by severing all major hepatic veins with reconstruction of the right hepatic vein. *Surg Today.* 2004; 34:482-484.
 23. Hasegawa K, Takayama T, Orii R, Sano K, Sugawara Y, Imamura H, Kubota K, Makuuchi M. Effect of hypoventilation on bleeding during hepatic resection: A randomized controlled trial. *Arch Surg.* 2002; 137:311-315.
 24. Hashimoto T, Kokudo N, Orii R, Seyama Y, Sano K, Imamura H, Sugawara Y, Hasegawa K, Makuuchi M. Intraoperative blood salvage during liver resection: A randomized controlled trial. *Ann Surg.* 2007; 245:686-691.
 25. Takayama T, Makuuchi M, Kubota K, Harihara Y, Hui AM, Sano K, Ijichi M, Hasegawa K. Randomized comparison of ultrasonic vs clamp transection of the liver. *Arch Surg.* 2001; 136:922-928.
 26. Sakamoto Y, Yamamoto J, Kokudo N, Seki M, Kosuge T, Yamaguchi T, Muto T, Makuuchi M. Bloodless liver resection using the monopolar floating ball plus ligasure diathermy: Preliminary results of 16 liver resections. *World J Surg.* 2004; 28:166-172.
 27. Seyama Y, Makuuchi M, Takayama T, Cescon M, Kokudo N. Can a small ultrasonic dissector equipped for electrocautery improve the results of hepatic resection? *Hepatogastroenterology.* 2005; 52:1845-1848.
 28. Ikeda M, Hasegawa K, Sano K, Imamura H, Beck Y, Sugawara Y, Kokudo N, Makuuchi M. The vessel sealing system (LigaSure) in hepatic resection: A randomized controlled trial. *Ann Surg.* 2009; 250:199-203.
 29. Imamura H, Takayama T, Sugawara Y, Kokudo N, Aoki T, Kaneko J, Matsuyama Y, Sano K, Maema A, Makuuchi M. Pringle's manoeuvre in living donors. *Lancet.* 2002; 360:2049-2050.
 30. Makuuchi M, Mori T, Gunvén P, Yamazaki S, Hasegawa H. Safety of hemihepatic vascular occlusion during resection of the liver. *Surg Gynecol Obstet.* 1987; 164:155-158.
 31. Kyoden Y, Imamura H, Sano K, Beck Y, Sugawara Y, Kokudo N, Makuuchi M. Value of prophylactic abdominal drainage in 1269 consecutive cases of elective liver resection. *J Hepatobiliary Pancreat Sci.* 2010; 17:186-192.
 32. Ishizawa T, Hasegawa K, Kokudo N, Sano K, Imamura H, Beck Y, Sugawara Y, Makuuchi M. Risk factors and management of ascites after liver resection to treat hepatocellular carcinoma. *Arch Surg.* 2009; 144:46-51.
 33. Tamura S, Sugawara Y, Kokudo N. Donor evaluation and hepatectomy for living-donor liver transplantation. *J Hepatobiliary Pancreat Surg.* 2008; 15:79-91.
 34. Tamura S, Sugawara Y, Kaneko J, Yamashiki N, Kishi Y, Matsui Y, Kokudo N, Makuuchi M. Systematic grading of surgical complications in live liver donors according to Clavien's system. *Transpl Int.* 2006; 19:982-987.
 35. Togashi J, Sugawara Y, Tamura S, Yamashiki N, Kaneko J, Aoki T, Hasegawa K, Beck Y, Makuuchi M, Kokudo N. Donor quality of life after living donor liver transplantation: A prospective study. *J Hepatobiliary Pancreat Sci.* 2011; 18:263-267.

36. Yamashiki N, Sugawara Y, Tamura S, Kaneko J, Matsui Y, Togashi J, Ohki T, Yoshida H, Omata M, Makuuchi M, Kokudo N. Noninvasive estimation of hepatic steatosis in living liver donors: Usefulness of visceral fat area measurement. *Transplantation*. 2009; 88:575-581.
37. Yamashiki N, Sugawara Y, Tamura S, Kaneko J, Nojiri K, Omata M, Makuuchi M. Selection of liver-transplant candidates for adult-to-adult living donor liver transplantation as the only surgical option for end-stage liver disease. *Liver Transpl*. 2006; 12:1077-1083.
38. Kokudo N, Sugawara Y, Imamura H, Sano K, Makuuchi M. Tailoring the type of donor hepatectomy for adult living donor liver transplantation. *Am J Transplant*. 2005; 5:1694-1703.
39. Togashi J, Sugawara Y, Hashimoto M, Tamura S, Kaneko J, Aoki T, Hasegawa K, Kokudo N. Oral valganciclovir versus intravenous ganciclovir as preemptive treatment for cytomegalovirus infection after living donor liver transplantation: A randomized trial. *Biosci Trends*. 2011; 5:217-222.
40. Hashimoto M, Sugawara Y, Tamura S, Kaneko J, Matsui Y, Togashi J, Makuuchi M. Bloodstream infection after living donor liver transplantation. *Scand J Infect Dis*. 2008; 40:509-516.
41. Akamatsu N, Sugawara Y, Kaneko J, Tamura S, Makuuchi M. Preemptive treatment of fungal infection based on plasma (1 → 3) β-D-glucan levels after liver transplantation. *Infection*. 2007; 35:346-351.
42. Sugawara Y, Makuuchi M, Kaneko J, Ohkubo T, Imamura H, Kawarasaki H. Correlation between optimal tacrolimus doses and the graft weight in living donor liver transplantation. *Clin Transplant*. 2002; 16:102-106.

(Received April 23, 2012)

Guide for Authors

1. Scope of Articles

Drug Discoveries & Therapeutics welcomes contributions in all fields of pharmaceutical and therapeutic research such as medicinal chemistry, pharmacology, pharmaceutical analysis, pharmaceuticals, pharmaceutical administration, and experimental and clinical studies of effects, mechanisms, or uses of various treatments. Studies in drug-related fields such as biology, biochemistry, physiology, microbiology, and immunology are also within the scope of this journal.

2. Submission Types

Original Articles should be well-documented, novel, and significant to the field as a whole. An Original Article should be arranged into the following sections: Title page, Abstract, Introduction, Materials and Methods, Results, Discussion, Acknowledgments, and References. Original articles should not exceed 5,000 words in length (excluding references) and should be limited to a maximum of 50 references. Articles may contain a maximum of 10 figures and/or tables.

Brief Reports definitively documenting either experimental results or informative clinical observations will be considered for publication in this category. Brief Reports are not intended for publication of incomplete or preliminary findings. Brief Reports should not exceed 3,000 words in length (excluding references) and should be limited to a maximum of 4 figures and/or tables and 30 references. A Brief Report contains the same sections as an Original Article, but the Results and Discussion sections should be combined.

Reviews should present a full and up-to-date account of recent developments within an area of research. Normally, reviews should not exceed 8,000 words in length (excluding references) and should be limited to a maximum of 100 references. Mini reviews are also accepted.

Policy Forum articles discuss research and policy issues in areas related to life science such as public health, the medical care system, and social science and may address governmental issues at district, national, and international levels of discourse. Policy Forum articles should not exceed 2,000 words in length (excluding references).

Case Reports should be detailed reports of the symptoms, signs, diagnosis, treatment, and follow-up of an individual patient. Case reports may contain a demographic profile of the patient but usually describe an unusual or novel occurrence. Unreported or unusual side effects or adverse interactions involving medications will also be considered. Case

Reports should not exceed 3,000 words in length (excluding references).

News articles should report the latest events in health sciences and medical research from around the world. News should not exceed 500 words in length.

Letters should present considered opinions in response to articles published in Drug Discoveries & Therapeutics in the last 6 months or issues of general interest. Letters should not exceed 800 words in length and may contain a maximum of 10 references.

3. Editorial Policies

Ethics: Drug Discoveries & Therapeutics requires that authors of reports of investigations in humans or animals indicate that those studies were formally approved by a relevant ethics committee or review board.

Conflict of Interest: All authors are required to disclose any actual or potential conflict of interest including financial interests or relationships with other people or organizations that might raise questions of bias in the work reported. If no conflict of interest exists for each author, please state "There is no conflict of interest to disclose".

Submission Declaration: When a manuscript is considered for submission to Drug Discoveries & Therapeutics, the authors should confirm that 1) no part of this manuscript is currently under consideration for publication elsewhere; 2) this manuscript does not contain the same information in whole or in part as manuscripts that have been published, accepted, or are under review elsewhere, except in the form of an abstract, a letter to the editor, or part of a published lecture or academic thesis; 3) authorization for publication has been obtained from the authors' employer or institution; and 4) all contributing authors have agreed to submit this manuscript.

Cover Letter: The manuscript must be accompanied by a cover letter signed by the corresponding author on behalf of all authors. The letter should indicate the basic findings of the work and their significance. The letter should also include a statement affirming that all authors concur with the submission and that the material submitted for publication has not been published previously or is not under consideration for publication elsewhere. The cover letter should be submitted in PDF format. For example of Cover Letter, please visit <http://www.ddtjournal.com/downloadcentre.php> (Download Centre).

Copyright: A signed JOURNAL PUBLISHING AGREEMENT (JPA) must be provided by post, fax, or as a scanned file before acceptance of the article. Only forms with a hand-written signature are accepted. This copyright will ensure the widest possible dissemination of information. A form facilitating transfer of copyright can be downloaded by clicking the appropriate link and can be returned to the e-mail address or fax number noted on the form (Please visit

Download Centre). Please note that your manuscript will not proceed to the next step in publication until the JPA form is received. In addition, if excerpts from other copyrighted works are included, the author(s) must obtain written permission from the copyright owners and credit the source(s) in the article.

Suggested Reviewers: A list of up to 3 reviewers who are qualified to assess the scientific merit of the study is welcomed. Reviewer information including names, affiliations, addresses, and e-mail should be provided at the same time the manuscript is submitted online. Please do not suggest reviewers with known conflicts of interest, including participants or anyone with a stake in the proposed research; anyone from the same institution; former students, advisors, or research collaborators (within the last three years); or close personal contacts. Please note that the Editor-in-Chief may accept one or more of the proposed reviewers or may request a review by other qualified persons.

Language Editing: Manuscripts prepared by authors whose native language is not English should have their work proofread by a native English speaker before submission. If not, this might delay the publication of your manuscript in Drug Discoveries & Therapeutics.

The Editing Support Organization can provide English proofreading, Japanese-English translation, and Chinese-English translation services to authors who want to publish in Drug Discoveries & Therapeutics and need assistance before submitting a manuscript. Authors can visit this organization directly at <http://www.iacmhr.com/iac-eso/support.php?lang=en>. IAC-ESO was established to facilitate manuscript preparation by researchers whose native language is not English and to help edit works intended for international academic journals.

4. Manuscript Preparation

Manuscripts should be written in clear, grammatically correct English and submitted as a Microsoft Word file in a single-column format. Manuscripts must be paginated and typed in 12-point Times New Roman font with 24-point line spacing. Please do not embed figures in the text. Abbreviations should be used as little as possible and should be explained at first mention unless the term is a well-known abbreviation (e.g. DNA). Single words should not be abbreviated.

Title page: The title page must include 1) the title of the paper (Please note the title should be short, informative, and contain the major key words); 2) full name(s) and affiliation(s) of the author(s); 3) abbreviated names of the author(s); 4) full name, mailing address, telephone/fax numbers, and e-mail address of the corresponding author; and 5) conflicts of interest (if you have an actual or potential conflict of interest to disclose, it must be included as a footnote on the title page of the manuscript; if no conflict of interest exists for each author, please state "There is no conflict of interest to disclose"). Please visit [Download Centre](#) and refer to the title page of the manuscript sample.

Abstract: A one-paragraph abstract consisting of no more than 250 words must be included. The abstract should briefly state the purpose of the study, methods, main findings, and conclusions. Abbreviations must be kept to a minimum and non-standard abbreviations explained in brackets at first mention. References should be avoided in the abstract. Key words or phrases that do not occur in the title should be included in the Abstract page.

Introduction: The introduction should be a concise statement of the basis for the study and its scientific context.

Materials and Methods: The description should be brief but with sufficient detail to enable others to reproduce the experiments. Procedures that have been published previously should not be described in detail but appropriate references should simply be cited. Only new and significant modifications of previously published procedures require complete description. Names of products and manufacturers with their locations (city and state/country) should be given and sources of animals and cell lines should always be indicated. All clinical investigations must have been conducted in accordance with Declaration of Helsinki principles. All human and animal studies must have been approved by the appropriate institutional review board(s) and a specific declaration of approval must be made within this section.

Results: The description of the experimental results should be succinct but in sufficient detail to allow the experiments to be analyzed and interpreted by an independent reader. If necessary, subheadings may be used for an orderly presentation. All figures and tables must be referred to in the text.

Discussion: The data should be interpreted concisely without repeating material already presented in the Results section. Speculation is permissible, but it must be well-founded, and discussion of the wider implications of the findings is encouraged. Conclusions derived from the study should be included in this section.

Acknowledgments: All funding sources should be credited in the Acknowledgments section. In addition, people who contributed to the work but who do not meet the criteria for authors should be listed along with their contributions.

References: References should be numbered in the order in which they appear in the text. Citing of unpublished results, personal communications, conference abstracts, and theses in the reference list is not recommended but these sources may be mentioned in the text. In the reference list, cite the names of all authors when there are fifteen or fewer authors; if there are sixteen or more authors, list the first three followed by *et al.* Names of journals should be abbreviated in the style used in PubMed. Authors are responsible for the accuracy of the references. Examples are given below:

Example 1 (Sample journal reference):
Nakata M, Tang W. Japan-China Joint Medical Workshop on Drug Discoveries and Therapeutics 2008: The need of Asian pharmaceutical researchers' cooperation. *Drug Discov Ther.* 2008; 2:262-263.

Example 2 (Sample journal reference with more than 15 authors):
Darby S, Hill D, Auvinen A, *et al.* Radon in homes and risk of lung cancer: Collaborative analysis of individual data from 13 European case-control studies. *BMJ.* 2005; 330:223.

Example 3 (Sample book reference):
Shalev AY. Post-traumatic stress disorder: Diagnosis, history and life course. In: *Post-traumatic Stress Disorder, Diagnosis, Management and Treatment* (Nutt DJ, Davidson JR, Zohar J, eds.). Martin Dunitz, London, UK, 2000; pp. 1-15.

Example 4 (Sample web page reference):
World Health Organization. The World Health Report 2008 – primary health care: Now more than ever. http://www.who.int/whr/2008/whr08_en.pdf (accessed September 23, 2010).

Tables: All tables should be prepared in Microsoft Word or Excel and should be arranged at the end of the manuscript after the References section. Please note that tables should not in image format. All tables should have a concise title and should be numbered consecutively with Arabic numerals. If necessary, additional information should be given below the table.

Figure Legend: The figure legend should be typed on a separate page of the main manuscript and should include a short title and explanation. The legend should be concise but comprehensive and should be understood without referring to the text. Symbols used in figures must be explained.

Figure Preparation: All figures should be clear and cited in numerical order in the text. Figures must fit a one- or two-column format on the journal page: 8.3 cm (3.3 in.) wide for a single column, 17.3 cm (6.8 in.) wide for a double column; maximum height: 24.0 cm (9.5 in.). Please make sure that artwork files are in an acceptable format (TIFF or JPEG) at minimum resolution (600 dpi for illustrations, graphs, and annotated artwork, and 300 dpi for micrographs and photographs). Please provide all figures as separate files. Please note that low-resolution images are one of the leading causes of article resubmission and schedule delays. All color figures will be reproduced in full color in the online edition of the journal at no cost to authors.

Units and Symbols: Units and symbols conforming to the International System of Units (SI) should be used for physicochemical quantities. Solidus notation (*e.g.* mg/kg, mg/mL, mol/mm²/min) should be used. Please refer to the SI Guide www.bipm.org/en/si/ for standard units.

Supplemental data: Supplemental data might be useful for supporting and enhancing your scientific research and

Drug Discoveries & Therapeutics accepts the submission of these materials which will be only published online alongside the electronic version of your article. Supplemental files (figures, tables, and other text materials) should be prepared according to the above guidelines, numbered in Arabic numerals (*e.g.*, Figure S1, Figure S2, and Table S1, Table S2) and referred to in the text. All figures and tables should have titles and legends. All figure legends, tables and supplemental text materials should be placed at the end of the paper. Please note all of these supplemental data should be provided at the time of initial submission and note that the editors reserve the right to limit the size and length of Supplemental Data.

5. Submission Checklist

The Submission Checklist will be useful during the final checking of a manuscript prior to sending it to Drug Discoveries & Therapeutics for review. Please visit [Download Centre](#) and download the Submission Checklist file.

6. Online submission

Manuscripts should be submitted to Drug Discoveries & Therapeutics online at <http://www.ddtjournal.com>. The manuscript file should be smaller than 5 MB in size. If for any reason you are unable to submit a file online, please contact the Editorial Office by e-mail at office@ddtjournal.com

7. Accepted manuscripts

Proofs: Galley proofs in PDF format will be sent to the corresponding author *via* e-mail. Corrections must be returned to the editor (proof-editing@ddtjournal.com) within 3 working days.

Offprints: Authors will be provided with electronic offprints of their article. Paper offprints can be ordered at prices quoted on the order form that accompanies the proofs.

Page Charge: A page charge of \$140 will be assessed for each printed page of an accepted manuscript. The charge for printing color figures is \$340 for each page. Under exceptional circumstances, the author(s) may apply to the editorial office for a waiver of the publication charges at the time of submission.

(Revised October 2011)

Editorial and Head Office:

Pearl City Koishikawa 603
2-4-5 Kasuga, Bunkyo-ku
Tokyo 112-0003
Japan
Tel: +81-3-5840-9697
Fax: +81-3-5840-9698
E-mail: office@ddtjournal.com

JOURNAL PUBLISHING AGREEMENT (JPA)

Manuscript No.:

Title:

Corresponding author:

The International Advancement Center for Medicine & Health Research Co., Ltd. (IACMHR Co., Ltd.) is pleased to accept the above article for publication in Drug Discoveries & Therapeutics. The International Research and Cooperation Association for Bio & Socio-Sciences Advancement (IRCA-BSSA) reserves all rights to the published article. Your written acceptance of this JOURNAL PUBLISHING AGREEMENT is required before the article can be published. Please read this form carefully and sign it if you agree to its terms. The signed JOURNAL PUBLISHING AGREEMENT should be sent to the Drug Discoveries & Therapeutics office (Pearl City Koishikawa 603, 2-4-5 Kasuga, Bunkyo-ku, Tokyo 112-0003, Japan; E-mail: office@ddtjournal.com; Tel: +81-3-5840-9697; Fax: +81-3-5840-9698).

1. Authorship Criteria

As the corresponding author, I certify on behalf of all of the authors that:

- 1) The article is an original work and does not involve fraud, fabrication, or plagiarism.
- 2) The article has not been published previously and is not currently under consideration for publication elsewhere. If accepted by Drug Discoveries & Therapeutics, the article will not be submitted for publication to any other journal.
- 3) The article contains no libelous or other unlawful statements and does not contain any materials that infringes upon individual privacy or proprietary rights or any statutory copyright.
- 4) I have obtained written permission from copyright owners for any excerpts from copyrighted works that are included and have credited the sources in my article.
- 5) All authors have made significant contributions to the study including the conception and design of this work, the analysis of the data, and the writing of the manuscript.
- 6) All authors have reviewed this manuscript and take responsibility for its content and approve its publication.
- 7) I have informed all of the authors of the terms of this publishing agreement and I am signing on their behalf as their agent.

2. Copyright Transfer Agreement

I hereby assign and transfer to IACMHR Co., Ltd. all exclusive rights of copyright ownership to the above work in the journal Drug Discoveries & Therapeutics, including but not limited to the right 1) to publish, republish, derivate, distribute, transmit, sell, and otherwise use the work and other related material worldwide, in whole or in part, in all languages, in electronic, printed, or any other forms of media now known or hereafter developed and the right 2) to authorize or license third parties to do any of the above.

I understand that these exclusive rights will become the property of IACMHR Co., Ltd., from the date the article is accepted for publication in the journal Drug Discoveries & Therapeutics. I also understand that IACMHR Co., Ltd. as a copyright owner has sole authority to license and permit reproductions of the article.

I understand that except for copyright, other proprietary rights related to the Work (e.g. patent or other rights to any process or procedure) shall be retained by the authors. To reproduce any text, figures, tables, or illustrations from this Work in future works of their own, the authors must obtain written permission from IACMHR Co., Ltd.; such permission cannot be unreasonably withheld by IACMHR Co., Ltd.

3. Conflict of Interest Disclosure

I confirm that all funding sources supporting the work and all institutions or people who contributed to the work but who do not meet the criteria for authors are acknowledged. I also confirm that all commercial affiliations, stock ownership, equity interests, or patent-licensing arrangements that could be considered to pose a financial conflict of interest in connection with the article have been disclosed.

Corresponding Author's Name (Signature):

Date:

